SLOVAK UNIVERSITY OF TECHNOLOGY
IN BRATISLAVA

FACULTY OF CHEMICAL AND FOOD TECHNOLOGY

Reg. No.: FCHPT-4622-91950

# Safe and Tunable MPC for Uncertain Systems

DISSERTATION THESIS

**2026** **Ing. Erika Plšičík Pavlovičová**

**SLOVAK UNIVERSITY OF TECHNOLOGY IN BRATISLAVA**

**FACULTY OF CHEMICAL AND FOOD TECHNOLOGY**

Reg. No.: FCHPT-4622-91950

# Safe and Tunable MPC for Uncertain Systems

**DISSERTATION THESIS**

| | |
|---|---|
| Study programme: | Process Control |
| Study field: | Cybernetics |
| Training workspace: | Institute of Information Engineering, Automation, and Mathematics |
| Thesis supervisor: | doc. Ing. Juraj Oravec, PhD. |

**2026** **Ing. Erika Plšičík Pavlovičová**

Slovak University of Technology in Bratislava
Department of Information Engineering and Process Control

Faculty of Chemical and Food Technology
Academic year: 2025/2026
Reg. No.: FCHPT-4622-91950

# DISSERTATION THESIS TOPIC

| | |
|---|---|
| Student: | **Ing. Erika Plšičík Pavlovičová** |
| Student's ID: | 91950 |
| Study programme: | Process Control |
| Study field: | Cybernetics |
| Thesis supervisor: | doc. Ing. Juraj Oravec, PhD. |
| Head of department: | prof. Ing. Miroslav Fikar, DrSc. |
| Workplace: | Institute of Information Engineering, Automation, and Mathematics, FCHPT STU |

Topic: **Safe and Tunable MPC for Uncertain Systems**

Language of thesis: English

Specification of Assignment:

The main goal of this thesis is to develop the methods of robust model predictive control (MPC) design for uncertain linear time-invariant (LTI) systems representing industrial plants or embedded control applications.
The particular objectives are:
(i) to develop the Tube MPC design method providing real-time tuning of the control performance, while guaranteeing closed-loop system stability, recursive feasibility, and computationally efficient implementation;
(ii) to validate and analyze the considered Tube MPC design methods using numerical simulation or laboratory implementation;
(iii) to develop freely available software for the design of the selected robust control methods.

Length of thesis: 100

| | |
|---|---|
| Deadline for submission of Dissertation thesis: | 31. 05. 2026 |
| Approval of assignment of Dissertation thesis: | 22. 05. 2026 |
| Assignment of Dissertation thesis approved by: | prof. Ing. Miroslav Fikar, DrSc. – Chairperson of Field of Study Board |

# Acknowledgment

I am deeply grateful to my supervisor, Assoc. Prof. Ing. Juraj Oravec, PhD., for introducing me to process control and guiding me through both my master's and doctoral studies. His patience, willingness to help, and support in every situation meant a great deal to me. I am grateful for the trust he placed in me, for the many opportunities he created, and for encouraging me to become involved in activities beyond research. Under his supervision, I learned much more than process control and scientific work. The opportunity to participate in promotional activities, student events, and the Student Scientific Conference helped me develop communication, organizational, and management skills. Above all, I thank him for our PhD meetings, which I always looked forward to and which gave me motivation and new energy.

I am also grateful to Prof. Ing. Miroslav Fikar, DrSc., head of the department, for creating a supportive working environment at our institute and for the opportunities provided during my doctoral studies. My colleagues from the institute deserve thanks for the friendly atmosphere and many helpful discussions. I also thank all co-authors and collaborators who contributed to the results presented in this thesis, especially Juro, Lenka, and Miška, for their collaboration, advice, and encouragement. I would also like to thank Diana for keeping the caffeine level in my blood stable during the most demanding days.

I would like to thank my husband for his support throughout my studies, for his help, patience, and countless brainstorming sessions in which his main task was often simply to listen. I am especially grateful that he learned what Tube MPC is and how it works, so that he could explain it to others when I no longer had the energy to do so myself. I also want to mention Buddy, whose presence was a great emotional support after long and demanding days.

Na záver by som sa chcela poďakovať mojim rodičom za ich lásku, podporu a nekonečnú trpezlivosť. Ďakujem, že sa nikdy neprestali pýtať, čo to vlastne študujem a kde si budú môcť prečítať moje články, aj keď tomu stále celkom nerozumejú.

# Abstract

This dissertation addresses scalable, robust model predictive control (MPC) for constrained, uncertain systems. The first contribution develops set-based rigid and elastic tube MPC implementations in the freely available MATLAB toolbox MPT+. Rigid tube MPC is designed, tuned, and experimentally validated on a laboratory plate heat exchanger. The elastic tube MPC extension is validated on an embedded heat-exchanger platform, demonstrating satisfaction of input constraints and recovery after a forced actuation disruption. The second contribution focuses on implicit tube MPC as a scalable alternative to explicit set-based tube construction. The formulation is implemented in MPT+, validated on a large-scale reactor-separator benchmark, and experimentally evaluated on the laboratory smart greenhouse VESNA, accounting for actuator limits, environmental disturbances, and the coupled dynamics of controlled variables. An offset-free implicit tube MPC design and numerical implementation are developed for a hybrid heat-integrated distillation system affected by fouling and plant–model mismatch. The industrial case study evaluates robust offset-free tracking in setpoint-tracking and disturbance-rejection scenarios. Compared with conventional PID control, the controller improves tracking, reduces overshoot under conservative tuning, and enables shaping of energy consumption through MPC weighting matrices. Fuel cost and carbon dioxide emissions are also considered, indicating that robust predictive control supports safe and energy-conscious operation. The third contribution presents a real-time tunable implicit tube MPC formulation. Selected penalty factors are tuned online without recomputing the associated auxiliary tube MPC design problem. Fixed tube-design parameters and relaxed first-step constraints preserve recursive feasibility and stability while enabling runtime adaptation of the closed-loop behavior and reducing conservativeness. Numerical validation on the reactor-separator benchmark demonstrates that the tunable controller closely approximates the performance of the corresponding non-tunable implicit tube MPC, with only a negligible performance loss, while removing repeated tube redesign from the online tuning loop. The thesis provides scalable, practically implementable, and robust MPC strategies for constrained, uncertain systems, spanning set-based tube construction, implicit tube representations, and real-time tunable formulations.

# Abstrakt

Táto dizertačná práca sa zaoberá škálovateľným robustným prediktívnym riadením (MPC) pre ohraničené neurčité systémy. Prvým prínosom je vývoj implementácií MPC založeného na rigidných a elastických tubách vo voľne dostupnom MATLAB toolboxe MPT+ s využitím množinových operácií. MPC založené na rigidných tubách je navrhnuté, ladené a experimentálne validované na laboratórnom výmenníku tepla. Validácia MPC založeného na elastických tubách na vnorenej platforme výmenníka tepla potvrdzuje dodržanie vstupných ohraničení a návrat k riadeniu po výpadku akčného zásahu. Druhý prínos sa zameriava na MPC založené na implicitných tubách ako škálovateľnú alternatívu konštrukcii založenej na množinových operáciách. Formulácia je implementovaná v MPT+, validovaná na veľkorozmernom systéme reaktor-separátor a experimentálne overená na inteligentnom skleníku VESNA s ohraničenými akčnými členmi, poruchami z prostredia a previazanou dynamikou riadených veličín. MPC založené na implicitných tubách bez regulačnej odchýlky je navrhnuté pre hybridnú rektifikačnú kolónu s integrovaným ohrevom, zanášaním a nesúladom modelu s procesom. Priemyselná prípadová štúdia hodnotí robustné sledovanie referencie bez regulačnej odchýlky pri sledovaní žiadanej hodnoty a potláčaní porúch. V porovnaní s konvenčným PID riadením regulátor zlepšuje kvalitu riadenia, znižuje preregulovanie pri konzervatívnom ladení a upravuje spotrebu energie prostredníctvom váhových matíc MPC. Analýza zahŕňa aj náklady na palivo a emisie oxidu uhličitého, čím potvrdzuje podporu bezpečnej a energeticky úspornej prevádzky. Tretí prínos predstavuje formuláciu MPC založeného na implicitných tubách laditeľnú v reálnom čase. Vybrané penalizačné faktory sú ladené online bez opätovného prepočítania príslušnej pomocnej úlohy návrhu MPC založeného na tubách. Fixné parametre návrhu tuby a uvoľnené ohraničenia v prvom kroku zachovávajú rekurzívnu riešiteľnosť a stabilitu, pričom umožňujú meniť správanie uzavretého regulačného obvodu a znižovať konzervatívnosť. Numerická validácia na systéme reaktor-separátor potvrdzuje takmer ekvivalentnú kvalitu riadenia v porovnaní s neladiteľným MPC založeným na implicitných tubách, a to len so zanedbateľnou stratou kvality, pričom odstraňuje potrebu opakovane konštruovať tuby. Práca poskytuje škálovateľné a prakticky implementovateľné robustné MPC stratégie pre ohraničené neurčité systémy, od množinovej konštrukcie tuby cez implicitné reprezentácie tuby až po laditeľné formulácie v reálnom čase.

# Contents

# List of Figures

# List of Tables

Chapter 1

# Introduction

Industrial control systems are expected to operate close to physical, safety, and economic limits. Process plants, energy systems, and many others are affected by actuator saturation, constraints on system states, disturbances, plant–model mismatch, sensor noise, and operating conditions that change over time [53]. In such settings, the controller is expected not only to improve nominal performance but also to preserve constraint satisfaction and closed-loop system stability when the plant deviates from the prediction model [62]. These requirements have made model predictive control (MPC) one of the central methodologies of modern constrained control [33]. Its constrained-control foundations and practical design principles are developed across the broader MPC literature [5]. However, retaining these guarantees while reducing computational complexity and enabling real-time controller adaptation remains an open implementation-oriented challenge.

MPC formulates the control task as a finite-horizon constrained optimization problem built on a prediction model of the plant [33]. The optimization problem contains the multivariable plant dynamics, constraints on control inputs and system states, and performance objectives that express the desired trade-off among tracking accuracy, actuator usage, and economic or operational requirements [5]. Only the first optimized control input is applied to the plant. After the next measurement, the horizon is shifted and the optimization is solved again. The resulting implementation is called the receding-horizon control principle [33]. This repeated re-optimization introduces feedback and allows the controller to react to disturbances and modeling errors while preserving the constraint-aware structure of the design. This combination is particularly important in process control, where product quality, energy consumption, safety margins, and actuator limits interact in ways that are difficult to coordinate with conventional single-loop control structures [53]. Applications in energy and process systems show that predictive controllers can improve operating performance and reduce energy demand when compared with more classical control strategies [40]. Similar benefits have been reported for constrained predictive control in numerous process-industry applications [30].

The ability of MPC to handle constraints through optimization is also one of its main implementation limitations. The controller normally solves an optimization problem at every sampling instant, and the size of this problem grows with the number of system states, control inputs, constraints, and prediction steps. This computational burden is acceptable for many slow industrial processes, but it becomes restrictive for embedded hardware, fast sampling rates, high-dimensional systems, and robust formulations in which uncertainty has to be treated explicitly [62]. The development of MPC has therefore been shaped not only by control-theoretic guarantees, but also by the need to make these guarantees computationally tractable. This implementation drawback helps explain why proportional-integral-derivative (PID) controllers remain widespread in embedded and industrial practice, despite their limited ability to handle multivariable interactions and hard constraints [39].

This computational difficulty has also influenced the numerical methods and software tools used for MPC. A large part of this effort focuses on quadratic optimization, because quadratic programming (QP) problems appear directly in linear MPC [33] and as structured subproblems in many nonlinear MPC algorithms. Reviews of QP methods for nonlinear MPC emphasize the role of optimal-control structure in solver design [23]. Embedded implementation has also motivated code-generation and structured solver developments, as illustrated by CVXGEN [35] and OSQP [65]. Modelling environments used later in this thesis, in particular YALMIP [32] and the Multi-Parametric Toolbox [14], further show that implementation choices are part of the controller design problem itself.

An efficient way to reduce the online computational load is explicit MPC [4]. In this approach, all of the optimization burden is moved offline by treating the measured system state as a parameter [1]. The online controller then evaluates a precomputed feedback control law rather than solving the finite-horizon problem at every sampling instant. This makes explicit MPC relevant for microcontrollers and other resource-limited platforms, provided that the stored controller remains small enough [22].

The main limitation of explicit MPC is complexity growth. The memory needed to store the precomputed controller and the cost of online controller evaluation can increase rapidly with the system dimension, prediction horizon, and number of constraints. This has motivated approaches that keep the speed of explicit evaluation while reducing memory footprint or simplifying the control law. Examples include optimal region merging and complexity reduction of piecewise-affine partitions [12], clipping-based simplification [25], separation-function-based simplification exploiting input saturation properties [28], low-complexity controller design and verification in MPT3 [26], and polynomial approximation of explicit feedback control laws with stability and constraint-satisfaction guarantees [27]. Reachability-based methods remove regions that are irrelevant for the closed-loop evolution [24]. Lattice piecewise-affine approximations provide structured approximations of explicit control laws [73]. Neural-network approximations replace the stored partition by a learned mapping while attempting to retain acceptable closed-loop performance [6]. These developments show that embedded MPC is not only a matter of solving an optimization problem quickly, it is also a matter of choosing a representation that fits the available memory, arithmetic, and real-time scheduling constraints.

Implicit, or online, MPC follows the opposite implementation philosophy: the optimization problem is solved during operation rather than stored as a complete parametric solution. This avoids the memory burden of explicit partitions, but it leaves the online solver in the feedback loop. For embedded and implementation-oriented control, the choice between explicit and implicit MPC is therefore a design trade-off between memory, online computation, adaptability, and model dimension.

Computational tractability alone does not make a predictive controller safe in the presence of uncertainty. A nominal controller can react to disturbances through feedback, but nominal feasibility does not guarantee that constraints on system states and control inputs remain satisfied for all admissible disturbance realizations. Robust MPC addresses this limitation by incorporating uncertainty into the controller design. Early work on constrained predictive control under bounded uncertainty established the importance of robustifying the nominal prediction against model mismatch and disturbances [36]. The subsequent development of robust constrained MPC further clarified how recursive feasibility and closed-loop system stability can be preserved under uncertainty when the controller is designed with appropriate invariant sets and tightened constraints [29].

Tube-based MPC is a widely used robust predictive control strategy for constrained uncertain systems. Instead of optimizing over all possible disturbed trajectories, it predicts a nominal trajectory and keeps the true disturbed trajectory inside a tube around it. A local stabilizing feedback control law compensates for disturbances, while the nominal constraints are tightened so that the original plant constraints are satisfied for every admissible disturbance. Earlier work on persistent bounded disturbances used such constraint restrictions to keep the predictive controller feasible and constraint-satisfying [7]. A central rigid tube MPC formulation established this construction for constrained uncertain systems [36]. Efficient tube controllers further developed the use of robust positively invariant sets and constraint tightening [55], [38].

The tube framework has since been extended to output-feedback designs [37], reference tracking [31], homothetic tube parameterizations [58], elastic tubes [59], sampled-data systems [10], linear parameter-varying systems [15], and parallel explicit implementations [70]. From the implementation point of view, the robust controller keeps the interpretation of tube MPC, while its computational representation is better aligned with larger optimization problems and software-supported implementations.

The same tube idea has also influenced more recent uncertainty descriptions. Distributionally robust predictive control considers uncertainty not only in individual disturbance values, but also in the probability distributions from which disturbances are drawn [68]. Ambiguity-based tube MPC propagates uncertainty sets in probability space for nonlinear stochastic systems [72]. Wasserstein tube MPC retains the nominal trajectory and error-tube structure while modifying the tightening according to distributional ambiguity [2]. Tube-based distributionally robust MPC for nonlinear process systems continues the same line of work on robust constraint satisfaction with probabilistic descriptions of uncertainty [75]. These methods show that tube constructions remain useful under richer uncertainty descriptions, but they also increase the computational demands of uncertainty-aware predictive control.

A persistent bottleneck in classical tube MPC is the reliance on explicit set-based operations. Robust positively invariant sets, Pontryagin differences, and terminal sets define the tightened constraints and invariant regions used by the controller, but their explicit computation can become demanding or numerically intractable as the system dimension grows. This limits repeated controller redesign and restricts the use of rigid tube MPC in large-scale applications. Implicit tube MPC [56] addresses this difficulty by representing the tube through auxiliary variables and support-function-based constraints instead of explicitly constructing the tube cross-section. Implicit terminal ingredients continue this movement away from explicitly constructed terminal sets [60].

Reducing computational complexity is not the only reason to move beyond the classical rigid tube. A fixed tube cross-section can be conservative when the effect of disturbances changes along the prediction horizon or when the plant has operating regimes with different sensitivity to uncertainty. This has motivated non-rigid tube parameterizations, including fully parameterized and homothetic tubes [57], [58]. Elastic tube MPC [59] follows the same direction by allowing the tube cross-section to vary along the horizon while preserving robustness guarantees. More recent scaled-zonotopic formulations continue this direction by improving the scalability of flexible tube representations [9]. Time-varying cross-section tube MPC extends this idea further by treating the changing cross-section itself as part of the controller design [71]. A recent highly efficient approach of configuration-constrained tube MPC and self-optimizing terminal ingredients further illustrates the broader search for tube parameterizations that maintain constraint-satisfaction guarantees without unnecessary conservatism, see [69, 19, 21, 20], and references therein. Robust constraint satisfaction does not by itself guarantee accurate reference tracking. In process applications, persistent disturbances and plant–model mismatch often produce steady-state offsets if the prediction model does not capture the effect that causes the mismatch. Offset-free MPC addresses this issue by augmenting the prediction model with disturbance dynamics, estimating the disturbance online, and computing steady-state targets that are consistent with the estimated mismatch [47]. A tutorial account compares the disturbance-model approach with observer-based and velocity-form interpretations [45]. Further work clarifies the role of disturbance modeling and observer design in state-space predictive control [66], as well as practical formulation issues in offset-free MPC [46]. Robust setpoint tracking formulations connect the offset-free objective with constraint satisfaction under uncertainty [44]. This is particularly relevant in thermal and separation processes, where fouling, heat-transfer degradation, composition uncertainty, and unmeasured load changes can gradually shift the steady-state relation between manipulated and controlled variables [42].

For robust tube MPC, online tunability is more tightly coupled to the safety construction. Changing the penalty factors may also change the stabilizing feedback gain, the tube parameters, the tightened constraints, and the terminal ingredients. Asynchronous tube redesign offers one way to update a robust tube controller on demand, but repeated set computations remain restrictive for real-time or large-scale implementation [64]. This motivates robust MPC formulations in which closed-loop behavior can be tuned online without losing recursive feasibility and robust stability.

The literature survey provides separate components for robust, implicit, tunable MPC, however, these components are underdeveloped in control scenarios when the target is an MPC controller that is simultaneously constraint-aware, tunable, computationally scalable, and experimentally implementable. Robust tube MPC typically relies on fixed design ingredients, whereas online tuning may affect the feedback gain, terminal ingredients, and constraints. This thesis therefore investigates how stability-aware tube-based MPC formulations is modified and implemented so that their closed-loop behavior is tunable in real time while preserving recursive feasibility, robust stability, and implementability on the considered platforms.

## Thesis Goals

The main goal of this thesis is to develop and validate safe, constraint-aware, and tunable MPC design methods for large-scale and implementation-oriented platforms. The thesis focuses on MPC controllers that preserve constraint satisfaction under bounded disturbances, enable meaningful online tuning of closed-loop behavior, and remain computationally tractable in the considered design and deployment settings. More specifically, the thesis addresses the following goals:

1. **Safe tube MPC for uncertain systems: implementation, analysis, and validation.** The goal is to implement, analyze, and validate tube-based robust MPC strategies for constrained systems affected by bounded disturbances and plant–model mismatch. The analysis and validation cover laboratory, embedded, large-scale, and industrially oriented case studies.

2. **Real-time tunability of implicit tube MPC:** The goal is to develop a tunable implicit tube MPC strategy that allows the closed-loop behavior to be adjusted online through penalty tuning without requiring a complete redesign of the tube ingredients or repeated solution of the auxiliary tube-design optimization problem in real time.

3. **Open-source software-supported implementation of tube-based controllers:** The goal is to integrate the developed robust-control methods into Multi-Parametric Toolbox (MPT)+ and support reproducible controller design, closed-loop performance analysis, visualization, and implementation preparation for embedded platforms.

Chapter 2

# Theoretical Background

*This chapter establishes the theoretical background used throughout the thesis for constrained and robust predictive control. It establishes the notation and formulates the main assumptions, optimization problems, cost functions, constraints, and terminal ingredients of finite-horizon MPC for linear systems. The chapter then introduces implicit MPC, in which the optimization problem is solved online, and explicit MPC, in which the parametric solution is computed offline and evaluated online as a piecewise-affine control law. The following robust-control part of the chapter introduces the basic set-theoretic concepts needed for constraint satisfaction under uncertainty, with emphasis on robust positively invariant sets and their approximations. These notions lead naturally to tube-based MPC, in which the system state is decomposed into a nominal component and an error component. This separation allows the nominal MPC law to address performance and constraints, while a local feedback law keeps the actual system state inside a tube around the nominal trajectory.*

## 2.1 Model Predictive Control

Model Predictive Control (MPC) is an advanced control strategy that utilizes a mathematical model of a system to predict its future behavior and determine optimal control inputs. At each sampling instant, MPC solves a constrained finite-horizon optimal control problem, applies only the first control action, and repeats the procedure at the next time step. The receding horizon control approach introduces feedback into the control loop, enabling the controller to react to disturbances and model mismatch [62].

The strength of MPC lies in its ability to systematically handle multivariable systems and explicitly incorporate constraints on system states and control inputs. This makes it particularly suitable for applications where physical or safety limitations have to be satisfied. MPC also provides a unified framework integrating optimal control, estimation, and constraint handling [33].

### 2.1.1 Formulation of Conventional MPC Design Problem

Consider a discrete-time linear time-invariant (LTI) system of the form

$$\begin{aligned} x_{k+1} &= Ax_k + Bu_k, \\ x_0 &= x(0), \end{aligned} \tag{2.1}$$

where $x_k \in \mathbb{R}^n$ is the system state vector, $u_k \in \mathbb{R}^m$ is the control input vector, $A \in \mathbb{R}^{n\times n}$ is the state matrix, $B \in \mathbb{R}^{n\times m}$ is the input matrix, and $k \in \mathbb{N}_0$ denotes the discrete-time index.

The associated conventional MPC design problem is formulated as a finite-horizon optimal control problem:

$$\min_{U} \quad x_N^\top P x_N + \sum_{k=0}^{N-1} \left( x_k^\top Q x_k + u_k^\top R u_k \right) \tag{2.2a}$$

$$\text{s.t.} \quad x_{k+1} = Ax_k + Bu_k, \tag{2.2b}$$

$$x_k \in \mathbb{X}, \quad u_k \in \mathbb{U}, \tag{2.2c}$$

$$x_N \in \mathbb{X}_\mathrm{f}, \tag{2.2d}$$

$$x_0 = x(t), \tag{2.2e}$$

where $N \in \mathbb{N}$ is the prediction horizon, $U = [u_0^\top, \dots, u_{N-1}^\top]^\top \in \mathbb{R}^{mN}$ is the optimized control input sequence, $x_0, \dots, x_N$ are the predicted system states, and $x(t) \in \mathbb{R}^n$ is the measured or estimated system state at the current sampling instant. The matrices $Q \in \mathbb{R}^{n\times n}$ and $R \in \mathbb{R}^{m\times m}$ define the stage-cost penalties, while $P \in \mathbb{R}^{n\times n}$ defines the terminal penalty. The sets $\mathbb{X} \subseteq \mathbb{R}^n$ and $\mathbb{U} \subseteq \mathbb{R}^m$ impose constraints on system states and control inputs, and $\mathbb{X}_\mathrm{f} \subseteq \mathbb{R}^n$ is the terminal constraint set.

**Assumption 2.1** (Prediction model and constraints)**.** *The pair $(A, B)$ is controllable. The constraint sets $\mathbb{X}$ and $\mathbb{U}$ are compact, convex, and contain the origin in their strict interiors. The weighting matrices are square and satisfy $Q \succeq 0$, i.e., $Q$ is positive semidefinite, and $R \succ 0$, i.e., $R$ is positive definite. Moreover, the pair $(Q^{1/2}, A)$ is detectable.*

**Assumption 2.2** (Terminal set and terminal penalty)**.** *There exists a local terminal controller $\kappa_\mathrm{f} : \mathbb{X}_\mathrm{f} \to \mathbb{U}$ such that the terminal set $\mathbb{X}_\mathrm{f}$ is control invariant for the nominal model* (2.1)*, i.e., for every $x \in \mathbb{X}_\mathrm{f}$, the successor state $Ax + B\kappa_\mathrm{f}(x)$ remains in $\mathbb{X}_\mathrm{f}$ and the terminal control input $\kappa_\mathrm{f}(x)$ remains admissible. Moreover, the terminal penalty $V_\mathrm{f}(x) = x^\top P x$ satisfies*

$$V_\mathrm{f}\big(Ax + B\kappa_\mathrm{f}(x)\big) - V_\mathrm{f}(x) \leq -\ell(x, \kappa_\mathrm{f}(x)), \qquad \forall x \in \mathbb{X}_\mathrm{f}, \tag{2.3}$$

*where $\ell(x, u) = x^\top Q x + u^\top R u$.*

After solving (2.2), only the first optimizer $u_0^\star$ is applied to the system. At the next sampling instant, the current state is measured or estimated again and the finite-horizon problem is solved with the updated initial condition. This receding-horizon implementation gives MPC its feedback benefits and distinguishes it from an open-loop optimal control problem [62].

### 2.1.2 Recursive Feasibility and Stability

Recursive feasibility and closed-loop system stability are strong theoretical properties of a well-established MPC design problem. The problem in (2.2) is solved only over a finite horizon, but the resulting MPC controller is considered to operate indefinitely. It is therefore not enough to find an admissible control input sequence at the current sampling instant, but the optimization problem should remain feasible at future sampling instants, and the closed-loop system trajectory should approach the desired steady-state value [62].

Recursive feasibility means that feasibility of the optimization problem (2.2) propagates along the closed-loop system trajectory for given initial conditions. From this perspective, the relevant set is the $N$-step feasible set

$$\mathbb{X}_\mathrm{N} = \{x \in \mathbb{X} : \text{(2.2) is feasible for } x(t) = x\} \tag{2.4}$$

and recursive feasibility requires the MPC control law to produce a successor system state that again belongs to $\mathbb{X}_\mathrm{N}$. Under Assumption 2.2, this is addressed by the terminal constraint $x_N \in \mathbb{X}_\mathrm{f}$ together with the local terminal controller $\kappa_\mathrm{f}$. The control-invariance condition can be written as [5]

$$x \in \mathbb{X}_\mathrm{f} \quad \Rightarrow \quad Ax + B\kappa_\mathrm{f}(x) \in \mathbb{X}_\mathrm{f}, \qquad \kappa_\mathrm{f}(x) \in \mathbb{U}. \tag{2.5}$$

This gives the conventional shifted-sequence argument for recursive feasibility. After the first optimal control input is applied, the remaining optimized control inputs are shifted by one step and the local terminal controller is appended at the end. The shifted sequence provides a feasible candidate for the next optimization problem, so feasibility at the current step implies feasibility at the next one [62].

For MPC design problem (2.2), asymptotic stability is usually guaranteed by using the optimal value function $V_N^\star(x)$ formulated as a Lyapunov function. In this role, the optimal cost is required not only to be finite, but also to decrease along the closed-loop system trajectory. For the quadratic stage cost in (2.2a), with $\ell(x,u) = x^\top Qx + u^\top Ru$, this is commonly expressed as the Lyapunov descent condition

$$V_N^\star(x(t+1)) - V_N^\star(x(t)) \leq -\ell(x(t), u_0^\star). \tag{2.6}$$

The prediction model, cost, and terminal properties in Assumptions 2.1 and 2.2 provide the usual ingredients to achieve this decrease [62]. The terminal penalty represents the cost beyond the finite prediction horizon, while the terminal set and local controller ensure that the controller has a feasible continuation after the horizon ends. Under these assumptions, the origin is asymptotically stable for all initial system states in the feasible set $\mathbb{X}_\mathrm{N}$.

The value function and terminal ingredients are therefore crucial not only for the nominal MPC problem (2.2), but also for several MPC variants built on the same finite-horizon formulation. For the linear MPC problem (2.2) with quadratic costs and polyhedral constraints, the optimal resulting value function is piecewise quadratic over the polytopic MPC critical regions defining the domain of the feasibility set, which also supports stability analysis in the multi-parametric setting [4], see Section 2.1.4.

In robust tube MPC, the analogous principles are applied to the nominal trajectory and combined with invariant error bounds and tightened constraints to preserve constraint satisfaction for all admissible disturbances, see Section 2.2.1.

### 2.1.3 Implicit MPC Design Framework

In its conventional form, MPC is implemented implicitly by solving the optimization problem online at each sampling instant. For linear systems with quadratic cost and polyhedral constraints, the online optimization problem (2.2) is a quadratic programming (QP) problem [23]. However, the computational complexity of solving a QP online represents one of the main limitations of MPC, especially for systems with fast dynamics or limited computational resources. This is particularly relevant in embedded implementations, where both computational power and memory are constrained. The most relevant aspects for successful real-time implementation are therefore directly tied to the structure of the optimization problem, the numerical method used to solve it, the memory layout of the implementation, and the predictability of the online computation.

To address these challenges, various numerical methods have been developed. Code-generation tools such as CVXGEN [35] illustrate how small embedded convex programs can be turned into predictable custom solvers. Operator-splitting solvers such as OSQP [65] are attractive when structured quadratic programs must be solved repeatedly. Embedded implementations of linear MPC solvers, including HPIPM [11], also highlight the importance of exploiting problem structure and numerical linear algebra in real-time deployment.

### 2.1.4 Explicit MPC Design Framework

An alternative approach to reducing online computational complexity is explicit MPC, which shifts the computational burden from the online phase to an offline precomputation step [1]. In explicit MPC, the optimization problem is formulated as a multi-parametric quadratic program (mp-QP), where the current system state $x(t)$ is treated as a parameter. The solution of this parametric problem is a piecewise affine function of the system state [4].

As a result, the control law can be written as a piecewise-affine function of the system states:

$$u^\star(x) = F_i x + g_i, \quad \text{if } x \in \mathcal{R}_i, \tag{2.7}$$

where $u^\star(x)$ is the optimizer evaluated at the current system state, $i$ is the index of the active critical region, $F_i \in \mathbb{R}^{m\times n}$ and $g_i \in \mathbb{R}^m$ define the affine control law in that region, and $\mathcal{R}_i \subseteq \mathbb{R}^n$ are polyhedral regions forming a partition of the system state space.

The offline phase consists of computing these polyhedral sets, known as critical regions, together with their associated affine control laws. During online operation, the control action is obtained by determining which critical region contains the current system state and evaluating the corresponding affine function. Software tools such as the

Multi-Parametric Toolbox [14] have made this construction accessible for constrained and explicit MPC design.

This significantly reduces the online computational effort, as the optimization problem is replaced by a point-location problem usually having a form of a suitable lookup table and a simple matrix-vector multiplication. This makes explicit MPC particularly suitable for real-time and embedded applications when the number of critical regions and the memory footprint are manageable.

However, the number of critical regions typically grows exponentially with the system dimension, number of constraints, and prediction horizon. This leads to high memory requirements and increased complexity of the critical region search. As a result, explicit MPC is mainly applicable to systems of moderate size.

Despite these limitations, explicit MPC provides valuable insight into the structure of the optimal control law. It also forms the basis for approximate and hybrid approaches that aim to balance computational efficiency and scalability [1].

## 2.2 Robust Model Predictive Control

The conventional MPC formulation relies on a nominal prediction model and assumes perfect knowledge of system dynamics. In practice, however, real systems are affected by model mismatch, parameter variations, external disturbances, and measurement errors. These effects may lead to deviations between predicted and actual trajectories, potentially resulting in degraded performance or violation of constraints [62].

Robust Model Predictive Control (RMPC) extends the MPC formulation by explicitly accounting for such uncertainties. The goal is to ensure that the system constraints are satisfied for all admissible realizations of uncertainty while maintaining acceptable control performance [36].

A general uncertain system can be described as [62]

$$x_{k+1} = f(x_k, u_k, \xi_k), \tag{2.8}$$

where $\xi_k \in \Xi \subset \mathbb{R}^{n_\xi}$ represents a generic uncertainty, $\Xi$ is a compact set containing the origin, and $f : \mathbb{R}^n \times \mathbb{R}^m \times \mathbb{R}^{n_\xi} \to \mathbb{R}^n$ is the uncertain prediction model. A common specialization is the uncertain linear time-invariant (LTI) system with additive bounded disturbances [38]

$$x_{k+1} = Ax_k + Bu_k + Ed_k, \qquad d_k \in \mathbb{D}, \tag{2.9a}$$
$$w_k := Ed_k, \qquad \mathbb{W} := E\mathbb{D}. \tag{2.9b}$$

Here $d_k \in \mathbb{D} \subset \mathbb{R}^{n_d}$ is the disturbance input before multiplication by the disturbance matrix $E \in \mathbb{R}^{n \times n_d}$, while $w_k \in \mathbb{R}^n$ is the additive disturbance acting directly on the system state equation. Thus, $\mathbb{D}$ is the admissible set for the disturbance input and $\mathbb{W}$ is its image in the system state space. When $E = I$, the two descriptions coincide. In the tube MPC formulations below, this disturbance is written in the equivalent additive form [29]

$$x_{k+1} = Ax_k + Bu_k + w_k, \quad w_k \in \mathbb{W}. \tag{2.10}$$

where the additive disturbance satisfies $\mathbb{W} \subset \mathbb{R}^n$. Unless stated otherwise, the disturbance set used in the robust tube construction is represented as the polyhedron [38]

$$\mathbb{W} = \left\{ w \in \mathbb{R}^n : e_i^\top w \leq 1, \quad \forall i \in \mathcal{I}_\mathrm{W} \right\}, \tag{2.11}$$

where $e_i \in \mathbb{R}^n$ denotes the normal vector of the $i$th disturbance set inequality and $\mathcal{I}_\mathrm{W}$ is the corresponding finite index set. If the disturbance is specified before the matrix $E$, the set $\mathbb{D}$ describes admissible disturbance inputs and the additive disturbance set is its image $\mathbb{W} = E\mathbb{D}$.

Uncertainty may also enter through system parameters, where the matrices $A$ and $B$ are not fixed but belong to a prescribed uncertainty set. However, additive disturbance models (2.9) are especially common when external disturbances or modeling errors are considered explicitly in robust MPC [55].

The main requirement in RMPC is that constraints are satisfied for all admissible additive disturbances, equivalently for all admissible disturbance inputs mapped through $w = Ed$ [36], i.e.,

$$x_k \in \mathbb{X}, \quad u_k \in \mathbb{U}, \quad \forall w_k \in \mathbb{W}. \tag{2.12}$$

Thus, the same constraints on system states and control inputs are required to hold for every admissible disturbance realization.

Several robust MPC formulations were developed to handle this requirement. For random uncertainty realizations, one possible approach is stochastic MPC [68], which describes uncertainty through probability distributions and accepts probabilistic, rather than deterministic, constraint guarantees, with recent chance-constrained formulations extending this viewpoint to data-driven settings [8]. Scenario-based robust MPC replaces the uncertainty set by sampled disturbance trajectories and can provide probabilistic guarantees when sufficiently many scenarios are considered [62]. However, these probabilistic methods do not provide rigorous guarantees of hard constraint satisfaction.

In contrast, the well-known min–max MPC formulation provides guarantees of constraint satisfaction for bounded additive disturbances. The min–max MPC controller is based on the solution of an optimization problem that optimizes against the worst-case disturbance sequence and therefore gives a direct robust formulation [63].

For the additive model (2.10), the min–max design approach leads to a finite-horizon optimization problem in which the predicted control input sequence is chosen with respect to the most adverse admissible disturbance sequence over the horizon. This can be written as the following worst-case finite-horizon problem [63], [61]:

$$
\begin{aligned}
\min_{u_0,\ldots,u_{N-1}} \ \max_{w_0,\ldots,w_{N-1}\in\mathbb{W}} \quad & x_N^\top P x_N + \sum_{k=0}^{N-1} \left( x_k^\top Q x_k + u_k^\top R u_k \right) && \text{(2.13a)}\\
\text{s.t.} \quad & x_{k+1} = A x_k + B u_k + w_k, && \text{(2.13b)}\\
& x_k \in \mathbb{X}, \quad u_k \in \mathbb{U}, \quad w_k \in \mathbb{W}, && \text{(2.13c)}\\
& x_N \in \mathbb{X}_\mathrm{N}, && \text{(2.13d)}\\
& x_0 = x(t), \qquad k = 0,\ldots,N-1. && \text{(2.13e)}
\end{aligned}
$$

The inner maximization represents the disturbance sequence that gives the largest cost, while the outer minimization chooses a control input sequence for that worst case. In feedback min–max MPC, the future control inputs may also be written as corrected control inputs that depend on the previously realized disturbances, for example

$$
u_k = v_k + \sum_{i=0}^{k-1} M_{k,i} w_i, \qquad k = 0,\ldots,N-1, \tag{2.14}
$$

where $v_k$ is the nominal part of the control input and $M_{k,i}$ are feedback-policy matrices. Because all admissible disturbance realizations are considered explicitly, the formulation gives a clear worst-case robust interpretation.

The main drawbacks of min–max MPC are twofold: from the control-performance perspective, this method provides highly conservative performance, and from the implementation viewpoint, this approach leads to an optimization problem with numerous inequality constraints.

Its computational complexity originates in the min–max optimization problem, which traverses disturbance sequences and becomes computationally intractable as the horizon, system dimension, and disturbance description grow. Moreover, since the min–max controller is designed for the worst-case disturbance realization, the resulting control action can also be conservative in less severe operating conditions.

This limitation motivates the implementation of less conservative and more computationally tractable robust MPC formulations.

Throughout this thesis, the tube MPC method is considered for robust MPC design to address the main implementation challenges.

### 2.2.1 Tube-Based MPC

Compared to min–max MPC design that evaluates computationally expensive worst-case optimization in (2.13), tube-based MPC handles the uncertainties through a robust invariant set constructed around a nominal trajectory.

Consider the additive system (2.10) subject to the disturbance set (2.11) and the hard constraints (2.12). The sets $\mathbb{X}$ and $\mathbb{U}$ are assumed to contain the origin in their strict interiors.

For a stabilizing feedback gain $K_{\mathrm{S}}$, the conventional rigid tube MPC problem follows a robust tube construction based on constraint tightening and invariant tubes [38]. The invariant-set approximation used to construct the tube cross-section is based on a finite-step procedure for robust positively invariant sets [54]. The resulting optimization problem is written as

$$\min_{\hat{x}_0,\hat{u}_0,\dots,\hat{u}_{N-1},\hat{x}_N} \quad \hat{x}_N^\top P \hat{x}_N + \sum_{k=0}^{N-1} \left( \hat{x}_k^\top Q \hat{x}_k + \hat{u}_k^\top R \hat{u}_k \right) \tag{2.15a}$$

$$\text{s.t.} \quad \hat{x}_{k+1} = A\hat{x}_k + B\hat{u}_k, \tag{2.15b}$$

$$\hat{u}_k \in \mathbb{U} \ominus K_{\mathrm{S}}\mathbb{T}, \tag{2.15c}$$

$$\hat{x}_k \in \mathbb{X} \ominus \mathbb{T}, \tag{2.15d}$$

$$\hat{x}_N \in \mathbb{X}_{\mathrm{N}} \ominus \mathbb{T}, \tag{2.15e}$$

$$x(t) - \hat{x}_0 \in \mathbb{T}, \tag{2.15f}$$

$$k = 0, 1, \dots, N-1. \tag{2.15g}$$

Here $\hat{x}_k$ and $\hat{u}_k$ are the nominal counterparts of the predicted variables in the MPC problem, and the weights $Q$, $R$, and $P$ have the same role as in the nominal MPC formulation (2.2). The gain $K_{\mathrm{S}} \in \mathbb{R}^{m\times n}$ is chosen such that $A + BK_{\mathrm{S}}$ is Schur stable. The set $\mathbb{T} \subseteq \mathbb{R}^n$ is an offline-computed robust positively invariant (RPI) tube cross-section, and $\mathbb{X}_{\mathrm{N}} \subseteq \mathbb{R}^n$ is the terminal set. In the finite-sum construction used below, $\mathbb{T}$ is given by

$$\mathbb{T} = (1-\alpha)^{-1} \oplus_{j=0}^{N_{\mathrm{S}}-1} (A+BK_{\mathrm{S}})^j \, \mathbb{W}, \tag{2.16}$$

where $N_{\mathrm{S}}$ is the finite disturbance-propagation length and $\alpha \in [0,1)$ is the associated scalar scaling parameter [54]. The value of $\alpha$ is evaluated as

$$\alpha = \max_{i \in \mathcal{I}_{\mathrm{W}}} \alpha_i \leq \alpha_{\mathrm{tol}}, \tag{2.17a}$$

$$\alpha_i = \mathrm{h}\left(\mathbb{W}, \left((A+BK_{\mathrm{S}})^{N_{\mathrm{S}}}\right)^{\top} e_i\right), \quad \forall i \in \mathcal{I}_{\mathrm{W}}. \tag{2.17b}$$

Here $\alpha_{\mathrm{tol}} \in [0,1)$ is a prescribed tolerance and $\mathrm{h}(\mathbb{W}, v)$ is the support function of $\mathbb{W}$ in direction $v \in \mathbb{R}^n$,

$$\mathrm{h}(\mathbb{W}, v) = \max_{w} \quad v^{\top} w, \tag{2.18a}$$

$$\text{s.t.} \quad e_i^{\top} w \leq 1, \quad \forall i \in \mathcal{I}_{\mathrm{W}}. \tag{2.18b}$$

The resulting receding-horizon control law is given by

$$\mu_{\mathrm{MPC}}(x) = \hat{u}_0^{\star} + K_{\mathrm{S}} \left(x - \hat{x}_0^{\star}\right), \tag{2.19}$$

where the optimizers $\hat{u}_0^{\star}$ and $\hat{x}_0^{\star}$ are obtained from (2.15).

**Assumption 2.3** (Terminal set and terminal penalty)**.** *Consider the nominal prediction model $\hat{x}_{k+1} = A\hat{x}_k + B\hat{u}_k$ used in problem* (2.15) *and the corresponding tube MPC feedback control law* (2.19)*, with a fixed stabilizing feedback gain $K_{\mathrm{S}}$ such that $A+BK_{\mathrm{S}}$ is Schur stable. Assume that the terminal set $\mathbb{X}_{\mathrm{N}}$ and terminal penalty $P$ satisfy:*

(A1) ***Terminal set.*** *The terminal set $\mathbb{X}_{\mathrm{N}}$ is compact, invariant, contains the origin in its strict interior, and satisfies*

$$(A+BK_{\mathrm{S}})\hat{x} \in \mathbb{X}_{\mathrm{N}}, \qquad \forall \hat{x} \in \mathbb{X}_{\mathrm{N}}, \tag{2.20}$$

$$\hat{x} \in \mathbb{X} \ominus \mathbb{T}, \qquad K_{\mathrm{S}}\hat{x} \in \mathbb{U} \ominus K_{\mathrm{S}}\mathbb{T}, \qquad \forall \hat{x} \in \mathbb{X}_{\mathrm{N}}. \tag{2.21}$$

(A2) ***Terminal penalty.*** *The matrix $P$ is chosen as a stabilizing Lyapunov terminal penalty associated with the terminal controller $K_{\mathrm{S}}$, i.e.,*

$$(A+BK_{\mathrm{S}})^{\top} P (A+BK_{\mathrm{S}}) - P \preceq -(Q + K_{\mathrm{S}}^{\top} R K_{\mathrm{S}}). \tag{2.22}$$

*Consequently,*

$$\begin{aligned} V_{\mathrm{f}}\big((A+BK_{\mathrm{S}})\hat{x}\big) - V_{\mathrm{f}}(\hat{x}) &\leq \ell(\hat{x}, K_{\mathrm{S}}\hat{x}), \\ V_{\mathrm{f}}(\hat{x}) := \hat{x}^{\top} P \hat{x}, \qquad \ell(\hat{x}, \hat{u}) &:= \hat{x}^{\top} Q \hat{x} + \hat{u}^{\top} R \hat{u}. \end{aligned} \tag{2.23}$$

Under Assumption 2.3, the receding-horizon tube MPC law (2.19) is recursively feasible and preserves constraint satisfaction for all admissible disturbances whenever the initial condition is feasible for (2.15), by the conventional tube MPC argument [38].

Chapter 3

# Set-Based Tube MPC for Constrained Systems

*This chapter presents the development and validation of set-based tube MPC strategies for constrained systems. The focus is on robust controllers whose safety guarantees are obtained by surrounding a nominal prediction with a disturbance tube and by tightening the original constraints accordingly. The research presented here addresses the practical challenges of ensuring safety and constraint satisfaction in the presence of bounded disturbances and plant–model mismatch, with emphasis on laboratory and embedded validation. The practical deployment of tube MPC depends on how efficiently the robust invariant sets defining the tube geometry can be computed and represented. A set-based formulation gives a clear geometric interpretation of robustness, but it also relies on offline set operations, in particular Minkowski sums and Pontryagin differences. This chapter demonstrates how these design steps can be handled systematically with the developed MPT+ tool and applied to physical processes, providing the set-based baseline for the implicit and tunable formulations developed in the following chapters.*

*The chapter is structured around two main research contributions. First, Section 3.1 discusses the implementation and experimental validation of rigid tube MPC on a laboratory plate heat exchanger, building on the results published in [17]. This section demonstrates how robust tubes can be used to handle constraints on system states and control inputs in a physical process. Second, Section 3.2 presents the elastic tube MPC implementation and embedded validation, extending the results from [18] to allow for time-varying tube cross-sections that reduce conservatism. Both methodologies discussed in this chapter are supported by MPT+, which streamlines the design, simulation, and implementation of these robust controllers [16].*

## 3.1 Rigid Tube MPC

Rigid tube MPC is the baseline approach for the robust control methods considered in this thesis. It combines a nominal MPC problem with a stabilizing feedback law that keeps the real system state inside a robust positively invariant tube around the nominal trajectory. The main benefit of this construction is a clear and verifiable route to robust constraint satisfaction. A robust tube MPC formulation based on nominal prediction, invariant tubes, and constraint tightening provides the theoretical basis for this construction [38]. Efficient tube-controller variants further clarify how such tubes can be computed and used in constrained control [55].

The formulation considered in this section is the set-based tube MPC problem introduced in Section 2.2.1. The controller is (2.15) together with the feedback law (2.19). Its safety properties follow from the invariant tube construction (2.16), the tightened constraints in (2.15c)–(2.15d), and Assumption 2.3. The contribution considered here is the practical realization of this design in MPT+[1] and its experimental validation on a laboratory plate heat exchanger. MPT+ extends the original MPT workflow from nominal and explicit MPC design toward robust tube MPC synthesis [14]. The software package was introduced as an MPC design and tuning environment in [16]. The user works with the familiar model, constraint, and penalty objects, while the toolbox constructs the tube-related ingredients required by the theory. In this dissertation, the rigid tube case therefore serves as the baseline implementation of the safe-MPC part of the work.

The explicit construction of sets is also the main limitation of this baseline: the tube cross-section and tightened constraints are computed geometrically, which is appropriate for low-dimensional systems but becomes restrictive for larger process models. This motivates the implicit extensions developed later in the thesis.

### 3.1.1 Rigid Tube MPC Implementation in MPT+

The MPT+ implementation was developed to make the workflow in (2.15) available without requiring the user to manually construct all robust sets. The design starts from an MPT-style model definition: the user specifies the matrices $A$, $B$, and $E$, the constraints on system states and control inputs, the disturbance-input set $\mathbb{D}$ and its induced additive set $\mathbb{W} = E\mathbb{D}$, the quadratic penalties, and the prediction horizon. MPT+ then computes or accepts the stabilizing feedback gain, constructs an invariant tube approximation, evaluates the tightened constraints, and returns a controller object

[1] `https://github.com/holaza/mptplus`

that can be simulated or evaluated at measured system states.

MPT+ was introduced as an extension of the MPT3 workflow rather than as a separate modeling environment. The package can be installed through `tbxManager`[2],

```
tbxmanager install mptplus
```

or added manually to the MATLAB path. In both cases, MPT+ depends on MPT3[3] and uses the same modeling objects for uncertain LTI systems, constraints, and quadratic penalties [14]. This is important in the dissertation context because the robust tube ingredients are introduced without changing the modeling layer used for nominal MPC and explicit MPC. The robust controller is constructed by the class `TMPCController`, while the underlying model remains an `ULTISystem`.

This implementation exposes the design parameters that matter in practice: prediction horizon, weights $Q$ and $R$, disturbance-input bounds, and available margins for system states and control inputs. These quantities are the same parameters that were tuned in the heat-exchanger experiment below. The double-integrator benchmark is used as a compact, reproducible construction of the controller object before moving to the laboratory plant. It contains the same robust-design elements as the experimental case: an additive disturbance channel, hard constraints, automatic terminal ingredients, and an inspectable tube. The uncertain LTI system is defined as

$$x_{k+1} = \begin{bmatrix} 1 & 1 \\ 0 & 1 \end{bmatrix} x_k + \begin{bmatrix} 0.5 \\ 1 \end{bmatrix} u_k + \begin{bmatrix} 1 & 0 \\ 0 & 1 \end{bmatrix} d_k, \tag{3.1}$$

with initial condition $x_0 = [-5, -2]^\top$. In MPT+, the model is created as follows:

```
model = ULTISystem('A', [1, 1; 0, 1], 'B', [0.5; 1], 'E', [1, 0; 0, 1]);
x0 = [-5; -2];
```

Here $d_k \in \mathbb{D}$ is the disturbance input and the additive system state disturbance used by the tube construction is $w_k = Ed_k \in \mathbb{W}$. Since the example uses $E = I$, the componentwise bounds entered through `model.d` also describe $\mathbb{W}$. The disturbance-input constraints and the constraints on system states and control inputs are then specified directly on the model object:

```
model.d.min = [-0.1; -0.1];
model.d.max = [ 0.1;  0.1];
```

[2] https://www.tbxmanager.com/
[3] https://www.mpt3.org/

```
model.x.min = [-200; -2];
model.x.max = [ 200;  2];
model.u.min = -1;
model.u.max =  1;
```

The quadratic weights are attached to the variables representing system states and control inputs. The optional parameter `LQRstability` lets MPT+ compute the stabilizing feedback gain, the Lyapunov terminal penalty, and the terminal set automatically. This option provides a direct software realization of the terminal ingredients required in Assumption 2.3:

```
model.x.penalty = QuadFunction([1, 0; 0, 1]);
model.u.penalty = QuadFunction(0.01);
options = {'LQRstability', 1};
N = 9;
```

The rigid tube MPC controller is then constructed and evaluated from the initial system state:

```
iMPC = TMPCController(model, N, options);
u = iMPC.evaluate(x0);
```

For the benchmark data above, the first evaluated control move is $u = 1$, which is the control input applied by the tube feedback law.

For a more detailed inspection of the optimization variables, MPT+ can be asked to return the compact vector containing the optimal nominal control input and nominal initial system state:

```
options = {'LQRstability', 1, 'solType', 0};
iMPC = TMPCController(model, N, options);
ux = iMPC.optimizer(x0);
```

For the presented example, this vector corresponds to

$$\hat{u}_0^\star = 0.7026, \qquad \hat{x}_0^\star = [-5.0516,\ -1.7500]^\top.$$

The difference between `evaluate` and `optimizer` is therefore useful: the former returns the plant control input generated by the tube feedback law, whereas the latter exposes the nominal decision variables of the robust MPC problem.

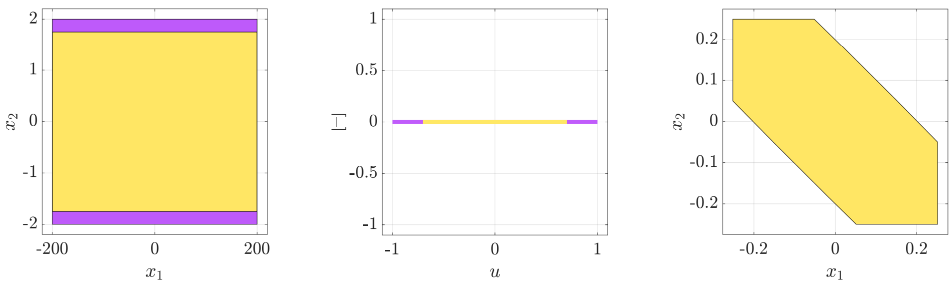


**a)** State sets $\mathbb{X}$ and $\mathbb{X} \ominus \mathbb{T}$. **b)** Input sets $\mathbb{U}$ and $\mathbb{U} \ominus K_{\mathrm{S}}\mathbb{T}$. **c)** Tube cross-section $\mathbb{T}$.

**Figure 3.1:** Designed sets for rigid tube MPC in MPT+ for the double-integrator benchmark: the state and input constraint tightening and the tube cross-section.

The computed tube-design ingredients are also accessible from the controller object. This is useful for analyzing how the robust controller tightens the original constraints. In the benchmark, the stabilizing feedback gain returned by the controller is approximately $K_{\mathrm{S}} = [-0.6609, \ -1.3261]$:

```
K = iMPC.TMPCparams.K;
Tube = iMPC.TMPCparams.Tube;
figure, Tube.plot();

X_tight = iMPC.TMPCparams.Xset;
figure, X_tight.plot();

U_tight = iMPC.TMPCparams.Uset;
figure, U_tight.plot();
```

The plots in Figure 3.1 a)–b) depict the geometric representation of constraint tightening in the rigid tube MPC design enforced by the tube shown in Figure 3.1 c). The constraints on the system state have the form $\mathbb{X} \ominus \mathbb{T}$, and the constraints on the control inputs are given by $\mathbb{U} \ominus K_{\mathrm{S}}\mathbb{T}$. These tightened constraints are considered by the nominal prediction. As can be observed in Figure 3.1 a)–b), the volume of these sets is obviously smaller than the original admissible sets $\mathbb{X}$, $\mathbb{U}$, respectively. Consequently, the tightened sets lead to conservative decision-making, as the tube $\mathbb{T}$ and its image under $K_{\mathrm{S}}$ reserve margins for all admissible disturbances within the extended control law in (2.19). The resulting controller object therefore contains the elements required by the rigid tube MPC design: the stabilizing feedback gain, the invariant tube approximation, and the tightened sets for system states and control inputs. Hence, the software implementation contains the same robust design ingredients used in (2.15), while keeping the controller construction close to the conventional MPT modeling interface.

In addition to constructing and visualizing these tube-design sets, the MPT+ toolbox can generate the corresponding explicit (multi-parametric) tube MPC controller from the implicit MPC controller object. In this mode, the multi-parametric solution is computed offline and stored in the explicit MPC controller object `eMPC`. The explicit controller is generated by converting `iMPC` to its multi-parametric representation, and the corresponding control law can then be evaluated directly:

```
eMPC = iMPC.toExplicit;
u_exp = eMPC.evaluate(x0);
```

The explicit MPC controller object is compatible with the graphical analysis tools inherited from MPT. The feasibility domain, i.e., the polytopic partition, the corresponding piecewise-affine feedback law, and the piecewise-quadratic value function can be visualized by

```
figure; eMPC.partition.plot();
figure; eMPC.feedback.fplot();
figure; eMPC.cost.fplot();
```

The plots in Figure 3.2 are useful when the stored explicit MPC policy has to be inspected or certified before deployment. Figure 3.2 illustrates how the robust tube design is represented after the offline multi-parametric solution, while the evaluated control input `u_exp` is already the final input applied to the controlled plant.

The available constructor options and output fields can be inspected directly in MATLAB by calling

```
help TMPCController
```

which is useful when switching between controller evaluation, optimizer inspection, simulation, and plotting during laboratory tuning.

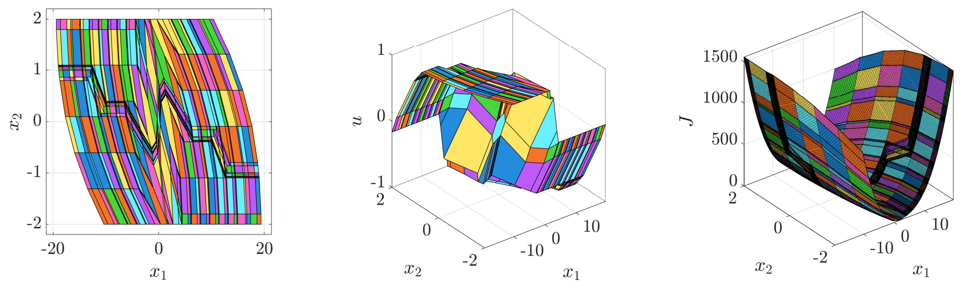


**a)** Polytopic partition. **b)** Piecewise-affine feedback law. **c)** Piecewise-quadratic value function.

**Figure 3.2:** Explicit representation of rigid tube MPC controller generated in MPT+: critical-region partition, feedback law, and value function.

### 3.1.2 Experimental Validation on a Laboratory Heat Exchanger

The rigid tube MPC workflow was validated on the Armfield PCT23 laboratory plate heat exchanger depicted in Figure 3.3. The plant consists of a three-stage indirect liquid-liquid plate heat exchanger, cold-medium retention tanks, a hot-medium tank, and two peristaltic pumps. The hot medium is preheated to 60 °C by an auxiliary proportional controller with gain 0.2. During the MPC experiment, the cold-medium flow is kept constant, the hot-water pump is the manipulated control input, and the controlled output is the outlet temperature of the cold medium. The process is nonlinear and asymmetric: heating and cooling responses do not have the same effective dynamics. This makes the setup useful for testing whether a robust MPC design can tolerate modeling mismatch while respecting physical limits on the control input.

The plant was identified from experimental data and represented by an augmented linear discrete-time model

$$A = \begin{bmatrix} 0.5897 & 0 \\ 3 & 1 \end{bmatrix}, \qquad B = \begin{bmatrix} 0.0426 \\ 0 \end{bmatrix}, \qquad E = \begin{bmatrix} 1 & 0 \\ 0 & 1 \end{bmatrix}. \tag{3.2}$$

The sampling time was $T_\mathrm{s} = 3\,\mathrm{s}$. The identified dominant time constant was approximately $T = 341\,\mathrm{s}$, which led to the prediction horizon $N = 60$. The disturbance bound was set to $w_\mathrm{max} = 0.8$ to account for measurement noise and residual nonlinear effects. The integral state in the prediction model provides offset-free tracking, following the conventional disturbance-compensation logic of offset-free MPC [45]. The reference

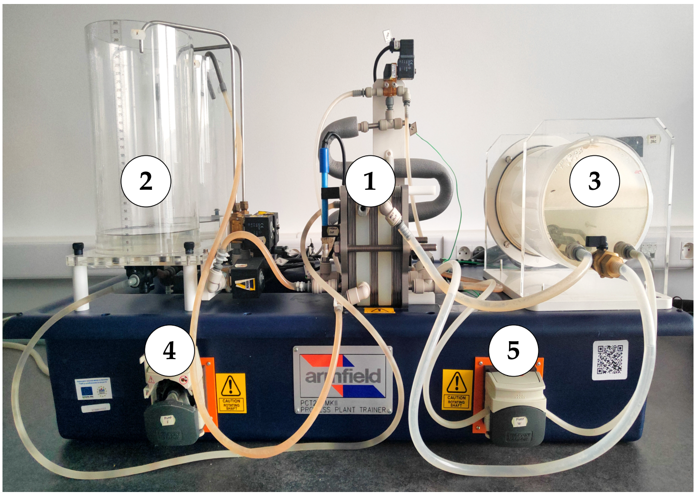


**Figure 3.3:** Laboratory plate heat exchanger used for rigid tube MPC validation: (1) heat exchanger, (2) cold medium tank, (3) hot medium tank, (4) cold medium pump, and (5) hot medium pump.

sequence 30 °C → 35 °C → 40 °C → 35 °C was used to evaluate both heating and cooling behavior.

Two settings for constraints on control inputs were investigated in deviation variables. The tighter setting,

$$-30 \leq u(t) \leq 20, \tag{3.3}$$

corresponds to operating the hot-medium pump within approximately 5 %–55 %. The relaxed setting,

$$-35 \leq u(t) \leq 50, \tag{3.4}$$

extends the admissible range to approximately 0 %–85 %. The quadratic tuning used in the experiment was

$$Q = \begin{bmatrix} 0.1 & 0 \\ 0 & 10 \end{bmatrix}, \qquad R = 150. \tag{3.5}$$

The smaller weight on the system state tunes the thermal response aggressiveness, while the larger weight penalizes the integral state responsible for offset-free behavior. The penalty on the control input was selected with the resource use of the hot medium in mind, not only the settling time. The laboratory implementation used the eLab interface for plant communication. The implementation was carried out in MATLAB

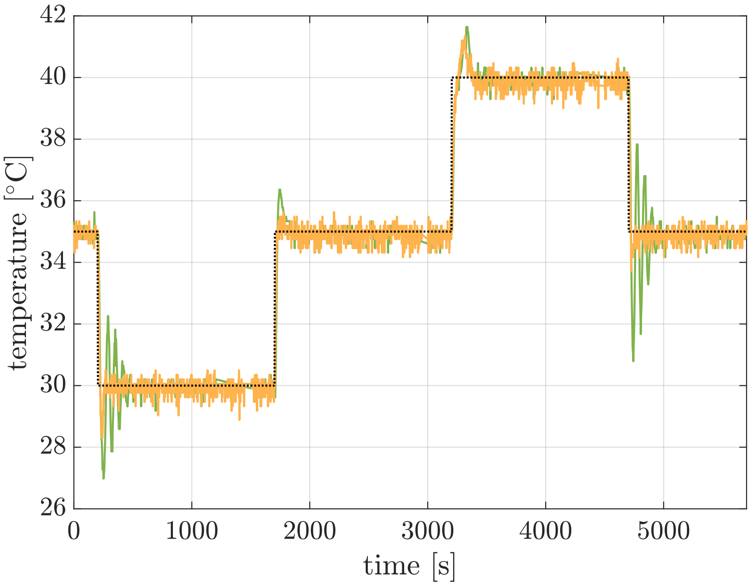


**Figure 3.4:** Measured outlet-temperature response of the laboratory heat exchanger under rigid tube MPC.

R2022b with YALMIP R20210331, MPT 3.2.1, MPT+, and Gurobi 10.0 on an i7 1.2 GHz CPU with 16 GB RAM.

The measured trajectories are depicted in Figures 3.4 and 3.5. The relaxed constraints on control inputs give faster temperature settling because the controller can use more actuator authority. The tighter setting is less aggressive and may require more time to reach the new operating point, but it also gives a more conservative use of the pump. The measured temperature was processed by a first-order discrete-time filter with time

**Table 3.1:** Rigid tube MPC performance on the heat exchanger with relaxed constraints on control inputs.

| Reference step | $t_\epsilon$ [s] | $e_{\max}$ [%] | $V$ [L] | $E$ [kJ] |
|---|---|---|---|---|
| $35 \to 30\,°\mathrm{C}$ | 55 | 62 | 3.9 | 621 |
| $30 \to 35\,°\mathrm{C}$ | 22 | 33 | 4.6 | 725 |
| $35 \to 40\,°\mathrm{C}$ | 130 | 43 | 5.7 | 881 |
| $40 \to 35\,°\mathrm{C}$ | 40 | 43 | 5.2 | 810 |

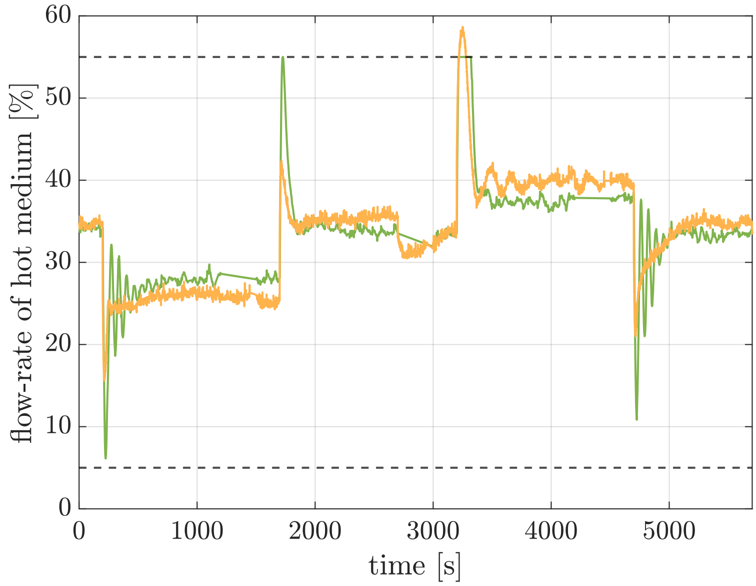


**Figure 3.5:** Measured hot-medium pump actuation under rigid tube MPC.

constant $T_{\mathrm{f}} = 0.5\,\mathrm{s}$ before being supplied to the controller, while the figures depict the measured plant trajectory.

The experimental comparison was evaluated using settling time $t_\epsilon$, maximum overshoot $e_{\max}$, consumed volume of hot medium $V$, and the corresponding energy demand $E$. The numerical values are reported in Tables 3.1 and 3.2. The relaxed constraints reduced overshoot and improved output tracking during the reported temperature steps, but this improvement was achieved by using more hot medium, thereby requiring more energy. The rigid tube MPC study is therefore not only a software demonstration.

**Table 3.2:** Rigid tube MPC performance on the heat exchanger with tight constraints on control inputs.

| Reference step | $t_\epsilon$ [s] | $e_{\max}$ [%] | $V$ [L] | $E$ [kJ] |
|---|---|---|---|---|
| $35 \to 30\,^\circ\mathrm{C}$ | 193 | 171 | 4.0 | 632 |
| $30 \to 35\,^\circ\mathrm{C}$ | 70 | 73 | 4.7 | 733 |
| $35 \to 40\,^\circ\mathrm{C}$ | 160 | 55 | 5.5 | 844 |
| $40 \to 35\,^\circ\mathrm{C}$ | 181 | 241 | 4.9 | 771 |

It indicates that robust constraint handling, actuator margins, and energy use are coupled tuning decisions, and that MPT+ makes these decisions accessible through the same controller object used for simulation and experimental evaluation.

## 3.2 Elastic Tube MPC

Rigid tube MPC considers one fixed cross-section $\mathbb{T}$ in (2.16) along the whole prediction horizon. This construction is robust and conceptually simple, but it may be conservative because the uncertainty allowance is the same at every prediction step, independently of the local margins for system states and control inputs and of disturbance amplification. Elastic tube MPC extends the tube-based design space by allowing a less rigid description of the predicted uncertainty propagation. In this formulation, the fixed-geometry assumption is relaxed by optimizing a tube-size parameter together with the nominal tube center, so that the tube size can adapt to local conditions, such as varying disturbance amplification or different margins for system states and control inputs [59].

Consider the uncertain LTI system in (2.10) with additive disturbance and the rigid tube MPC formulation in (2.15). Elastic tube MPC preserves the same overall structure as rigid tube MPC, but replaces the fixed tube cross-section $\mathbb{T}$ in (2.16) with an elastic tube template that can be scaled along the prediction horizon.

Let the normalized tube template be the polytope

$$\mathcal{S}(\mathbf{1}) = \{s \in \mathbb{R}^n \mid H_{\mathrm{S}} s \leq \mathbf{1}\}, \tag{3.6}$$

where $H_{\mathrm{S}} \in \mathbb{R}^{q_{\mathrm{S}} \times n}$, and $q_{\mathrm{S}}$ is the number of tube-template inequalities. Instead of using only the fixed set $\mathcal{S}(\mathbf{1})$, an elastic tube scales the individual inequalities through scaling parameters $a_k \in \mathbb{R}^{q_{\mathrm{S}}}_{\geq 0}$:

$$\mathcal{S}(a_k) = \{s \in \mathbb{R}^n \mid H_{\mathrm{S}} s \leq a_k\}. \tag{3.7}$$

The vector $a_k$ is therefore part of the optimization variables. Values $a_k > \mathbf{1}$ locally expand the tube cross-section, whereas smaller admissible values represent a contraction.

The predicted tube for system states and the corresponding tube for control inputs are written as

$$X_k = z_k \oplus \mathcal{S}(a_k), \tag{3.8a}$$

$$U_k = v_k \oplus K_{\mathrm{S}} \mathcal{S}(a_k), \tag{3.8b}$$

where $z_k$ is the center of the tube for system states and $v_k$ is the center of the tube for control inputs. The associated feedback control law is

$$u_k = \pi(x_k, z_k, v_k, a_k) := v_k + K_{\mathrm{S}}(x_k - z_k), \qquad x_k \in z_k \oplus \mathcal{S}(a_k). \tag{3.9}$$

This has the same structure as the rigid tube feedback law in (2.19), but the admissible deviation $x_k - z_k$ now belongs to the optimized set $\mathcal{S}(a_k)$ rather than to a fixed set $\mathbb{T}$.

The tube-propagation constraint is obtained by applying (2.10) to all system states in $X_k$, all control inputs generated by (3.9), and all disturbances in $\mathbb{W}$. With $A_{\mathrm{K}} := A + BK_{\mathrm{S}}$, robust one-step propagation requires

$$Az_k + Bv_k - z_{k+1} + A_{\mathrm{K}}\mathcal{S}(a_k) \oplus \mathbb{W} \subseteq \mathcal{S}(a_{k+1}). \tag{3.10}$$

Using the row-wise support-function representation already introduced in (2.18), this inclusion can be written as linear inequalities. Define

$$d_{\mathrm{W},i} = \mathrm{h}\left(\mathbb{W}, H_{\mathrm{S},i}^{\top}\right), \qquad i = 1, \dots, q_{\mathrm{S}}, \tag{3.11}$$

and let $L_{\mathrm{S}} \geq 0$ satisfy

$$L_{\mathrm{S}} H_{\mathrm{S}} = H_{\mathrm{S}} A_{\mathrm{K}}. \tag{3.12}$$

Then (3.10) is enforced by

$$H_{\mathrm{S}}(Az_k + Bv_k - z_{k+1}) + L_{\mathrm{S}} a_k + d_{\mathrm{W}} \leq a_{k+1}. \tag{3.13}$$

The nonnegative matrix $L_{\mathrm{S}}$ bounds the image of the elastic cross-section under $A_{\mathrm{K}}$, while $d_{\mathrm{W}}$ accounts for the additive disturbance set in (2.11).

To connect the elastic tube to the hard constraints in (2.12), consider a separated normalized description

$$\mathbb{X} = \{x \in \mathbb{R}^n \mid Gx \leq \mathbf{1}\}, \tag{3.14a}$$
$$\mathbb{U} = \{u \in \mathbb{R}^m \mid Hu \leq \mathbf{1}\}. \tag{3.14b}$$

Let $M_{\mathrm{X}} \geq 0$ and $M_{\mathrm{U}} \geq 0$ satisfy

$$M_{\mathrm{X}} H_{\mathrm{S}} = G, \tag{3.15a}$$
$$M_{\mathrm{U}} H_{\mathrm{S}} = HK_{\mathrm{S}}. \tag{3.15b}$$

The robust constraints on system states and control inputs are then imposed through

$$Gz_k + M_{\mathrm{X}} a_k \leq \mathbf{1}, \tag{3.16a}$$
$$Hv_k + M_{\mathrm{U}} a_k \leq \mathbf{1}. \tag{3.16b}$$

These inequalities are the elastic analog of the rigid tightened constraints in (2.15c)–(2.15d). If $\mathcal{S}(\mathbf{1})$ is chosen as the rigid tube cross-section and $a_k = \mathbf{1}$ is fixed, the elastic constraint tightening reduces to the fixed-cross-section interpretation used by rigid tube MPC.

Let

$$\epsilon = \{z_0, \dots, z_N,\ v_0, \dots, v_{N-1},\ a_0, \dots, a_N\}$$

collect the elastic tube decision variables. The elastic tube MPC problem can then be written as

$$\begin{aligned}
\min_{\epsilon} \quad & V_{\mathrm{f}}(z_N, a_N) + \sum_{k=0}^{N-1} \ell(z_k, v_k, a_k) && \text{(3.17a)}\\
\text{s.t.} \quad & H_{\mathrm{S}}(x(t) - z_0) \leq a_0, && \text{(3.17b)}\\
& a_k \geq 0, && \text{(3.17c)}\\
& H_{\mathrm{S}}(Az_k + Bv_k - z_{k+1}) + L_{\mathrm{S}} a_k + d_{\mathrm{W}} \leq a_{k+1}, && \text{(3.17d)}\\
& Gz_k + M_{\mathrm{X}} a_k \leq \mathbf{1}, && \text{(3.17e)}\\
& Hv_k + M_{\mathrm{U}} a_k \leq \mathbf{1}, && \text{(3.17f)}\\
& (z_N, a_N) \in \Phi_{\mathrm{f}}, && \text{(3.17g)}\\
& k = 0, 1, \dots, N-1. && \text{(3.17h)}
\end{aligned}$$

The initial condition (3.17b) enforces $x(t) \in z_0 \oplus \mathcal{S}(a_0)$. Constraint (3.17d) enforces robust tube propagation for all $w_k \in \mathbb{W}$. Constraints (3.17e) and (3.17f) impose robust satisfaction of constraints on system states and control inputs. Finally, $\Phi_{\mathrm{f}}$ is a terminal set in the lifted $(z, a)$ coordinates. It plays the same role as $\mathbb{X}_{\mathrm{N}}$ in Assumption 2.3, but now includes both the terminal tube center and the terminal tube size. For a scalar tube-size parametrization, this lift adds only one additional coordinate to the nominal state.

A common quadratic objective is

$$\begin{aligned}
V_{\mathrm{f}}(z_N, a_N) &= z_N^\top P_{\mathrm{z}} z_N + (a_N - \mathbf{1})^\top P_{\mathrm{a}} (a_N - \mathbf{1}), && \text{(3.18a)}\\
\ell(z_k, v_k, a_k) &= z_k^\top Q_{\mathrm{z}} z_k + v_k^\top Q_{\mathrm{v}} v_k + (a_k - \mathbf{1})^\top Q_{\mathrm{a}} (a_k - \mathbf{1}), && \text{(3.18b)}
\end{aligned}$$

with positive definite weights of compatible dimensions. Penalizing $(a_k - \mathbf{1})$ discourages unnecessary tube expansion while still allowing the controller to enlarge the tube when required for robust feasibility. Consequently, elastic tube MPC retains the robust constraint-satisfaction principles of tube MPC but reduces conservatism by adapting the tube cross-section along the prediction horizon.

### 3.2.1 Elastic Tube MPC Implementation in MPT+

The elastic tube MPC [59] module extends the analogous MPT+ workflow used for rigid tube MPC into an end-to-end design and analysis procedure. The user defines the uncertain system, constraints, disturbance-input set, cost weights, and prediction horizon, and selects the elastic tube option. The MPT+ extension presented in [18] then formulates the elastic tube propagation constraints, computes the stabilizing feedback gain, constructs the terminal ingredients, and returns a controller object that can be evaluated, simulated, and inspected from a measured system state. The implementation also computes the nontrivial matrices associated with elastic tube propagation, so the design task exposed to the user remains comparable to the rigid cases.

The elastic tube MPC implementation is illustrated on the disturbed double-integrator model:

```
model = ULTISystem('A', [1, 1; 0, 1], ...
                   'B', [0.5; 1], ...
                   'E', [1, 0; 0, 1]);
```

The constraints on system states, control inputs, and disturbance inputs are imposed by

```
model.x.min = [-200; -2];
model.x.max = [ 200;  2];
model.u.min = -1;
model.u.max =  1;
model.d.min = [-0.1; -0.1];
model.d.max = [ 0.1;  0.1];
```

The cost weights are selected in the same modeling style as for the rigid controller:

```
model.x.penalty = QuadFunction(eye(2));
model.u.penalty = QuadFunction(0.01);
```

The finite prediction horizon is set to $N = 9$, and the elastic controller is constructed by selecting the elastic tube type:

```
N = 9;
options = {'TubeType', 'elastic'};
ETMPC = TMPCController(model, N, options);
```

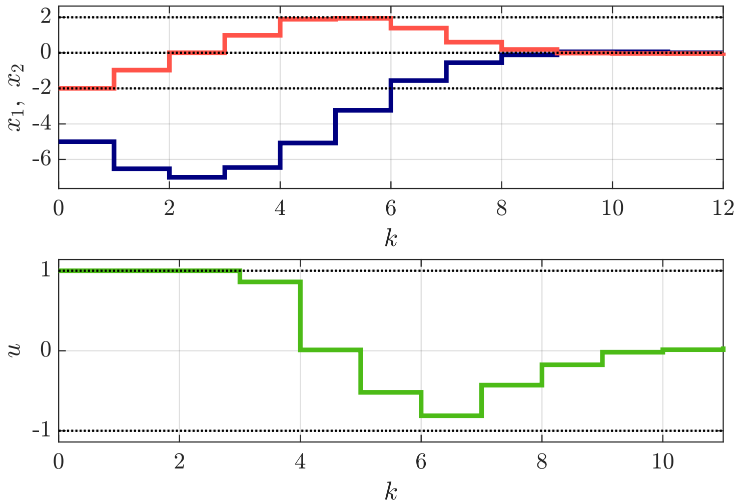


**Figure 3.6:** Elastic tube MPC closed-loop system trajectories for the disturbed double-integrator benchmark. The upper subplot depicts the system states $x_1$ (dark blue) and $x_2$ (red), while the lower subplot depicts the control input $u$ (green). Black dashed and dash-dotted lines denote the upper and lower constraints.

For the initial condition $x_0 = [-5,\ -2]^\top$, the first control action and a finite closed-loop system simulation are obtained by

```
x0 = [-5; -2];
u0 = ETMPC.evaluate(x0);

Nsim = 12;
ClosedLoopData = ETMPC.simulate(x0, Nsim);
```

The result object stores the simulated system states in `ClosedLoopData.X`. It stores the simulated control inputs in `ClosedLoopData.U`. The simulated trajectory is used to verify stable closed-loop behavior and satisfaction of the hard constraints imposed on the double-integrator benchmark. MPT+ also provides a dedicated visualization tool for the elastic tube propagation:

```
ETMPC.plotTube('ClosedLoop', true);
```

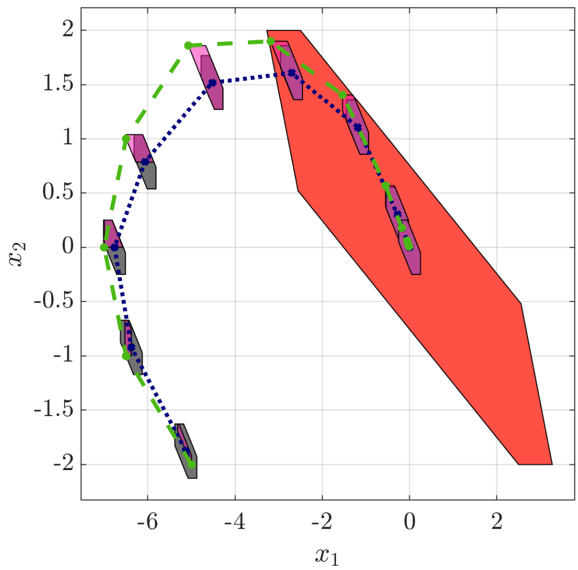


**Figure 3.7:** Closed-loop elastic tube MPC with time-varying tube $\mathcal{S}(a_k)$ (transparent purple), uncertain system states (green stars), nominal system states (dark blue crosses), the corresponding rigid tube (gray), and the terminal set (red).

This command visualizes how the tube cross-section $\mathcal{S}(a_k)$ expands and contracts along the trajectory. The resulting plot makes the conservatism of the robust controller inspectable and therefore tunable. Figures 3.6 and 3.7 illustrate the typical simulation output. The controller propagates the tube along the predicted trajectory and adapts its cross-section through the elasticity parameter. Compared with a fixed rigid tube, this gives a more informative design object: the user can inspect where uncertainty requires a larger margin and where the tube contracts because the predicted system state is safely inside the admissible region. The adaptive tube therefore preserves the robustness role of tube MPC while reducing the conservatism associated with a fixed cross-section.

### 3.2.2 Laboratory Case Study of Embedded Heat Exchanger

The elastic tube MPC workflow was validated on the Sensoric Shi-3-ld compact heat-exchanger platform associated with the Optimal Control Labs (OCL) material[4] and driven by an ESP32-S3 microcontroller [3]. The thermal module contains a $47\,\Omega$ heating resistor and an analog temperature sensor. The controlled variable is the measured temperature deviation, and the manipulated variable is the heater power in percent applied through a PWM signal. The platform has low-order but experimentally relevant thermal dynamics: the measured temperature is affected by sensor noise and ambient airflow, and the control input is constrained by the physical range of the heater.

The Sensoric Shi-3-ld board is compatible with the ESP32-S3-DevKitC-1 module. In the experiments considered in this dissertation, the board is equipped with an ESP32-S3-DEVKITC-1-N32R8V microcontroller. The microcontroller provides a 32-bit Xtensa LX7 processor running at 240 MHz, 32 MB of flash storage, 512 kB of SRAM, and 8 MB of PSRAM. The temperature is measured by a TC1047A analog sensor placed close to the heating resistor. The ESP32-S3 regulates the heating power by PWM actuation through a transistor, while thermal paste improves the heat transfer between the resistor and the sensor. At the maximum PWM duty cycle, the resistor reaches approximately 45 °C.

The control loop is depicted in Figure 3.8. The MPC computation is performed off-board, while the embedded board handles measurement and actuation through PWM. In the validation experiments, the MPC computation was performed in MATLAB and the robust MPC law was modified, tuned, and tested in MPT+. For the experimental run, the designed tube MPC law was generated in explicit form, so the online controller evaluation reduced to selecting and evaluating the corresponding precomputed feedback law. The same workflow can later be moved closer to the embedded target because MPT+ supports C++ and Python export of the resulting controller. This split is appropriate for controller validation, because the physical device provides real disturbances and hardware constraints.

The experimental model was obtained by exciting the system with a sequence of control input changes that covered both heating and cooling phases, followed by least-squares identification of the discrete-time step-response data. With sampling time $T_{\mathrm{s}} = 0.5\,\mathrm{s}$, the identified first-order model is

$$A = 0.96, \qquad B = 0.03, \qquad C = 1. \tag{3.19}$$

[4] `https://ocl.sk/`

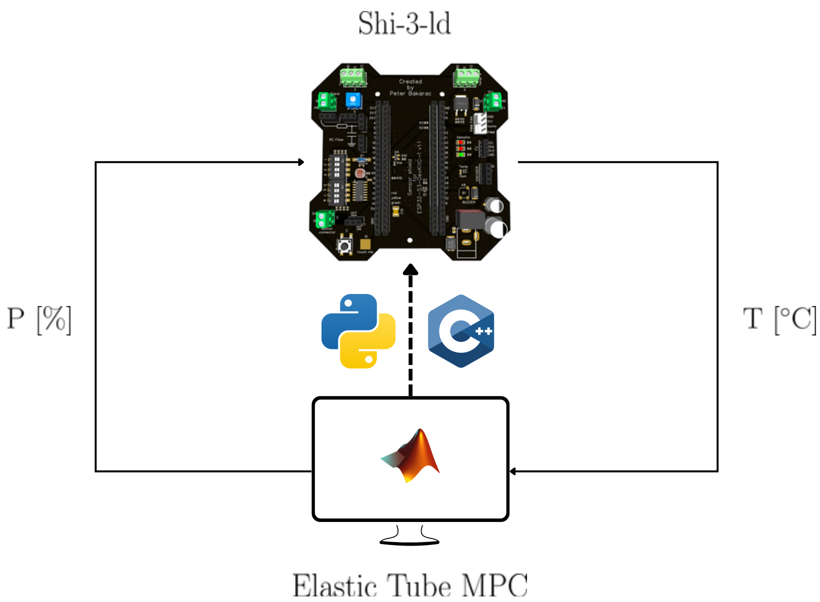


**Figure 3.8:** Laboratory setup of elastic tube MPC control loop for the compact heat-exchanger platform.

The disturbance matrix is $E = 1$, so the disturbance input and additive system state disturbance coincide. Ambient fluctuations, airflow, sensor noise, and residual modeling errors are represented by the disturbance-input set

$$\mathbb{D} = \{d \in \mathbb{R} \mid -0.1 \leq d \leq 0.1\}, \qquad \mathbb{W} = E\mathbb{D}. \tag{3.20}$$

The physical constraints on system states and control inputs are

$$20 \leq x(t) \leq 45\,^{\circ}\mathrm{C}, \qquad 0 \leq u(t) \leq 100\,\%. \tag{3.21}$$

The controller was constructed with prediction horizon $N = 10$ and scalar penalty factors $Q_{\mathrm{x}} = 70$ and $Q_{\mathrm{u}} = 1$. All feedback, terminal, and tube-propagation quantities were computed by MPT+.

In the experiment, the elastic tube MPC controller drives the temperature to the reference while keeping the heater control input within its admissible range, as depicted in Figure 3.9. From the initial deviation $x_0 = 0.2\,^{\circ}\mathrm{C}$, the measured temperature reached the reference $y_{\mathrm{ref}} = 31.6\,^{\circ}\mathrm{C}$ in approximately 10 s. During the initial interval of roughly 0–6 s, the actuator reached its upper bound. Afterward, the controller maintained the reference with only small fluctuations consistent with sensor noise and ambient

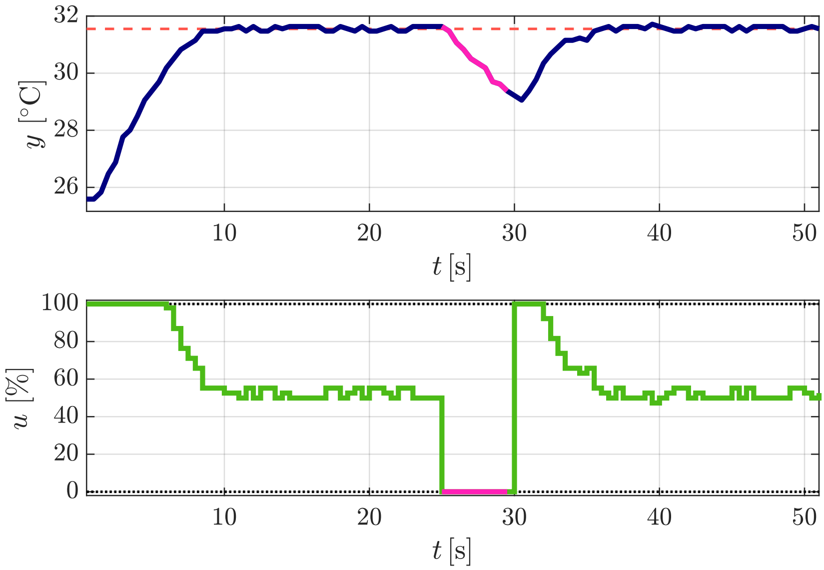


**Figure 3.9:** Experimental embedded heat-exchanger response under elastic tube MPC. The upper subplot depicts the reference $y_{\mathrm{ref}}$ (red dashed) and measured temperature $y$ (dark blue), while the lower subplot depicts heater actuation $u$ (green), constraints on the control input $0 \leq u \leq 100\,\%$ (black dotted), and the forced zero-input interval (magenta).

airflow. A temporary zero-input interval was introduced at $t = 25\,\mathrm{s}$ for $5\,\mathrm{s}$ to emulate an actuation disruption. Once the controller regained authority at $t = 30\,\mathrm{s}$, it recovered the reference in approximately $5\,\mathrm{s}$ without redesign or retuning. The measured response confirms that the controller respects constraints on the control input, compensates for ambient disturbances and modeling mismatch, and maintains the temperature with modest actuation once the reference is reached.

## 3.3 Discussion

This chapter has presented implementation-oriented set-based tube MPC strategies for constrained systems. The main emphasis was placed on formulations that preserve constraint satisfaction under bounded disturbances while remaining usable in reproducible software and experimental settings. Rigid tube MPC was implemented in MPT+ and validated on a laboratory plate heat exchanger, where the results quantify the effect of constraint tightening on tracking performance and energy demand.

The elastic tube MPC implementation extends the same MPT+ workflow by allowing the tube cross-section to vary along the prediction horizon. This reduces the conservatism of a fixed tube while keeping the robust tube interpretation. The embedded validation on a compact heat-exchanger platform showed input-constraint satisfaction and recovery after a forced zero-input interval, confirming that tube-based robust control can be moved from software design to experimentally constrained hardware.

The experimental results also highlight the practical boundary of set-based methods. Their strength is the combination of safety guarantees and geometric clarity: the tube, tightened constraints, and invariant sets have a direct interpretation. At the same time, this explicit representation becomes the main computational limitation. The offline computation of Minkowski differences, invariant sets, and tightened constraints becomes increasingly demanding for higher-dimensional systems or for systems with more complex constraint structures.

This scalability bottleneck motivates the transition to implicit tube formulations in the following chapters. The aim is to retain the robust constraint-handling objective of set-based tube MPC, while avoiding the need to explicitly construct all tube-related sets. This provides a natural bridge from the laboratory-scale set-based implementations studied here to larger process models where traditional set operations are no longer computationally practical.

Chapter 4

# Implicit Tube MPC for Large-Scale Systems

---

*This chapter focuses on implicit tube MPC as a scalable alternative to the set-based formulations investigated in Chapter 3. The motivation comes from the practical limitation of explicit set operations: while they provide a clear geometric interpretation of robustness, their use becomes increasingly demanding as the system dimension and constraint complexity grow. The implicit formulation replaces these set operations by auxiliary variables and support-function inequalities while preserving robust constraint satisfaction. This chapter demonstrates how the resulting design can be connected with the MPT+ workflow and applied to simulation, laboratory, and industrially oriented case studies, providing the scalable counterpart to the set-based formulations developed in Chapter 3.*

*The chapter is structured around three main research contributions. First, Sections 4.1 and 4.2 discuss the implicit rigid tube MPC formulation based on [56] and its implementation in MPT+. Second, Sections 4.3 and 4.4 validate the implementation on a large-scale reactor-separator benchmark, following the results presented in [49], and on the laboratory smart greenhouse VESNA, building on [41], [51], and [48]. Third, Section 4.5 presents the offset-free implicit tube MPC design, tuning, and implementation for the hybrid heat-integrated distillation system published in [50]. This industrially oriented case study combines robust tube-based constraint handling with offset-free tracking and evaluates the controller's ability to compensate for plant–model mismatch, remove steady-state offsets, and maintain energy-aware operation*

## 4.1 Formulation of Implicit Tube MPC

The explicit formulation (2.15) requires the tube cross-section (2.16) and the tightened constraints to be constructed through set-based operations. Consequently, the application range of the set-based tube MPC is restricted only to the systems with modest complexity. On the other hand, in implicit rigid tube MPC, these operations are replaced by auxiliary variables and support-function inequalities while preserving the same robust MPC guarantees [56].

The initial explicit set-based tube membership $x(t) - \hat{x}_0 \in \mathbb{T}$ is now represented implicitly through auxiliary variables $\omega_j \in \mathbb{R}^n$, $j = 0, \ldots, N_\mathrm{S} - 1$, satisfying the disturbance-set constraints. The realized implicit tube deviation $\mathcal{T} \in \mathbb{R}^n$ is

$$\mathcal{T} = (1-\alpha)^{-1} \sum_{j=0}^{N_\mathrm{S}-1} (A + BK_\mathrm{S})^j \omega_j. \tag{4.1}$$

For normalized constraints on system states and control inputs $c_l^\top x + d_l^\top u \leq 1$, $l = 1, \ldots, N_\mathrm{C}$, with $c_l \in \mathbb{R}^n$, $d_l \in \mathbb{R}^m$, and $N_\mathrm{C}$ denoting the number of normalized constraints on system states and control inputs, the tightened constraints can be written using the vector $f \in \mathbb{R}^{N_\mathrm{C}}$ with components

$$f_l = (1-\alpha)^{-1} \sum_{j=0}^{N_\mathrm{S}-1} \mathrm{h}\left(\mathbb{W}, \left((A + BK_\mathrm{S})^j\right)^\top \eta_l\right), \tag{4.2a}$$

$$\eta_l = c_l + K_\mathrm{S}^\top d_l, \qquad l = 1, 2, \ldots, N_\mathrm{C}. \tag{4.2b}$$

Then, the explicit tightened constraints and their implicit representation are equivalent in the following sense:

$$(\hat{x}_k \times \hat{u}_k) \in ((\mathbb{X} \ominus \mathbb{T}) \times (\mathbb{U} \ominus K_\mathrm{S}\mathbb{T})), \tag{4.3a}$$

$$c_l^\top \hat{x}_k + d_l^\top \hat{u}_k \leq 1 - f_l, \qquad l = 1, 2, \ldots, N_\mathrm{C}. \tag{4.3b}$$

The corresponding implicit tube MPC problem is

$$\min_{\substack{\hat{x}_0, \hat{u}_0, \omega_0, \ldots \\ \hat{u}_{N-1}, \hat{x}_N, \omega_{N_\mathrm{S}-1}}} \quad \hat{x}_N^\top P \hat{x}_N + \sum_{k=0}^{N-1} \left( \hat{x}_k^\top Q \hat{x}_k + \hat{u}_k^\top R \hat{u}_k \right) \tag{4.4a}$$

$$\begin{aligned}
\text{s.t.} \quad & \hat{x}_{k+1} = A\hat{x}_k + B\hat{u}_k, && (4.4\mathrm{b}) \\
& c_l^\top \hat{x}_k + d_l^\top \hat{u}_k \leq 1 - f_l, && (4.4\mathrm{c}) \\
& \left( c_l^\top + d_l^\top K_\mathrm{S} \right) \hat{x}_N \leq 1 - f_l, && (4.4\mathrm{d}) \\
& x(t) - \hat{x}_0 = \mathcal{T}, && (4.4\mathrm{e}) \\
& e_i^\top \omega_j \leq 1, && (4.4\mathrm{f}) \\
& i \in \mathcal{I}_\mathrm{W}, && (4.4\mathrm{g}) \\
& j = 0, 1, \ldots, N_\mathrm{S} - 1, && (4.4\mathrm{h}) \\
& k = 0, 1, \ldots, N - 1, && (4.4\mathrm{i}) \\
& l = 1, 2, \ldots, N_\mathrm{C}. && (4.4\mathrm{j})
\end{aligned}$$

The decision variables $\omega_j$ encode the admissible disturbance sequence that realizes the tube membership condition. The feedback control law remains the same and has the form (2.19). Thus, the implicit formulation is equivalent to the explicit rigid tube MPC formulation in terms of robustness, recursive feasibility, and stability, but avoids explicit Minkowski sums and Pontryagin differences in the offline problem construction.

The main differences between the set-based and implicit rigid tube MPC formulations are summarized in Table 4.1. In the offline phase, set-based tube MPC constructs the tube set and the tightened constraint sets explicitly. This construction relies on set operations, in particular Minkowski sums and Pontryagin differences, which become limiting for larger-scale systems. The implicit formulation addresses this limitation by replacing explicit set construction with support-function values and an implicit tube description. This extends the applicability of tube MPC to systems for which the explicit set-based construction becomes computationally intractable. On the other hand, the resulting online optimization problem of implicit tube MPC has a larger number of decision variables, since the auxiliary disturbance variables $\omega_j$, $j = 0, \ldots, N_\mathrm{S} - 1$, are optimized in addition to the nominal states and inputs.

The formulation proposed in [56] is the algebraic realization of the same rigid tube design summarized in Section 4.1. Instead of constructing $\mathbb{T}$ and the Pontryagin differences explicitly, it uses the auxiliary tube realization (4.1), the tightening vector (4.2), and the optimization problem (4.4). The safety interpretation is preserved: the nominal predictions are constrained so that the disturbed plant remains inside the admissible tube for all $w \in \mathbb{W}$.

**Table 4.1:** Comparison of set-based and implicit rigid tube MPC formulations.

<table>
<tr><th></th><th>Set-Based Tube MPC</th><th>Implicit Tube MPC</th></tr>
<tr><td>Tube</td><td>Static RPI convex set<br>$\mathbb{T} \subset \mathbb{X}$</td><td>Tube encoded by dynamic vector<br>$\mathcal{T} \in \mathbb{R}^n$</td></tr>
<tr><td>Offline construction</td><td>• determine $K_{\mathrm{S}}$, $N_{\mathrm{S}}$, and $\alpha$;<br>• construct the tube set $\mathbb{T}$;<br>• compute tightened sets using Minkowski sums and Pontryagin differences.</td><td>• determine $K_{\mathrm{S}}$, $N_{\mathrm{S}}$, and $\alpha$;<br>• compute support-function values and the shrinking vector $f_l$;<br>• avoid explicit construction of sets.</td></tr>
<tr><td>Online control</td><td>Optimized variables:<br>$\hat{x}_k, \hat{u}_k, \quad k = 0, \ldots, N-1$<br>Inequality constraints:<br>$x(t) - \hat{x}_0 \in \mathbb{T}$</td><td>Optimized variables:<br>$\hat{x}_k, \hat{u}_k, \quad k = 0, \ldots, N-1$<br>$\omega_j, \quad j = 0, \ldots, N_{\mathrm{S}} - 1$<br>Equality constraints:<br>$x(t) - \hat{x}_0 = \mathcal{T}$</td></tr>
</table>

The main benefit of implicit tube MPC design is that this approach addresses the computational limitations of set-based rigid tube MPC. Instead of explicitly constructing the tube cross-section and performing geometric set-based operations offline, the tube membership and constraint tightening are encoded through auxiliary variables and support-function-based conditions online.

## 4.2 Implicit Tube MPC Implementation in MPT+

The practical contribution of the implicit tube MPC MPT+ work is to make this formulation applicable for systems for which explicit robust set construction is numerically prohibitive. MPT+ implements implicit tube MPC as a controller option within the same user-friendly workflow used for rigid tube MPC. The model, constraints, disturbance-input set, penalty matrices, and horizon in (4.4) are provided in the usual way. The user then selects the implicit tube type, and MPT+ computes the stabilizing feedback gain, terminal ingredients, tube approximation parameters, and constraint tightening terms. The option `LQRstability` again delegates the computation of the LQ feedback, terminal penalty, and terminal set to the toolbox, which is important because the implicit formulation is otherwise algebraically heavier than the set-based rigid tube implementation.

From the user perspective, this is a convenient interface change. From the numerical perspective, it changes the class of systems that can be handled. The MPT+ toolbox no longer needs to explicitly construct high-dimensional tube sets or perform Minkowski and Pontryagin operations on them. The same robust safety interpretation is retained, but the computational burden is shifted from offline explicit geometry to online auxiliary variables and linear inequalities in a convex optimization problem that can be parsed and solved with conventional optimization tools handling QPs.

The implementation workflow is first demonstrated on the same double-integrator model as in (3.1), now with wider bounds on system states. The model and initial condition are defined by

```
model = ULTISystem('A', [1, 1; 0, 1], ...
                              'B', [0.5; 1], ...
                              'E', [1, 0; 0, 1]);
x0 = [-5; -2];
```

The constraints and disturbance-input bounds are specified as

```
model.x.min = [-200; -2];
model.x.max = [ 200;  2];
model.u.min = -1;
model.u.max =  1;
model.d.min = [-0.1; -0.1];
model.d.max = [ 0.1;  0.1];
```

The penalty matrices are again assigned through quadratic functions:

```
model.x.penalty = QuadFunction([1, 0; 0, 1]);
model.u.penalty = QuadFunction(0.01);
```

The key change is the option `TubeType`. Setting it to `implicit` instructs MPT+ to construct the implicit tube formulation instead of the rigid set-based tube:

```
options = {'TubeType', 'implicit', ...
                'LQRstability', 1};
N = 9;
```

The controller construction and evaluation are then identical from the user side:

```
implicit_MPC = TMPCController(model, N, options);
u = implicit_MPC.evaluate(x0);
```

Closed-loop simulation is performed by calling the controller object:

```
Nsim = 12;
CLdata = implicit_MPC.simulate(x0, Nsim);
```

The returned structure contains the closed-loop system state trajectory `CLdata.X`, the control input sequence `CLdata.U`, and disturbance-input samples `CLdata.D`. The important point is that no manual construction of the implicit tube or tightening vector is required. MPT+ computes the auxiliary parameters, such as the finite tube length $N_{\mathrm{S}}$ and the tolerance parameter $\alpha$, during controller construction.

## 4.3 Simulation Case Study on a Large-Scale System

The implicit tube MPC implementation was evaluated on the reactor-separator benchmark depicted in Figure 4.1, adopted from the benchmark model in [13, chap. 6.6]. The process contains two continuously stirred tank reactors and a separator with recycle. The first reactor receives feed stream $F_{10}$, the outlet of the first reactor is mixed with the additional feed $F_{20}$ before entering the second reactor, and the separator returns condensed vapor to the first reactor. The system state vector contains temperatures and concentrations of the reactant $A$ and products $B$ and $C$ in all three vessels. The manipulated variables are the heat flows $H_1$, $H_2$, and $H_3$. The benchmark has one unstable and two stable steady states, and the control objective is to drive the deviation variables to the unstable steady-state setpoint while respecting constraints on control inputs and positivity-related constraints on system states.

The benchmark case study is obviously more demanding than the laboratory heat exchanger used for the rigid tube experiment in Section 3.1.2. This benchmark system

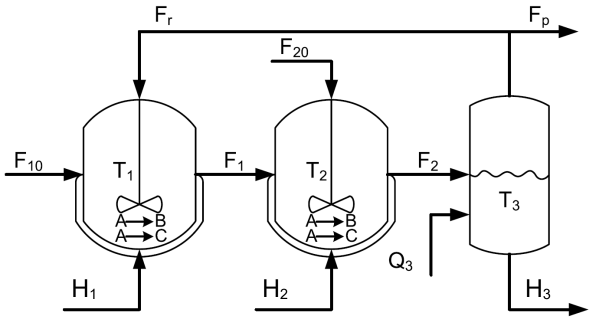


**Figure 4.1:** Reactor-separator benchmark plant used for implicit tube MPC validation [13].

has 12 system states, 3 manipulated control inputs, and coupled dynamics. The MPC design used sampling time $T_\mathrm{s} = 0.1\,\mathrm{h}$ and prediction horizon $N = 20$, with $R = \mathrm{diag}(1, 1, 1) \cdot 10^{-2}$ and $Q = \mathrm{diag}(Q_1, Q_2, Q_3)$, $Q_i = \mathrm{diag}(3200, 1, 1, 1) \cdot 10^3$. In this setting, the set-based rigid tube construction becomes numerically prohibitive because the required set-based operations grow exponentially with problem dimension. The implicit formulation avoids this obstacle and allows the robust controller to be constructed and simulated.

The controlled variables are expressed in deviation form with respect to the unstable steady state in Table 4.2:

$$x_{\mathrm{T},i}(t) := T_i(t) - T_i^s, \tag{4.5a}$$

$$x_{\mathrm{c_A},i}(t) := c_{\mathrm{A},i}(t) - c_{\mathrm{A},i}^s, \tag{4.5b}$$

$$x_{\mathrm{c_B},i}(t) := c_{\mathrm{B},i}(t) - c_{\mathrm{B},i}^s, \tag{4.5c}$$

$$x_{\mathrm{c_C},i}(t) := c_{\mathrm{C},i}(t) - c_{\mathrm{C},i}^s, \tag{4.5d}$$

**Table 4.2:** Steady-state values of the reactor-separator benchmark.

| $i$ | $T_i^s$ [K] | $c_{\mathrm{A},i}^s$ [kmol/m$^3$] | $c_{\mathrm{B},i}^s$ [kmol/m$^3$] | $c_{\mathrm{C},i}^s$ [kmol/m$^3$] | $H_i^s$ [kJ/h] |
|---|---|---|---|---|---|
| 1 | 369.53 | 3.31 | 0.17 | 0.04 | 0 |
| 2 | 435.25 | 2.74 | 0.44 | 0.11 | 0 |
| 3 | 435.25 | 2.88 | 0.49 | 0.12 | 0 |

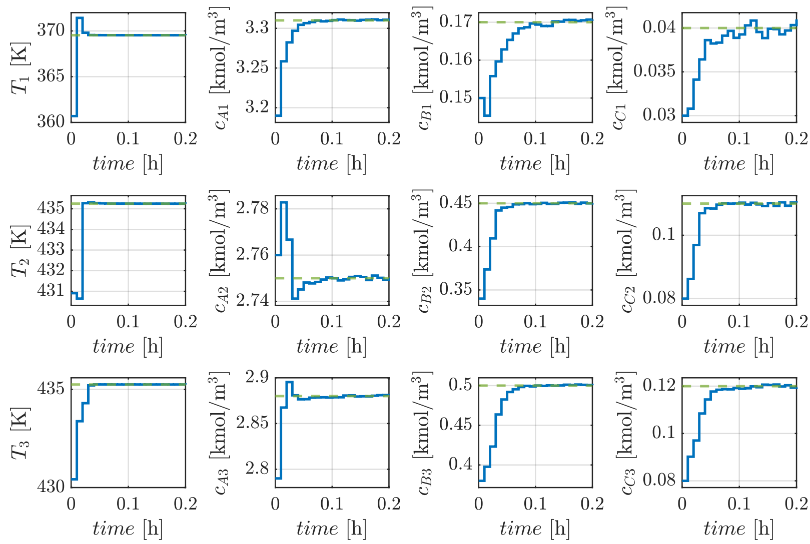


**Figure 4.2:** Closed-loop trajectories of reactor-separator system states under implicit tube MPC.

for $i \in \{1, 2, 3\}$. The manipulated variables are the heat-flow deviations

$$u_i(t) := H_i(t) - H_i^s, \qquad i \in \{1, 2, 3\}. \tag{4.6}$$

The bounds on control inputs, system states, and disturbance inputs are

$$\begin{bmatrix}-3 & -3.5 & -1.4\end{bmatrix}^\top 10^4 \leq u(t) \leq \begin{bmatrix}3 & 3.5 & 1.4\end{bmatrix}^\top 10^4, \tag{4.7a}$$

$$-x^s \leq x(t), \tag{4.7b}$$

$$-0.002I \leq d(t) \leq 0.002I. \tag{4.7c}$$

The second constraint enforces positivity of the physical temperatures and concentrations after conversion from deviation variables. The disturbance matrix is the identity matrix, so the additive disturbance used by the tube construction is $w(t) = d(t)$ and satisfies the same componentwise bounds.

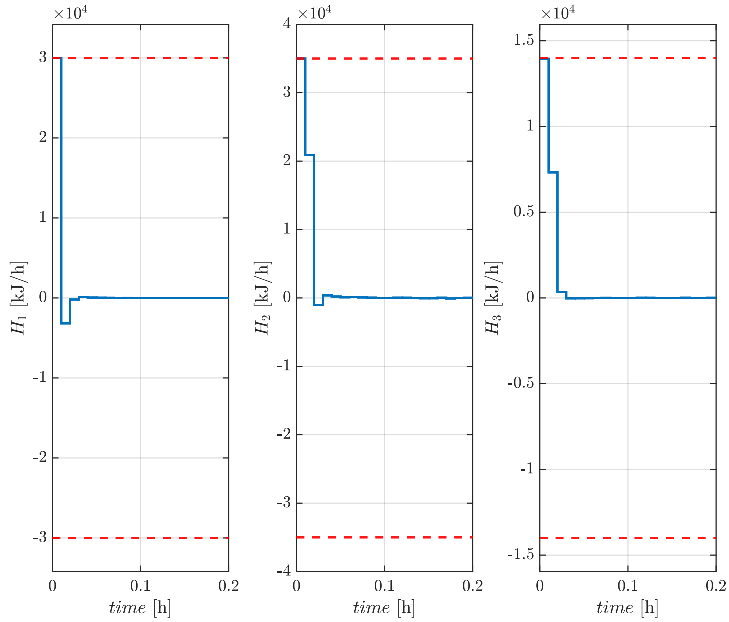


**Figure 4.3:** Closed-loop reactor-separator manipulated variables under implicit tube MPC.

Figures 4.2 and 4.3 summarize the closed-loop simulation. The controller drives the system state deviations toward the reference while maintaining the manipulated variables within their admissible range in the presence of randomly generated bounded disturbances. The simulation started from the deviation initial conditions

$$\begin{aligned} x_1(0) &= [-8.84, -0.12, -0.02, -0.01]^\top, \\ x_2(0) &= [-4.34, 0.01, -0.11, -0.03]^\top, \\ x_3(0) &= [-4.83, -0.09, -0.12, -0.04]^\top, \end{aligned} \tag{4.8}$$

for the first reactor, second reactor, and separator, respectively.

The computational data make the scalability benefit explicit. In the reported implementation in MATLAB, YALMIP provided the modeling layer for the optimization problem. The controller was constructed with MPT+, and the optimization problems were solved with MOSEK 10.0.40. MPT+ formulated the implicit tube MPC problem in 16.5361 s. The resulting optimization problem contained 984 constraints and 60 optimization variables. During the closed-loop simulation, the maximum, average, and minimum evaluation times were 0.1406 s, 0.0398 s, and 0.0156 s, respectively. The corresponding set-based rigid tube MPC design could not be constructed because the geometric set-based operations became numerically intractable. These results show that implicit tube MPC extends robust constraint-aware control from low-dimensional demonstrators to larger process systems where explicit tube geometry is no longer the right computational representation.

## 4.4 Experimental Case Study on a Laboratory Smart Greenhouse

The reactor-separator benchmark in the previous section demonstrates the scalability advantage of implicit tube MPC using numerical simulation. To complement this result with laboratory validation, this implementation-oriented framework is analyzed on a smart greenhouse VESNA[1] presented in [41]. VESNA is a laboratory smart greenhouse developed for research and education in control and sustainable food production [41], see Figure 4.4. The device was designed as a compact experimental platform for testing advanced monitoring and control methods on a real system with measurable environmental dynamics. Its construction is cuboid, with dimensions $0.5\,\mathrm{m} \times 0.5\,\mathrm{m} \times 1\,\mathrm{m}$, an aluminum frame, acrylic walls, metal reinforcement, and custom mechanical parts. The front side provides access to the internal growing space, while sensors, fans, control electronics, and the power supply are mounted around the side and back panels.

The greenhouse instrumentation, depicted in detail in Figure 4.4, covers the main variables that determine the internal microclimate. Temperature and relative humidity are measured inside the device, while additional sensors provide light intensity, carbon dioxide ($CO_2$) concentration, door-opening information, and ambient temperature and humidity. The available actuators include a heater, an air humidifier, side-wall fans used for ventilation and cooling, and growth LED strips mounted in the upper part of the chamber. This multi-sensor and multi-actuator structure motivates the use of implicit tube MPC beyond the two-input two-output experiment considered here: the present temperature–humidity controller is treated as a step toward a compact advanced robust MPC regulator for a broader multi-input multi-output VESNA control setup. The device is operated through ESP32-based microcontrollers and communicates with the supervisory controller through the Arduino IoT Cloud, which allows measured values to be downloaded and actuator commands to be uploaded during experimental runs. The communication and closed-loop control workflow, depicted in Figure 4.5,

[1] `https://vesna.uiam.sk/`

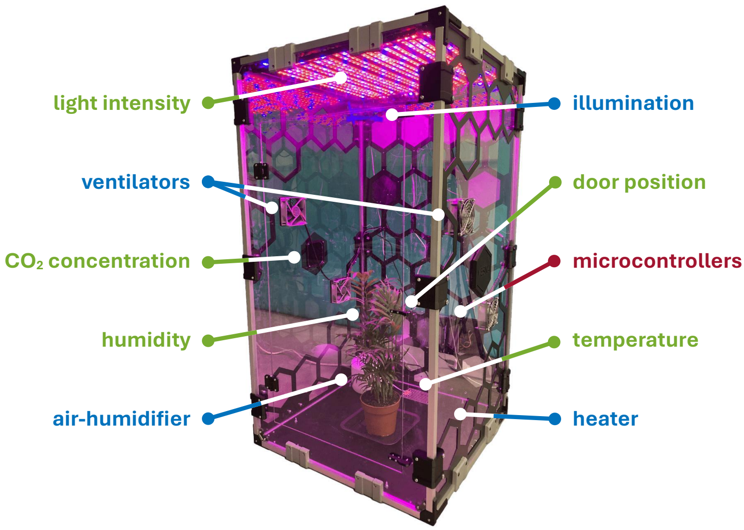


**Figure 4.4:** Laboratory smart greenhouse VESNA used for experimental validation – sensors (green), actuators (blue). control unit (red).

is handled by the VESNA CODE toolbox[2], a modular object-oriented framework developed in the MATLAB programming environment for implementing advanced optimization-based autonomous control on the VESNA platform [51]. The toolbox manages the network communication between the Arduino IoT Cloud and MATLAB. The collected process data are then used by the controller to compute optimal control inputs for the greenhouse actuators.

The experimental analysis in this section is aimed at control of the internal conditions of the smart greenhouse. The controlled variables are the internal temperature $T$ and relative humidity $h$. The associated manipulated variables are the electric supplies to the heater and the humidifier, respectively, with the corresponding actuators located in the lower part of the greenhouse, as depicted in Figure 4.4. Figure 4.6 depicts the non-negligible coupling, as observable from the response of temperature and humidity to a step change in the humidifier input from $0\,\%$ to $25\,\%$. The measured profiles indicate that the humidifier change affects both humidity and temperature, which confirms that these variables are physically coupled and complicates the use of separate control loops. Therefore, the aim of the experimental control-performance analysis is to use implicit tube MPC to address simultaneous temperature reference tracking and humidity disturbance rejection control problems under actuator constraints, interaction

[2] https://github.com/oravec-juraj/vesna/wiki/How-to-use-VESNA-CODE

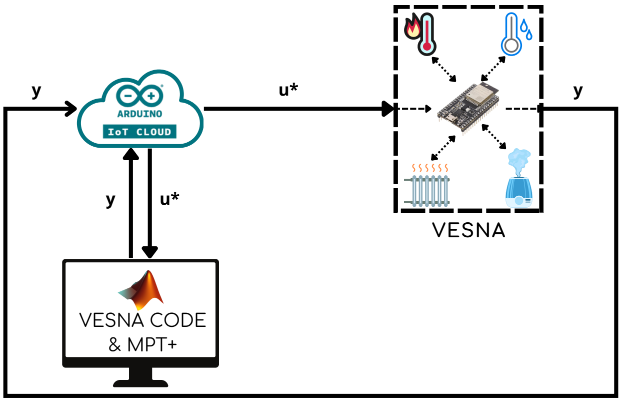


**Figure 4.5:** Communication and closed-loop control scheme connecting the VESNA greenhouse, Arduino IoT Cloud, VESNA CODE, and the supervisory controller.

between the controlled variables, and environmental disturbances.

### 4.4.1 Implicit Tube MPC Control Setup

The controller uses an offset-free prediction model in deviation variables, following the VESNA offset-free MPC construction reported in [51] and extended here to the tube MPC setting of [48]. The non-augmented model states describe the deviations of the measured temperature and humidity from their operating values. The vector $x_k = [x_{\mathrm{T},k}\ x_{\mathrm{h},k}]^\top$ collects these physical process-state deviations, where $x_{\mathrm{T},k}$ denotes the temperature deviation and $x_{\mathrm{h},k}$ denotes the humidity deviation. To remove steady-state tracking offsets caused by plant–model mismatch, measurement noise, and slowly varying environmental disturbances, each controlled variable is augmented with an integral state that accumulates the corresponding output error. The vector $\xi_k = [\xi_{\mathrm{T},k}\ \xi_{\mathrm{h},k}]^\top$ collects the integral states associated with the temperature and humidity errors. In deviation form, the reference is shifted to the origin, so the integral states evolve as accumulated deviations of the controlled variables. The augmented state $\widetilde{x}_k = [x_k^\top\ \xi_k^\top]^\top$ combines the physical and integral states. Since the controller is designed in a robust tube MPC framework, the prediction model also includes an additive disturbance term. The resulting augmented state-space model is

$$\widetilde{x}_{k+1} = \widetilde{A}\widetilde{x}_k + \widetilde{B}u_k + \widetilde{E}\widetilde{d}_k, \tag{4.9a}$$

$$y_k = \widetilde{C}\widetilde{x}_k, \tag{4.9b}$$

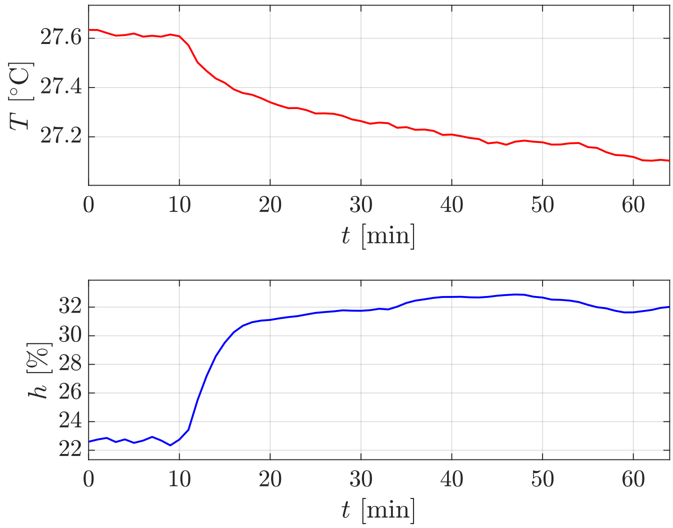


**Figure 4.6:** Measured influence of a humidifier step on temperature and relative humidity in VESNA.

where $u_k = [u_{\mathrm{T},k} \; u_{\mathrm{h},k}]^\top$ contains the heater and humidifier input deviations and $\widetilde{d}_k$ denotes the additive disturbance. The matrices of the discrete-time augmented state-space model, with sampling time $T_\mathrm{s} = 60\,\mathrm{s}$, are defined as

$$\widetilde{A} = \begin{bmatrix} A & 0 \\ -T_\mathrm{s}C & I \end{bmatrix}, \qquad \widetilde{B} = \begin{bmatrix} B \\ 0 \end{bmatrix}, \qquad \widetilde{C} = \begin{bmatrix} C & 0 \end{bmatrix}, \qquad \widetilde{E} = I_4. \tag{4.10}$$

In this representation, the physical states predict the greenhouse response, while the integral states store the accumulated tracking error and provide the offset-free behavior. The non-augmented matrices are

$$A = \begin{bmatrix} 0.7942 & 0 \\ 0 & 0.7747 \end{bmatrix}, \qquad B = \begin{bmatrix} 0.0261 & 0 \\ 0 & 0.8148 \end{bmatrix}, \qquad C = I_2. \tag{4.11}$$

The offset-free implicit tube controller is constructed for the experimental constraints defined in deviation form as

$$\begin{bmatrix} -10 \\ -20 \end{bmatrix} \leq x_k \leq \begin{bmatrix} 10 \\ 30 \end{bmatrix} \tag{4.12}$$

for the system states corresponding to the physical temperature within the interval

**Table 4.3:** Tuning of weight matrices for implicit tube MPC control on VESNA.

| Setup | $Q_{\mathrm{x,T}}$ | $Q_{\mathrm{i,T}}$ | $R_{\mathrm{T}}$ | $Q_{\mathrm{x,h}}$ | $Q_{\mathrm{i,h}}$ | $R_{\mathrm{h}}$ |
|---|---|---|---|---|---|---|
| A | 1000 | 10000 | 15 | 1 | 1 | 15 |
| B | 1000 | 10000 | 15 | 1 | 10 | 15 |
| C | 1000 | 10000 | 15 | 1 | 100 | 15 |

19 – 39 °C and humidity in the range 5 – 55%, and

$$\begin{bmatrix} -128 \\ -13 \end{bmatrix} \leq u_k \leq \begin{bmatrix} 128 \\ 13 \end{bmatrix} \tag{4.13}$$

for control inputs. Constraints in (4.13) define the admissible ranges for the control actions around the nominal operating point in the interval 0 – 100% for the power of heater and 0 – 25% for humidifier, respectively. The constraints are defined for the physical temperature and humidity states, while the integral states remain unconstrained.

The additive disturbance constraints are dedetermined as

$$\begin{bmatrix} -0.5 \\ -1 \\ -0.1 \\ -1 \end{bmatrix} \leq \widetilde{d}_k \leq \begin{bmatrix} 0.5 \\ 1 \\ 0.1 \\ 1 \end{bmatrix}. \tag{4.14}$$

The investigated controller tunings are summarized in Table 4.3. The penalty matrix of the augmented model is defined as

$$\begin{bmatrix} Q_{\mathrm{x}} & \mathbf{0} \\ \mathbf{0} & Q_{\mathrm{i}} \end{bmatrix}, \tag{4.15}$$

where the partial matrix $Q_{\mathrm{x}}$ penalizes the physical states and $Q_{\mathrm{i}}$ penalizes the integral states. The temperature-related weights are kept fixed across all setups, while the humidity output weight $Q_{\mathrm{i,h}}$ is increased from setup A to setup C. This tuning sequence is used to evaluate how humidity-control aggressiveness affects both the humidity response and the coupled temperature dynamics. In the presented case study, the prediction horizon $N = 50$ was considered across all control setups.

### 4.4.2 Control Performance Analysis of Implicit Tube MPC

The main objective of the case study is to ensure offset-free control of temperature to the reference value of 30 °C, while the humidity is kept close to the steady-state value of 25 %. Control profiles of temperature reference tracking are depicted in Figure 4.7.

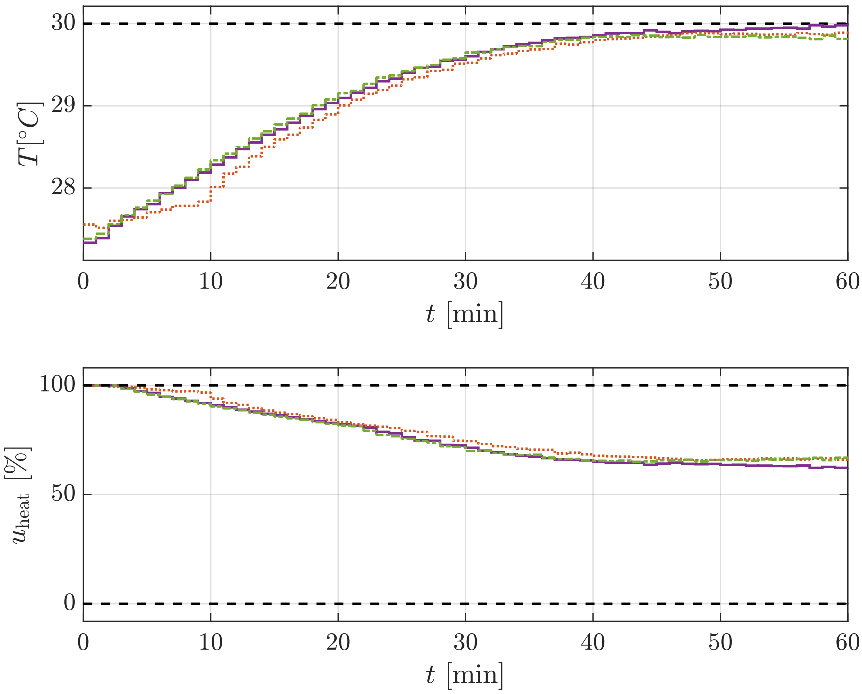


**Figure 4.7:** Measured temperature reference-tracking responses obtained with implicit tube MPC for different control setup A (dashed green), setup B (dotted orange), setup C (solid purple).

The measured temperature trajectories confirm that the implicit tube MPC controller reaches the required reference for all tested tunings. Since the temperature-related weights are identical in all control setups, the small differences in the responses mainly reflect the influence of the humidity-loop tuning and the temperature–humidity coupling discussed above. The corresponding humidity responses are depicted in Figure 4.8. The controller keeps humidity within the predefined steady-state neighborhood ($\pm 1\,\%$) in all configurations, while the transient behavior illustrates the expected trade-off between faster disturbance rejection and smoother actuator use.

The control performance is quantified by the settling time $t_{\mathrm{set}}$, the integral of squared output error ISE, the integral of squared input ISI, the actuator energy use $E$, and the associated $CO_2$ emissions $m(CO_2)$. The temperature-tracking criteria in Table 4.4 indicate that all three tunings reached the reference without reported constraint

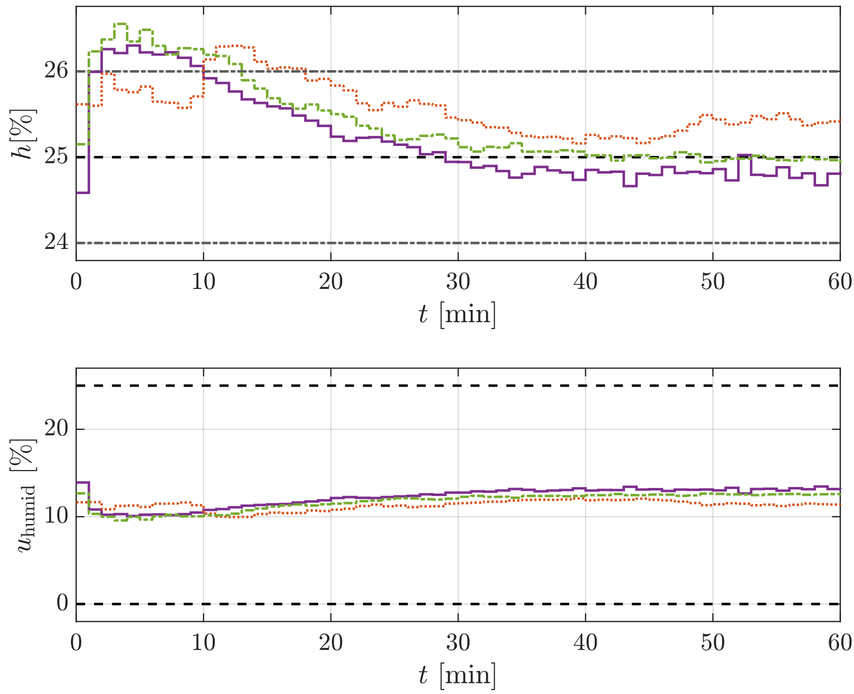


**Figure 4.8:** Measured humidity disturbance-rejection responses obtained with implicit tube MPC for different control setups: setup A (dashed green), setup B (dotted orange), setup C (solid purple).

violation and with negligible steady-state offset. Control setup A gives the best tracking and the smoothest input trajectory, while control setup C achieves comparable settling time with the lowest energy use and associated $CO_2$ emissions. Setup B is slightly slower and less favorable in the listed temperature criteria.

The humidity disturbance-rejection criteria in Table 4.5 indicate the analogous tuning compromise. Control setup A achieves the smallest humidity offset error with moderate actuator effort. Setup C reaches the humidity neighborhood fastest, but requires the largest input action resulting in the highest humidifier energy use. Setup B is slowest, but gives the smoothest input profile and the lowest energy use and associated $CO_2$ emissions.

The VESNA experiments confirm the practical relevance of the implicit tube MPC

**Table 4.4:** Control performance of implicit tube MPC in the VESNA temperature reference-tracking task.

| Setup | $t_{\mathrm{set}}$ [min] | $\mathrm{ISE_T}$ | $\mathrm{ISI_T}$ | $E_{\mathrm{T}}$ [kJ] | $m_{\mathrm{T}}(\mathrm{CO_2})$ [g] |
|---|---|---|---|---|---|
| A | 27 | 71.42 | 14000 | 102.10 | 7.54 |
| B | 29 | 84.31 | 17300 | 104.93 | 7.75 |
| C | 27 | 73.98 | 20200 | 101.87 | 7.53 |

**Table 4.5:** Control performance of implicit tube MPC in the VESNA humidity disturbance-rejection task.

| Setup | $t_{\mathrm{set}}$ [min] | $\mathrm{ISE_h}$ | $\mathrm{ISI_h}$ | $E_{\mathrm{h}}$ [kJ] | $m_{\mathrm{h}}(\mathrm{CO_2})$ [g] |
|---|---|---|---|---|---|
| A | 13 | 199.12 | 98.39 | 8.31 | 0.61 |
| B | 18 | 617.23 | 18.11 | 8.06 | 0.60 |
| C | 10 | 546.97 | 123.51 | 8.68 | 0.64 |

formulation. The controller was implemented on a physical greenhouse operated through a cloud communication layer, and the reported measurements include the effects of sensor noise, actuator limitations, environmental disturbances, and plant–model mismatch. At the same time, the implicit tube MPC.

## 4.5 Simulation Case Study of Industrial System

The previous sections discussed implicit tube MPC as a scalable robust control construction. This section illustrates the same idea on an industrially motivated separation process, where the uncertainty is not an abstract modeling term but a gradual physical degradation of heat-transfer equipment. The case study considers a hybrid heat-integrated distillation system (HHIDiS), in which the heat integration is realized through a plate-type heat and mass exchanger (HME). The control problem combines robust constraint handling, offset-free tracking, computationally tractable implementation, and energy-aware operation.

The process scheme is depicted in Figure 4.9. The system separates a binary mixture using two coupled distillation columns. The sections R1 and S2 form the heat-integrated part of the system, while the S1 and R2 sections provide additional process dynamics and stabilization. A detailed discussion of the HHIDiS dynamic model and the associated industrial constraints is given in [34]. In the considered HHIDiS setup,

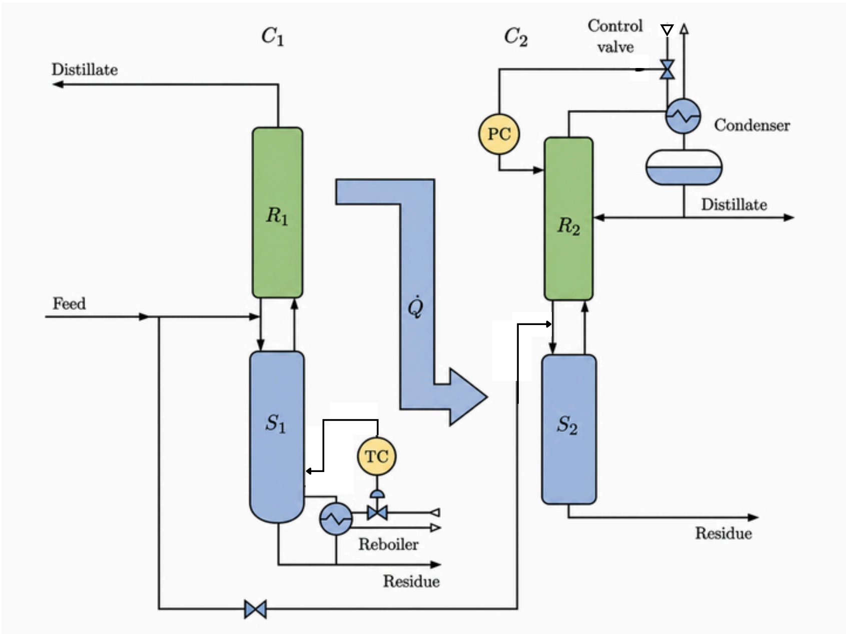


**Figure 4.9:** Process scheme of the considered HHIDiS.

in contrast to a conventional heat-integrated distillation column (HIDiC), the pressure difference between the integrated sections is produced by a pump and a valve. This configuration is attractive from an implementation point of view because it reduces equipment complexity, but it also creates a challenging control problem: the coupled heat and mass exchange is affected by fouling, and the resulting parameter changes modify the closed-loop dynamics over time.

The goal of the control case study is to design a robust controller that will provide reliable control performance under uncertainty. The control case study considers two controlled variables. The condenser pressure is regulated by the cooling-water mass flow rate, while the reboiler temperature is regulated by the heating-water mass flow rate. These variables define two control loops with a single input and a single output, but the operating objective is broader than setpoint tracking alone. The designed controller must also respect physical limits on the manipulated variables and maintain safety margins for the pressure and temperature system states. Fouling is represented through changes in the heat-transfer resistances of the condenser, reboiler, and integrated exchanger. Four fouling levels are considered, ranging from clean operation to high fouling according to Tubular Exchanger Manufacturers Association (TEMA)-based recommendations [67]. The values therefore reflect conventional heat-exchanger fouling-resistance guidelines rather than additional identified plant parameters. The condenser has a larger tube-side resistance under medium and high fouling, which makes the pressure loop particularly sensitive to degraded heat transfer.

### 4.5.1 Implicit Tube MPC Control Setup

The designed robust controller is based on the offset-free implicit tube MPC formulation. The offset-free part augments the prediction model with integral action to address the problem that constant plant–model mismatch and persistent disturbances lead to steady-state tracking errors [47]. The robust part treats the fouling-induced parameter variation as bounded uncertainty. The implicit tube construction then keeps the robust tube conditions inside the optimization problem without requiring explicit geometric construction of the tube cross-section [56]. This is important for the complex HHIDiS case study, where repeated set-based operations would make the controller design less practical.

The offset-free tube MPC control structure is depicted in Figure 4.10. The measured controlled variable is processed through the augmented prediction model, while the tube MPC controller computes the admissible manipulated-variable update subject to tightened constraints. This structure connects the integral offset-free mechanism with the robust tube tightening used to handle fouling-induced uncertainty.

For each controlled loop, the identified first-order model is augmented by an integral state. This gives a two-state offset-free prediction model of the form

$$x_{q,k+1} = A_q x_{q,k} + B_q u_{q,k} + E_q d_{q,k}, \qquad q \in \{\mathrm{C}, \mathrm{R}\}, \tag{4.16}$$

where $q = \mathrm{C}$ denotes the Condenser Pressure Control Loop and $q = \mathrm{R}$ denotes the Reboiler Temperature Control Loop. The models used in the HHIDiS study are

$$A_{\mathrm{C}} = \begin{bmatrix} 0.9598 & 0 \\ 1 & 1 \end{bmatrix}, \qquad B_{\mathrm{C}} = \begin{bmatrix} -2.2579 \\ 0 \end{bmatrix}, \qquad E_{\mathrm{C}} = \begin{bmatrix} 1 & 0 \\ 0 & 1 \end{bmatrix}, \tag{4.17a}$$

$$A_{\mathrm{R}} = \begin{bmatrix} 0.9435 & 0 \\ 1 & 1 \end{bmatrix}, \qquad B_{\mathrm{R}} = \begin{bmatrix} 0.6053 \\ 0 \end{bmatrix}, \qquad E_{\mathrm{R}} = \begin{bmatrix} 1 & 0 \\ 0 & 1 \end{bmatrix}. \tag{4.17b}$$

In (4.17), the first augmented system state corresponds to the controlled-variable deviation, whereas the second system state accumulates the tracking error and provides the offset-free property. The uncertain variables collect the effect of fouling and the residual nonlinear mismatch. In the robust tube construction, the additive disturbance

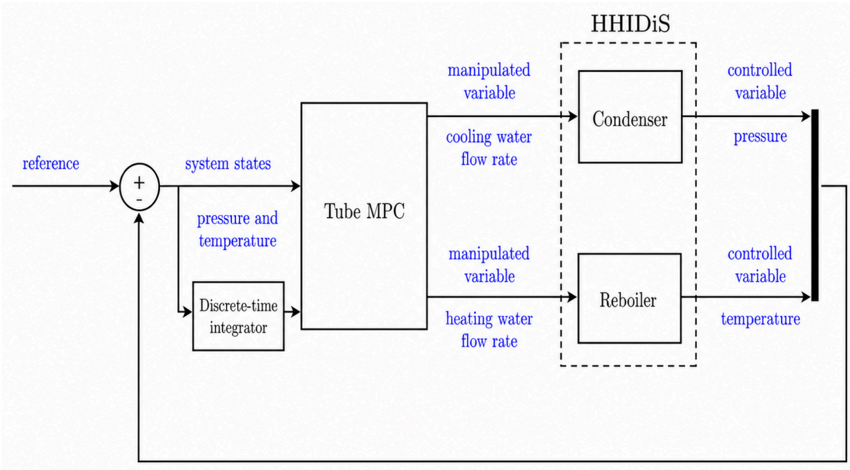


**Figure 4.10:** Control scheme of the offset-free tube MPC used for the HHIDiS case study.

set is the image $\mathbb{W}_q = E_q \mathbb{D}_q$. Since $E_q = I$, the reported componentwise disturbance-input bounds also define $\mathbb{W}_q$. The numerical design values are

$$T_\mathrm{s} = 0.1\,\mathrm{s}, \qquad w_{\max,\mathrm{C}} = 34, \qquad w_{\max,\mathrm{R}} = 6 \cdot 10^{-3}, \tag{4.18}$$

where the uncertainty bounds are expressed in the deviation units of the corresponding controlled variables.

The physical manipulated variables are imposed in deviation coordinates as

$$-v_q^\mathrm{s} \le u_{q,k} \le 2v_q^\mathrm{s}, \qquad v_\mathrm{C}^\mathrm{s} = 224.57\,\mathrm{kg/s}, \quad v_\mathrm{R}^\mathrm{s} = 111.97\,\mathrm{kg/s}. \tag{4.19}$$

The controlled-variable safety margins are

$$-5000 \le x_{\mathrm{C},k} \le 5000, \tag{4.20a}$$
$$-2 \le x_{\mathrm{R},k} \le 2. \tag{4.20b}$$

The integral system states are left formally unconstrained. The offset-free model (4.16) is combined with the implicit tube tightening from Section 4.1. For each loop $q$, this gives the following optimization problem:

$$
\begin{aligned}
\min_{\hat{x}_{q,k},\hat{u}_{q,k},\omega_{q,j}} \quad & \hat{x}_{q,N}^\top P_q \hat{x}_{q,N} + \sum_{k=0}^{N-1} \left(\hat{x}_{q,k}^\top Q_q \hat{x}_{q,k} + \hat{u}_{q,k}^\top R_q \hat{u}_{q,k}\right) && \text{(4.21a)}\\
\text{s.t.} \quad & \hat{x}_{q,k+1} = A_q \hat{x}_{q,k} + B_q \hat{u}_{q,k}, && \text{(4.21b)}\\
& c_{q,l}^\top \hat{x}_{q,k} + d_{q,l}^\top \hat{u}_{q,k} \leq 1 - f_{q,l}, && \text{(4.21c)}\\
& \left(c_{q,l}^\top + d_{q,l}^\top K_{\mathrm{S},q}\right) \hat{x}_{q,N} \leq 1 - f_{q,l}, && \text{(4.21d)}\\
& x_q(t) - \hat{x}_{q,0} = \mathcal{T}_q, && \text{(4.21e)}\\
& \omega_{q,j} \in \mathbb{W}_q, \qquad k = 0,\dots,N-1, \quad j = 0,\dots,N_{\mathrm{S},q}-1. && \text{(4.21f)}
\end{aligned}
$$

Here $\mathcal{T}_q$ denotes the implicit tube defined in (4.1). The matrix $Q_q$ penalizes the controlled-variable and integral system states, while $R_q$ penalizes the manipulated-variable movement. The term $f_{q,l}$ is the implicit tube shrinking vector computed from the uncertainty set $\mathbb{W}_q$.

The prediction horizon used in the reported HHIDiS controller tuning is $N = 200$. Thus, the controller retains the offset-free industrial tracking structure. At the same time, the admissible nominal trajectories are tightened so that the actual fouling-affected plant remains inside the robust tube.

The comparison baseline is formed by well-tuned PID controllers. The predictive controller was constructed and simulated in a MATLAB-based setup. The designed robust controller was constructed in MPT+, the optimization problem was parsed through YALMIP [32] and solved using MOSEK. The closed-loop simulations were then generated in MATLAB/Simulink R2023b on an i5 1.7 GHz CPU with 16 GB RAM.

The main tuning parameters are the quadratic weights on the augmented system states and control inputs. As in conventional MPC, increasing the penalty on control inputs produces smoother control actions, while increasing the penalty on system states gives a faster and more aggressive response. This tuning freedom is used to compare conservative and aggressive robust MPC settings. Among the eight analyzed tube MPC configurations, the dissertation discussion focuses on setup A and setup H, listed in Table 4.6. Setup A represents a conservative tuning that favors damped responses and small actuator movement, whereas setup H is more aggressive and targets faster error reduction.

Two operating scenarios are considered. In the first scenario, the condenser pressure performs a reference step, while the reboiler temperature is evaluated as a disturbance-rejection loop. In the second scenario, the roles are reversed: the condenser pressure

**Table 4.6:** Selected tube MPC tuning setups used for the HHIDiS performance comparison.

| Setup | $Q_{\mathrm{C},1}$ | $Q_{\mathrm{C},2}$ | $R_{\mathrm{C}}$ | $Q_{\mathrm{R},1}$ | $Q_{\mathrm{R},2} \cdot 10^6$ | $R_{\mathrm{R}}$ |
|---|---|---|---|---|---|---|
| A | 75 | 0.3 | 1 | 5 | 0.1 | 0.5 |
| H | 75 | 0.5 | 1 | 5 | 2.0 | 0.5 |

is evaluated under disturbance rejection and the reboiler temperature performs the reference-tracking task. The closed-loop quality is evaluated using the root mean square error (RMSE) of the tracking error. For reference-tracking responses, the maximum overshoot is also evaluated because it directly reflects the trade-off between fast response and conservative operation.

### 4.5.2 Control Performance Analysis of Implicit Tube MPC

Figures 4.11–4.14 present the representative closed-loop responses. The robust MPC trajectories demonstrate the expected tuning trade-off. A conservative setup gives slower but well-damped responses and can remove overshoot in the temperature tracking task across the considered fouling levels. A more aggressive setup reduces the RMSE and improves the speed of response, but it may introduce visible oscillations when the fouling level is high. The PID controllers provide acceptable nominal behavior, but their performance degrades when the heat-transfer characteristics move away from the tuning condition.

The numerical RMSE values are given in Tables 4.7 and 4.8. In scenario I, setup A improves the condenser pressure reference tracking for all fouling levels, while its reboiler disturbance-rejection response is intentionally conservative. Setup H gives the largest improvement for the low-fouling case, reducing the pressure-loop RMSE from 355.6 to 229.6, i.e. by approximately 35.4 % relative to the PID baseline. In scenario II, both tube MPC setups reduce the pressure-loop disturbance-rejection error for all fouling levels. Setup H also improves the reboiler temperature reference-tracking RMSE, reducing the error by 11–20 % across the four fouling cases.

The overshoot values in Table 4.9 indicate the other side of the same tuning decision. The conservative tube MPC setup A eliminates overshoot in the reboiler temperature reference-tracking task for all fouling levels. Setup H remains substantially less oscillatory than the PID controller in this metric, but overshoot increases again under medium and high fouling. The conservative tuning is therefore particularly relevant

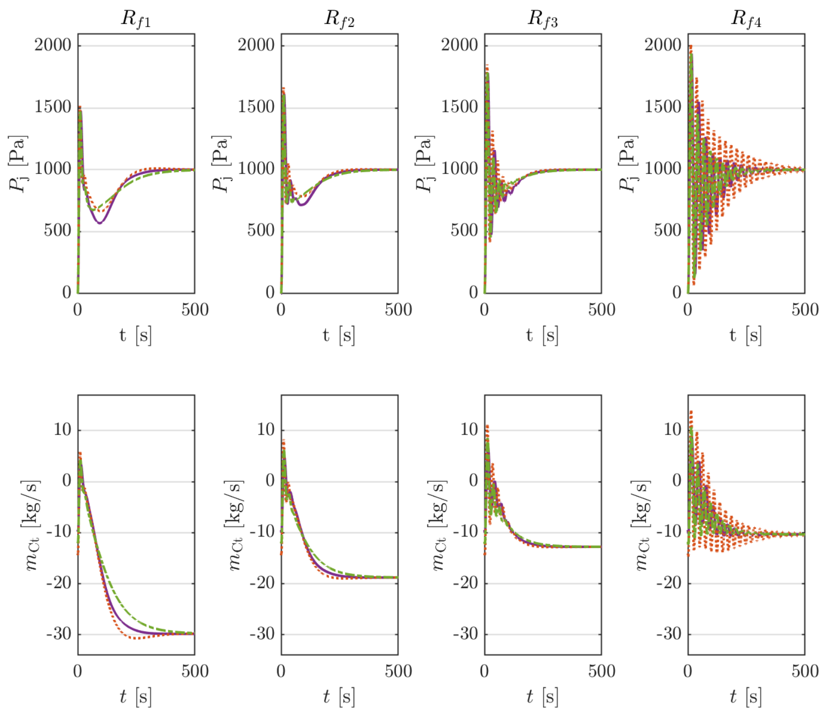


**Figure 4.11:** Condenser-pressure response for the condenser-pressure step scenario.

**Table 4.7:** RMSE values for HHIDiS control scenario I: condenser pressure reference tracking and reboiler temperature disturbance rejection.

| | Condenser pressure RMSE | | | Reboiler temperature RMSE ($\times 10^{-3}$) | | |
|---|---|---|---|---|---|---|
| Fouling | PID | Setup A | Setup H | PID | Setup A | Setup H |
| $R_{f,0}$ | 328.7 | 257.5 | 262.5 | 5.8 | 10.5 | 7.5 |
| $R_{f,1}$ | 355.6 | 236.5 | 229.6 | 5.9 | 5.8 | 4.7 |
| $R_{f,2}$ | 304.1 | 238.7 | 243.6 | 4.9 | 5.4 | 4.5 |
| $R_{f,3}$ | 406.0 | 308.9 | 373.3 | 7.1 | 6.0 | 5.3 |

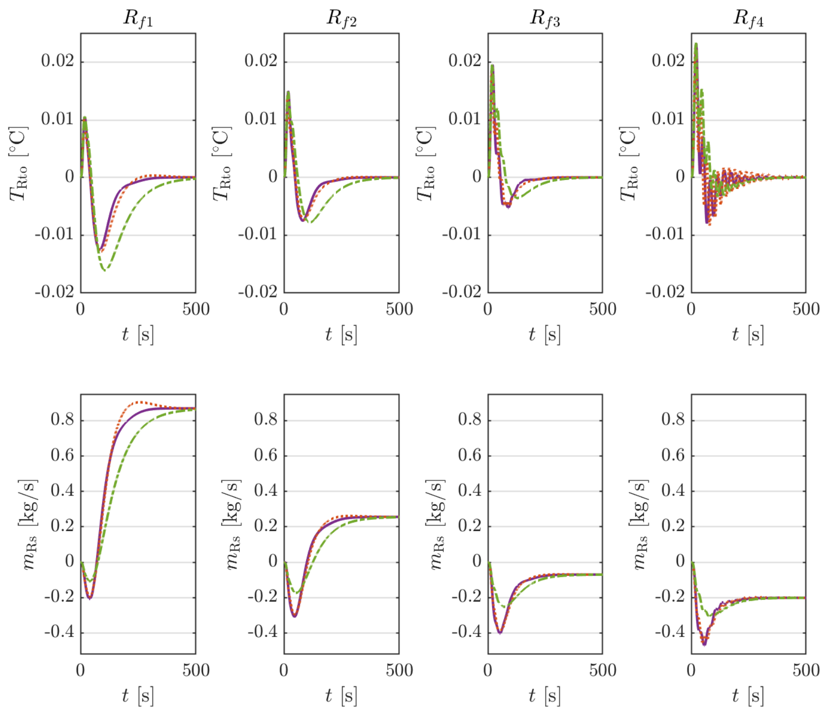


**Figure 4.12:** Reboiler-temperature response during the condenser-pressure step scenario.

**Table 4.8:** RMSE values for HHIDiS control scenario II: condenser pressure disturbance rejection and reboiler temperature reference tracking.

| | Condenser pressure RMSE | | | Reboiler temperature RMSE ($\times 10^{-3}$) | | |
|---|---|---|---|---|---|---|
| Fouling | PID | Setup A | Setup H | PID | Setup A | Setup H |
| $R_{f,0}$ | 525.8 | 381.0 | 411.4 | 36.0 | 46.5 | 32.0 |
| $R_{f,1}$ | 431.5 | 315.2 | 324.9 | 36.0 | 41.5 | 29.3 |
| $R_{f,2}$ | 402.9 | 275.7 | 280.4 | 34.9 | 39.6 | 28.1 |
| $R_{f,3}$ | 374.4 | 261.3 | 266.8 | 35.7 | 39.1 | 29.8 |

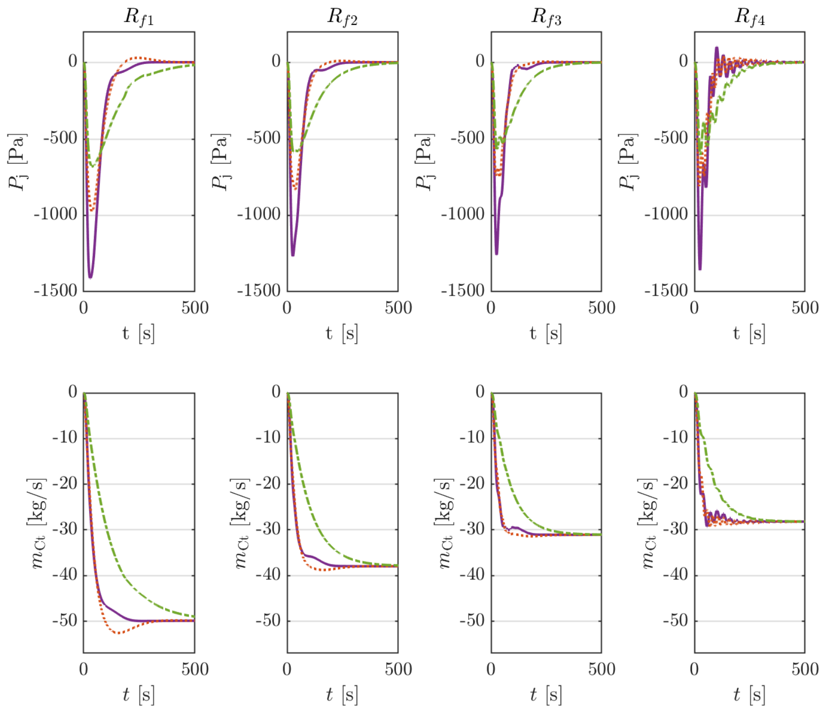


**Figure 4.13:** Condenser-pressure response during the reboiler-temperature step scenario.

for industrial operation because it favors smooth trajectories and avoids overshoot, which is often preferable when safety margins and product quality are more important than the shortest settling time.

The case study also evaluates the operational consequences of control tuning. The heating-water demand in the reboiler is translated into fuel-oil consumption and the associated $CO_2$ emissions. The results in Figures 4.15 and 4.16 indicate that robust MPC can reduce the energy demand and fuel cost when the tuning is selected with this objective in mind. In particular, conservative settings can decrease the heating-medium consumption for lower fouling levels and remain competitive with PID control under stronger fouling. In the reboiler step-change scenario, the conservative robust MPC settings are especially beneficial because they directly penalize unnecessary changes in the heating medium.

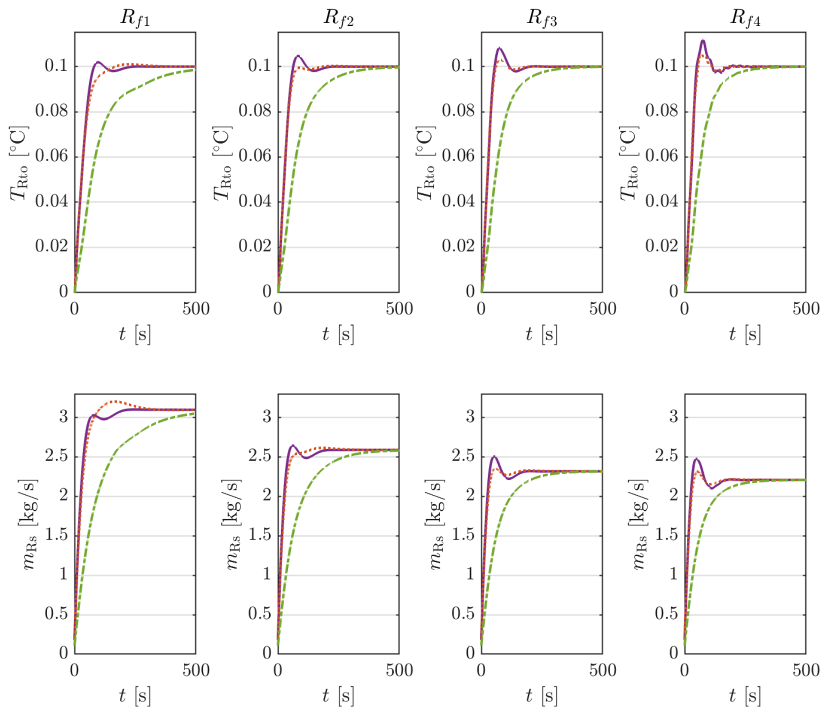


**Figure 4.14:** Reboiler-temperature response for the reboiler-temperature step scenario.

**Table 4.9:** Maximum overshoot in the reboiler temperature reference-tracking task of control scenario II.

| Fouling | PID [%] | Setup A [%] | Setup H [%] |
|---|---|---|---|
| $R_{f,0}$ | 1.90 | 0 | 1.02 |
| $R_{f,1}$ | 4.71 | 0 | 0.28 |
| $R_{f,2}$ | 8.25 | 0 | 3.14 |
| $R_{f,3}$ | 11.81 | 0 | 5.33 |

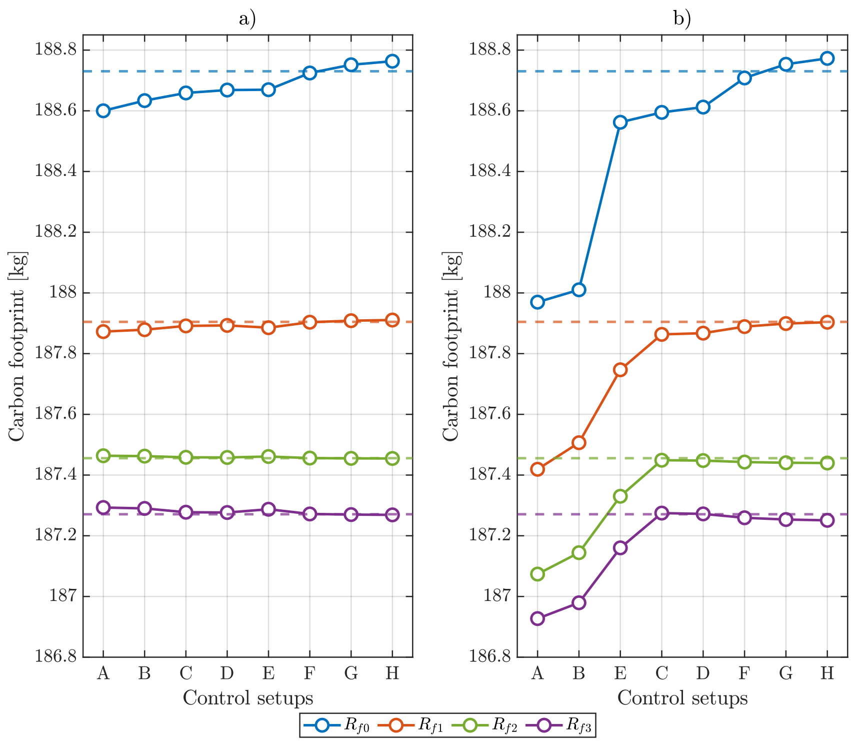


**Figure 4.15:** Comparison of $CO_2$ emissions associated with heating-medium consumption.

The same weighting matrices that tune closed-loop performance also provide a practical mechanism for shaping energy use. Increasing the penalty on control inputs discourages aggressive manipulated-variable movement, which can reduce heating-water consumption and therefore reduce both operating cost and $CO_2$ emissions. The robust offset-free implicit tube MPC formulation therefore contributes to safe operation in two senses: it preserves constraint-aware operation under fouling-induced uncertainty, and it enables control tuning that supports more economical and environmentally favorable operation.

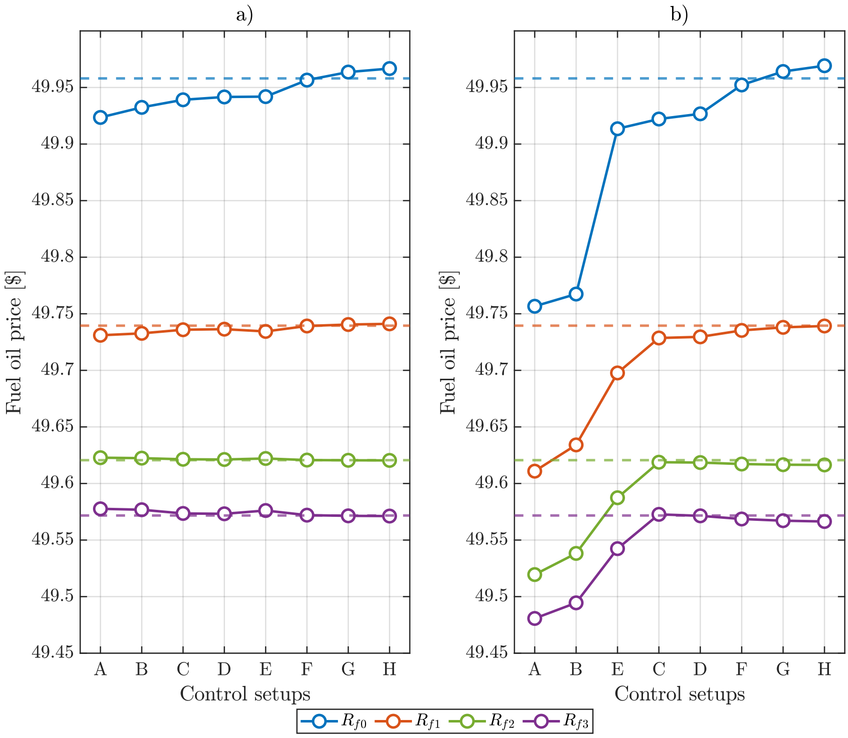


**Figure 4.16:** Comparison of fuel-oil costs associated with heating-medium consumption.

## 4.6 Discussion

This chapter has presented and applied the implicit tube MPC formulation as a software-supported workflow for scalable robust control. Compared to the set-based implementation in Chapter 3, the implicit formulation avoids explicit invariant-set construction and represents the tube through auxiliary variables and support-function-based constraints. The MPT+ implementation and the reactor-separator benchmark demonstrate that this construction can be applied to higher-dimensional process models where repeated explicit set operations would be impractical.

The extensive laboratory case study of smart greenhouse control complements the numerical scalability analysis by presenting the robust control of a real laboratory process. The greenhouse experiments include cloud-based communication, actuator limitations, environmental disturbances, sensor noise, and the coupling between temperature and humidity. The temperature reference-tracking and humidity disturbance-rejection results indicate the expected tuning trade-offs: more aggressive settings can reduce settling time, while smoother settings reduce input movement, energy use, and associated $CO_2$ emissions. This confirms that implicit tube MPC is not only a computational reformulation, but also a practical controller design approach for repeated experimental tuning on physical systems.

The other relevant contribution of the chapter is the offset-free implicit tube MPC case study for the HHIDiS. This application extends the implicit formulation to an energy-intensive industrial system affected by fouling and plant–model mismatch. In the reported scenarios, the selected tube MPC tunings reduced pressure-loop RMSE relative to the PID baseline, with the largest listed reduction approximately 35 %. Setup H also reduced the reboiler-temperature tracking RMSE in scenario II by 11-20 %. Conservative tuning eliminated overshoot in the reboiler-temperature tracking task, whereas more aggressive tuning reduced selected error measures at the cost of increased oscillations. The industrial case study also indicates that robust offset-free control can be evaluated beyond tracking metrics. The selected robust MPC settings lowered the reported heating-medium use, fuel cost, and associated $CO_2$ emissions in the considered energy comparison. The chapter therefore connects the scalability motivation of implicit tube MPC with experimental validation and with the energy-aware industrial application that forms its main contribution.

Chapter 5

# Tunable Implicit Tube MPC for Large-Scale Systems

---

*This chapter introduces a novel framework for real-time tunable implicit tube model predictive control, building upon the research published in [52]. While traditional robust MPC formulations often rely on fixed tuning parameters, the methodology presented here enables dynamic adjustment of penalty factors to optimize closed-loop performance in response to changing operating conditions or control objectives.*

*The primary contribution of this chapter is the development of a numerically tractable implicit tube MPC design that enables the effective adoption of time-varying penalty factors $\hat{Q}$ and $\hat{R}$. In the context of tube-based MPC, modifying these factors has a direct impact on the controller structure. Specifically, any change in the penalty matrices may necessitate a recomputation of the linear quadratic regulator (LQR)-based feedback gain $K_{\mathrm{S}}$, which in turn influences the geometry of the robust invariant set. Technically, the proposed approach ensures that the implicit tube, which serves as an approximation of the minimum robust positive invariant set, is updated consistently with the linear controller gain. The construction of this tube is governed by the number of iterations $N_{\mathrm{S}}$ and its volume is determined by the scaling factor $\alpha$. By systematically accounting for $\hat{Q}$, $\hat{R}$, and $K_{\mathrm{S}}$ in real time, the controller maintains constraint satisfaction and robustness even as the control law and the underlying tube are modified. This flexibility allows for a more agile response to performance requirements without sacrificing the safety guarantees inherent in the tube-based MPC framework.*

## 5.1 Tunable Implicit Tube MPC Design

The main bottleneck of conventional tube MPC design is that changing the penalty matrices $Q$ and $R$ changes the stabilizing feedback gain $K_\mathrm{S}$, the terminal ingredients, and the tube-design quantities $N_\mathrm{S}$, $\alpha$, and $f$. A direct implementation would therefore require recomputing the tube parameters through (2.17), (2.18), and (4.2) whenever the tuning parameter changes. The aim is therefore to transform the MPC optimization problem in (4.4) into a form that enables real-time tuning of the penalty factors $Q$, $R$. The formulation below removes this online redesign step by fixing conservative tube-design parameters over the full admissible tuning range and by relaxing the first-step constraints without sacrificing the recursive-feasibility argument inherited from Assumption 2.3.

For known bounds on the time-varying penalty factors $Q$ and $R$, a given pair of penalty factors determines the corresponding terminal penalty matrix $P$ and the stabilizing feedback gain $K_\mathrm{S}$ in the MPC optimization problem and in the control law (2.19). Online construction of the implicit tube representation $\mathcal{T}$ would then require evaluating the corresponding values of $N_\mathrm{S}$ and $\alpha$ by solving the auxiliary problems (2.17), (2.18). The tunable implicit tube MPC design developed in this section keeps fixed values of the parameters $N_\mathrm{S}$, $\alpha$, and $f$ over the admissible tuning range, which removes the need to solve the auxiliary tube-design problems at each tuning instant and enables real-time adaptation of the penalty factors while preserving the robust MPC guarantees. In addition, the first-step constraints are restated to reduce conservatism and, where possible, reduce the closed-loop cost.

### 5.1.1 Relaxed First-Step Constraints

The first modification concerns the constraints on system states and control inputs at $k = 0$, i.e., at the initial step of the prediction horizon.

**Lemma 5.1** (Relaxed constraints on system states and control inputs)**.** *Let Assumption 2.3 hold. Given the tube MPC optimization problem in* (2.15)*, relaxing the constraints on system states and control inputs in* (2.15d)*,* (2.15c) *for $k = 0$ into the form*

$$\hat{x}_0 \in \mathbb{X}, \tag{5.1a}$$

$$u(t) = \hat{u}_0 + K_\mathrm{S}(x(t) - \hat{x}_0) \in \mathbb{U}, \tag{5.1b}$$

*preserves the closed-loop system stability and recursive feasibility of the tube MPC optimization problem in* (2.15)*.*

**Proof 5.1.** *The proof verifies that replacing the tightened constraints at stage $k = 0$ by the relaxed constraints in* (5.1) *preserves feasibility, constraint satisfaction, and closed-loop stability. If the relaxed system state constraint* (5.1a) *and the initial tube condition* (2.15f) *are feasible at the initial time instant $t$, then, by the tube MPC construction, $x(t) = \hat{x}_0 + e(t)$ with $e(t) \in \mathbb{T}$ holds. Since the tube cross-section $\mathbb{T}$ is an admissible set and the relaxed control input constraint* (5.1b) *explicitly enforces*

$$u(t) = \hat{u}_0 + K_{\mathrm{S}}(x(t) - \hat{x}_0) \in \mathbb{U}$$

*to hold, therefore, the constraints on system states and control inputs in* (2.12) *are satisfied at time $t$. For all prediction steps $k > 0$, the original tube MPC constraints* (2.15d)–(2.15c) *remain the same, and constraint satisfaction follows from the conventional tube MPC argument. Consequently, the terminal constraint* (2.15e) *guarantees the existence of a feasible shifted solution, implying recursive feasibility. Since the terminal cost* (2.15a) *and terminal constraint* (2.15e) *are the same, under Assumption 2.3, the tube MPC Lyapunov argument applies. Consequently, the closed-loop stability properties induced by the terminal ingredients are preserved.*

The proof of Lemma 5.1 follows the concept of free initial conditions [7], its later extension [74], and a recent parameterized formulation [71]. Consequently, Lemma 5.1 can be interpreted as a generalized result within the implicit rigid tube MPC framework [56], adapted to fixed tube-design parameters, support-function-based constraint tightening, and the real-time tunable control policy considered in this chapter.

**Remark 5.2.** *Introducing the relaxed constraints on system states and control inputs in* (5.1) *can extend the feasibility set of the tube MPC optimization problems in* (2.15), (4.4)*. Under a relaxed constraint, a point may be feasible for the relaxed constraint while being infeasible for the original constraint. Moreover, this approach can reduce the cost function value. Consequently, relaxed constraints can lead to improved closed-loop control performance compared with the original solutions of* (2.15), (4.4) *evaluated subject to* (2.15d), (2.15c).

**Remark 5.3** (Reachability interpretation)**.** *The effect of relaxing the tightened constraint on the system state at the initial prediction step can be interpreted in terms of backward reachability to the terminal set. For a fixed prediction horizon $N$, the feasibility region of the MPC problem corresponds to the set of system states that can be steered to the terminal set $\mathbb{X}_{\mathrm{N}}$ in $N$ steps under the tightened constraints on system states and control inputs, and therefore explicitly depends on $N$. While the conventional tube MPC formulation enforces $\hat{x}_0 \in \mathbb{X} \ominus \mathbb{T}$, the relaxation used here modifies only the constraint at $k = 0$ to $\hat{x}_0 \in \mathbb{X}$, leaving all constraints for $k \geq 1$, including the terminal constraint, unchanged. Consequently, the enlarged feasibility* *region can be characterized as the set of system states that can be driven in one step into the* $(N-1)$*-step feasible set associated with the conventional formulation. Although this relaxation may lead to different nominal predictions and closed-loop trajectories, recursive feasibility is preserved, since the tightened constraints for all future prediction steps and the terminal condition remain identical to those of the conventional tube MPC design, and the usual shifting argument applies.*

### 5.1.2 Criterion for Real-Time Penalty Tuning

Tuning is introduced through a convex combination of the boundary values of the penalty factors $Q$ and $R$ in (4.4) [43]:

$$\hat{Q} = (1-\phi)Q_{\mathrm{L}} + \phi\, Q_{\mathrm{H}}, \quad 0 \leq \phi \leq 1, \tag{5.2a}$$

$$\hat{R} = (1-\rho)R_{\mathrm{L}} + \rho\, R_{\mathrm{H}}, \quad 0 \leq \rho \leq 1, \tag{5.2b}$$

where the subscripts $_{\mathrm{L}}$, $_{\mathrm{H}}$ denote the low and high limits on the penalty matrices, respectively. This tuning strategy considers diagonal penalty matrices, such that $\lambda_{i,\mathrm{L}} \leq \lambda_{i,\mathrm{U}}$, $\forall i = 1, \ldots, r$, where $\lambda$ denotes the vector of eigenvalues of the penalty matrix and $r$ is the rank of the tuned penalty matrix, see [43]. The scalar $\rho \in [0,1]$ is referred to as the scaling parameter governing the interpolation of the control input weighting matrix.

**Assumption 5.1** (Single-parameter affine tuning)**.** *The real-time tuning of the MPC objective* (4.4a) *is restricted to a single tuning parameter. At any given time instant, either the penalty on system states* $\hat{Q}$ *or the penalty on control inputs* $\hat{R}$ *is tuned via an affine (convex) combination of two predefined matrices, while the other weighting matrix is kept fixed. Specifically,*

$$\hat{Q} = (1-\phi)Q_L + \phi Q_H, \quad \phi \in [0,1], \quad \hat{R} = R_L = R_H,$$

*or*

$$\hat{R} = (1-\rho)R_L + \rho R_H, \quad \rho \in [0,1], \quad \hat{Q} = Q_L = Q_H.$$

*Thus, tuning is governed by a single scalar parameter, while the other penalty matrix remains fixed.*

Assumption 5.1 ensures a unique and interpretable influence of tuning on the closed-loop behavior, avoids ambiguity caused by simultaneous variation of $Q$ and $R$, and, consequently, simplifies real-time implementation by limiting tuning to a single scalar parameter.

**Remark 5.4** (Tuning based on the penalty on control inputs)**.** *The formulation in this chapter focuses on tuning the penalty on control inputs, $\hat{R}$, according to* (5.2b)*. This is a practical design choice adopted for clarity and implementation simplicity under Assumption 5.1. A similar extension may be possible for tuning of $\hat{Q}$ according to* (5.2a)*, but the present formulation does not claim full generality with respect to simultaneous or unrestricted tuning of both weighting matrices.*

Designing implicit tube MPC in (4.4) requires solving the auxiliary optimization problems in (4.2), (2.17) to evaluate $\alpha^\star$, $N_\mathrm{S}^\star$, and $f^\star$. When the scaling factor $\rho$ is tuned, the associated penalty factors $Q$, $R$ are changed. To avoid solving the auxiliary optimization problems in (4.2) and (2.17) whenever the scaling factor $\rho$ is tuned, conservative values of the parameters $\hat{N}_\mathrm{S}$, $\hat{\alpha}$, and $\hat{f}$ are selected offline according to (5.3). In practice, a generally valid procedure for selecting the parameters $\hat{N}_\mathrm{S}$, $\hat{\alpha}$, and $\hat{f}$ is to grid the considered tuning interval for $\rho \in [0, 1]$ offline, evaluate these parameters over the tuning range, and take their maxima. However, in many practical cases, the extrema are observed at the boundary tunings, and this intensive gridding is not required, i.e., it is sufficient to select

$$\hat{\alpha} = \max(\alpha_{\mathrm{tol,L}}, \alpha_{\mathrm{tol,H}}), \tag{5.3a}$$

$$\hat{N}_\mathrm{S} = \max(\hat{N}_{\mathrm{S,L}}, \hat{N}_{\mathrm{S,H}}), \tag{5.3b}$$

$$\hat{f}_l = \max(\hat{f}_{l,\mathrm{L}}, \hat{f}_{l,\mathrm{H}}), \quad l = 1, 2, \ldots, N_\mathrm{C}, \tag{5.3c}$$

where the parameters denoted with subscripts $_\mathrm{L}$, $_\mathrm{H}$ correspond to the evaluation of the low and high limits of the penalty factors in (5.2), respectively. The original constraints in (4.3) are reformulated for $k = 0$ into the relaxed but still feasible form in (5.1). As a consequence, the conservativeness of the parameters in (5.3) affects the predictions for $k \geq 1$. Meanwhile, the control performance for $k = 0$ is not affected, and the corresponding value of $u(t)$ applied to the system (2.10) is close to the original value from (4.4).

Given a pair of penalty factors $\hat{Q}$ and $\hat{R}$, and the corresponding matrices $\hat{P}$ and $\hat{K}_{\mathrm{S}}$ determined by solving the Riccati equation, the tunable implicit rigid tube MPC problem has the following form:

$$\min_{\substack{\hat{x}_0, \hat{u}_0, \omega_0, \ldots \\ \hat{u}_{N-1}, \hat{x}_N, \omega_{\hat{N}_{\mathrm{S}}-1}}} \quad \hat{x}_N^\top \hat{P} \hat{x}_N + \sum_{k=0}^{N-1} \left( \hat{x}_k^\top \hat{Q} \hat{x}_k + \hat{u}_k^\top \hat{R} \hat{u}_k \right) \tag{5.4a}$$

$$\text{s.t.} \quad \hat{x}_{k+1} = A\,\hat{x}_k + B\,\hat{u}_k, \tag{5.4b}$$

$$c_l^\top \hat{x}_0 + d_l^\top (\hat{u}_0 + \hat{K}_{\mathrm{S}} \hat{\mathcal{T}}) \leq 1, \tag{5.4c}$$

$$c_l^\top \hat{x}_k + d_l^\top \hat{u}_k \leq 1 - \hat{f}_l, \quad k = 1, 2, \ldots, N-1, \tag{5.4d}$$

$$\left( c_l^\top + d_l^\top \hat{K}_{\mathrm{S}} \right) \hat{x}_N \leq 1 - \hat{f}_l, \tag{5.4e}$$

$$x(t) - \hat{x}_0 = \hat{\mathcal{T}}, \tag{5.4f}$$

$$e_i^\top \omega_j \leq 1, \tag{5.4g}$$

$$i \in \mathcal{I}_{\mathrm{W}}, \tag{5.4h}$$

$$j = 0, 1, \ldots, \hat{N}_{\mathrm{S}} - 1, \tag{5.4i}$$

$$k = 0, 1, \ldots, N-1, \tag{5.4j}$$

$$l = 1, \ldots, N_{\mathrm{C}}. \tag{5.4k}$$

where the implicit tube realization $\hat{\mathcal{T}}$ has a form analogous to (4.1):

$$\hat{\mathcal{T}} = (1 - \hat{\alpha})^{-1} \sum_{j=0}^{\hat{N}_{\mathrm{S}}-1} \left( A + B\hat{K}_{\mathrm{S}} \right)^j \omega_j \;. \tag{5.5}$$

**Remark 5.5** (Fixed terminal ingredients)**.** *To avoid the need to re-verify the prediction horizon length $N$ and to redesign the terminal penalty and terminal set whenever the penalty factors are tuned, the terminal ingredients can be fixed a priori. In particular, the terminal cost matrix $\hat{P}$ is chosen offline together with an associated terminal feedback gain $K_{\mathrm{Z}}$ such that the pair $(\hat{P}, K_{\mathrm{Z}})$ satisfies the conventional stabilizing terminal conditions for tube MPC, i.e., $K_{\mathrm{Z}}$ provides nominal closed-loop stability and the corresponding terminal set is positively invariant and constraint admissible. Under these conditions, the terminal constraint* (5.4e) *has the fixed form*

$$\left( c_l^\top + d_l^\top K_{\mathrm{Z}} \right) \hat{x}_N \leq 1 - \hat{f}_l, \tag{5.6}$$

*independently of the tuned penalty factors. Consequently, real-time tuning of the MPC weights does not affect the validity of the terminal constraint, nor the associated stability and recursive feasibility guarantees. Formal proofs of admissibility and closed-loop stability for fixed terminal ingredients in the implicit tube MPC setting are in [56].*

**Remark 5.6** (Non-relaxed constraints). *The implicit tube realization $\mathcal{T}$ in* (4.1) *is an auxiliary vector variable that represents the error membership constraint. The tunable implicit tube MPC optimization problem can also be designed subject to the original non-relaxed constraints on system states and control inputs* (2.15c), (2.15d) *in their implicit form. Then, the constraints in* (5.4c), (5.4d) *are replaced with*

$$c_l^\top \hat{x}_k + d_l^\top \hat{u}_k \leq 1 - \hat{f}_l. \tag{5.7}$$

**Theorem 5.7.** *Consider the uncertain LTI system* (2.10) *subject to constraints* (2.12) *and disturbance set* (2.11)*. Suppose that Assumptions 2.3 and 5.1 hold. Let the penalty matrices be tuned in the admissible range* (5.2)*. For each $\rho \in [0, 1]$, let the corresponding stabilizing feedback gain $\hat{K}_\mathrm{S}(\rho)$, terminal penalty $\hat{P}(\rho)$, and terminal set $\hat{\mathbb{X}}_\mathrm{N}(\rho)$ satisfy Assumption 2.3. Assume that the fixed tube-design parameters $(\hat{\alpha}, \hat{N}_\mathrm{S}, \hat{f})$ used in* (5.4) *satisfy*

$$\hat{\alpha} \geq \alpha^\star(\rho), \qquad \hat{N}_\mathrm{S} \geq N_\mathrm{S}^\star(\rho), \qquad \hat{f}_l \geq f_l^\star(\rho), \quad l = 1, \ldots, N_C, \tag{5.8}$$

*for the full admissible tuning range $\rho \in [0, 1]$. Then, the tunable implicit tube MPC problem* (5.4) *is recursively feasible and the resulting receding-horizon closed loop is robustly stable.*

**Proof 5.2.** *The MPC problem in* (5.4) *is a relaxation of the implicit rigid tube MPC problem in* (4.4)*, and therefore inherits its properties. For fixed parameters $(\hat{\alpha}, \hat{N}_\mathrm{S}, \hat{f})$, the two optimization problems differ only in the treatment of the initial-step constraint: according to Lemma 5.1, the problem* (5.4) *replaces the original tightened constraint at $k = 0$ by* (5.4c)*. All remaining constraints coincide. Therefore, it is sufficient to prove that this constraint does not violate the recursive feasibility and closed-loop system stability conditions. First, as the constraint in* (5.4c) *is equivalent to* (5.1)*, it directly follows from Lemma 5.1 that* (5.4c) *satisfies the recursive feasibility condition. Next, closed-loop stability follows from recursive feasibility in the presence of the terminal cost* (5.4a) *and terminal constraint* (5.4e) *satisfying Assumption 2.3. Consequently, closed-loop stability is preserved. The remainder of the proof is the same as the proof of Theorem 2 in [56].*

Choosing fixed values of $\hat{N}_\mathrm{S} \geq N_\mathrm{S}^\star(\rho)$ preserves feasibility of the implicit tube realization $\hat{\mathcal{T}}$ in (5.5) for all $\rho \in [0, 1]$. On the other hand, implementing $\hat{\alpha} \geq \alpha^\star(\rho)$ in (5.8) may lead to a more conservative implicit tube realization $\hat{\mathcal{T}}$ and to conservative values of $\hat{f}_l \geq f_l^\star(\rho)$, $l = 1, \ldots, N_\mathrm{C}$. Consequently, the control performance may be suboptimal compared to (4.4) evaluated with the corresponding optimal values $\alpha^\star(\rho)$ and $f_l^\star(\rho)$.

## 5.2 Numerical Example

The numerical case study investigates the closed-loop performance of the tunable implicit tube MPC optimization problem in (5.4). The original non-tunable implicit tube MPC design [56] is used as the performance reference. The reference MPC optimization problem in (4.4) needs to be redesigned entirely whenever the penalty factors are tuned. The results presented in this section were generated using an Intel(R) Core(TM) i5-1240P CPU 1.70 GHz, 16 GB RAM, MATLAB R2023b, YALMIP R20230622, MPT v3.2.1, MOSEK v10.0, Gurobi v11.01.

### 5.2.1 Control Setup and Offline Tube Design

To provide a fair comparison, the same large-scale reactor-separator benchmark as in Section 4.3 is considered. Further details on the process model, constraints, disturbance bounds, and initial conditions are given in Table 4.2 and equations (4.5)–(4.8). This case study therefore only introduces the tunable penalty design. The penalty on system states is kept the same as in the setup in Section 4.3,

$$Q = \begin{bmatrix} Q_1 & 0 & 0 \\ 0 & Q_2 & 0 \\ 0 & 0 & Q_3 \end{bmatrix},$$

where $Q_i = \mathrm{diag}(3200, 1, 1, 1) \cdot 10^3$ for $i = 1, 2, 3$. The penalty on control inputs is tuned between $R_\mathrm{L} = 1 \cdot 10^{-4} \cdot I$ and $R_\mathrm{H} = 10 \cdot I$ according to the single-parameter tuning law in (5.2).

The tunable tube MPC design criteria in (5.4) were precomputed offline and fixed for all values of $\rho \in [0, 1]$ according to (5.8): $\hat{N}_\mathrm{S} = 29$, $\hat{\alpha} = 24.4657 \cdot 10^{-4}$. In contrast, the parameters for the non-tunable tube MPC optimization problems in (4.4) must be redesigned for each setting of $\rho$. The optimized values of $N_\mathrm{S}^\star$ and $\alpha^\star$ are summarized in Table 5.1. Using fixed values of $\hat{N}_\mathrm{S}$, $\hat{\alpha}$, and $\hat{f}$ in the construction of the tightened constraints yields a feasibility domain that is independent of the scaling parameter $\rho$. Tuning therefore affects only the closed-loop behavior through the $(Q, R)$-dependent gain $K_\mathrm{S}$, while the admissible set of initial conditions is preserved. A non-tunable redesign may reduce conservativeness for a particular tuning, but requires computationally expensive recomputation of the tube-related parameters.

The calculation of $N_\mathrm{S}^\star$ and $\alpha^\star$ takes, on average, 1.7 s, while the recalculation of $f^\star$ requires an additional 0.95 s. For this benchmark, the non-tunable implicit MPC could still be redesigned when the penalty matrices are changed. For systems with faster dynamics, however, this recomputation may exceed the available sampling

**Table 5.1:** Tube-design parameters for different tuning values.

| Tuning | $N_{\mathrm{S}}^{\star}$ | $\alpha^{\star} \cdot 10^{-4}$ |
|---|---|---|
| $\rho = 0$ | 13 | 24.4657 |
| $\rho = 0.25$ | 21 | 3.2873 |
| $\rho = 0.50$ | 23 | 1.9005 |
| $\rho = 0.75$ | 26 | 2.3704 |
| $\rho = 1$ | 29 | 2.1442 |

period and prevent real-time implementation. The tunable formulation removes this online burden by computing the tube parameters offline once and keeping them fixed throughout the control process.

Trajectories of the optimal values of $\alpha^{\star}$ and $N_{\mathrm{S}}^{\star}$ for different settings of $\rho$, along with the corresponding values considered by the tunable tube MPC, $\hat{\alpha}$ and $\hat{N}_{\mathrm{S}}$, are depicted in Figure 5.1. The presented profiles demonstrate the need to redesign the optimal values of these parameters whenever different tuning is considered for the non-tunable tube MPC in (2.15). The tunable MPC, on the other hand, considers conservative values defined in (5.8), providing safe control without the need to redesign the parameters when the tuning parameters change. As reported later in Table 5.2, the price paid for this conservatism is negligible in terms of the closed-loop performance loss.

### 5.2.2 Closed-Loop Performance

As already observed in Section 4.3, the set-based tube MPC design is numerically intractable for this benchmark. The comparison in this chapter therefore focuses on the real-time tunable implicit tube MPC in (5.4) and the original non-tunable implicit tube MPC [56] in (4.4).

The closed-loop simulations use the same initial condition as the implicit tube MPC case study in (4.8). This keeps the comparison focused on the tunable formulation rather than on a different operating scenario. The obtained control trajectories for the non-tunable (solid lines) and tunable (dashed lines) tube MPC formulations are depicted in Figures 5.2 and 5.3, respectively. The figures compare the performance of the tunable implicit tube MPC (5.4) and the non-tunable implicit tube MPC (4.4) for the limiting values of the tuning parameter $\rho$, i.e., $\rho = 0$ and $\rho = 1$. The trajectories exhibit only minor differences between the non-tunable (4.4) and tunable implicit tube MPC (5.4) approaches. The same observation is supported by Figures 5.4 and 5.5, which present the results for the intermediate tuning value $\rho = 0.5$.

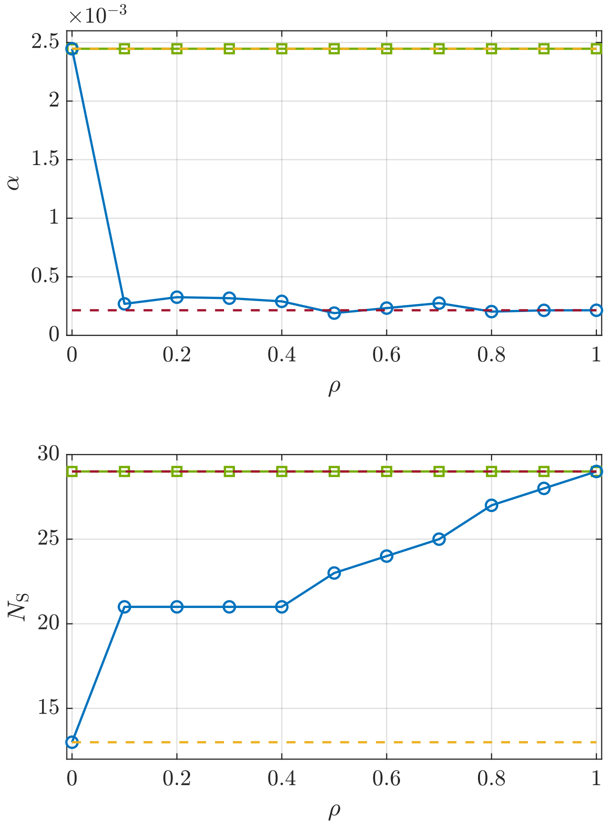


**Figure 5.1:** Evaluation of the parameters $\alpha$ (upper figure) and $N_\mathrm{S}$ (lower figure) for different settings of the scaling factor $\rho$: values associated with $R_\mathrm{L}$ (dashed yellow), values associated with $R_\mathrm{H}$ (dashed red), optimal values $\alpha^\star$ and $N_\mathrm{S}^\star$ evaluated for the non-tunable tube MPC optimization problem (blue circles), and values $\hat{\alpha}$ and $\hat{N}_\mathrm{S}$ considered by the tunable tube MPC (green squares) according to (5.8).

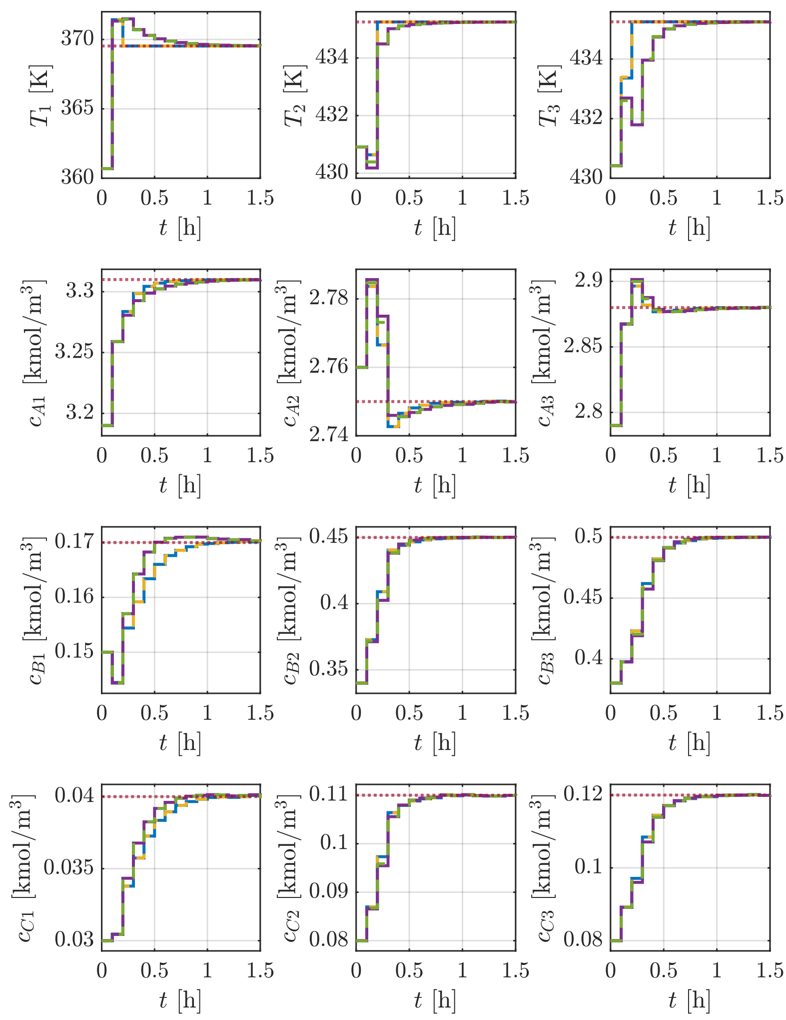


**Figure 5.2:** Closed-loop control trajectories of CVs: non-tunable tube MPC for scaling factor $\rho = 0$ (solid blue), tunable tube MPC for $\rho = 0$ and relaxed constraints (dashed yellow), non-tunable tube MPC for $\rho = 1$ (solid purple), tunable tube MPC for $\rho = 1$ and relaxed constraints (dashed green), steady-state values (dotted red).

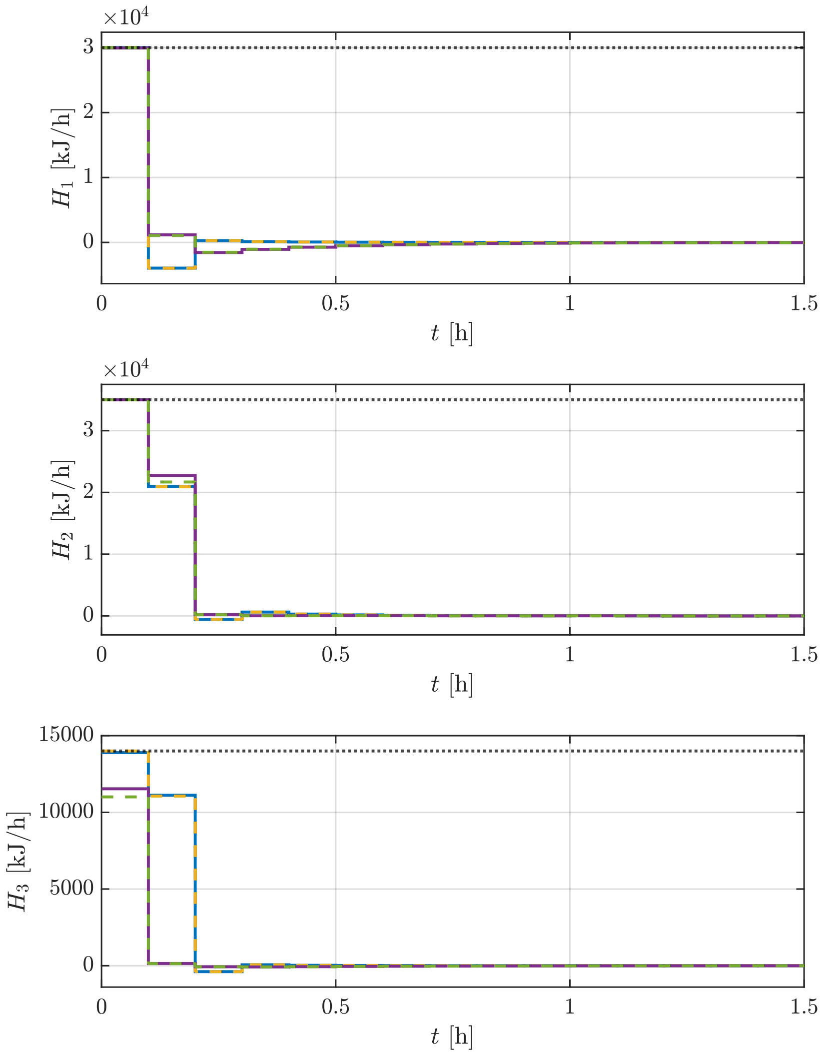


**Figure 5.3:** Closed-loop control trajectories of MVs: non-tunable tube MPC for scaling factor $\rho = 0$ (solid blue), tunable tube MPC for $\rho = 0$ and relaxed constraints (dashed yellow), non-tunable tube MPC for $\rho = 1$ (solid purple), tunable tube MPC for $\rho = 1$ and relaxed constraints (dashed green), constraints on control inputs (dotted black).

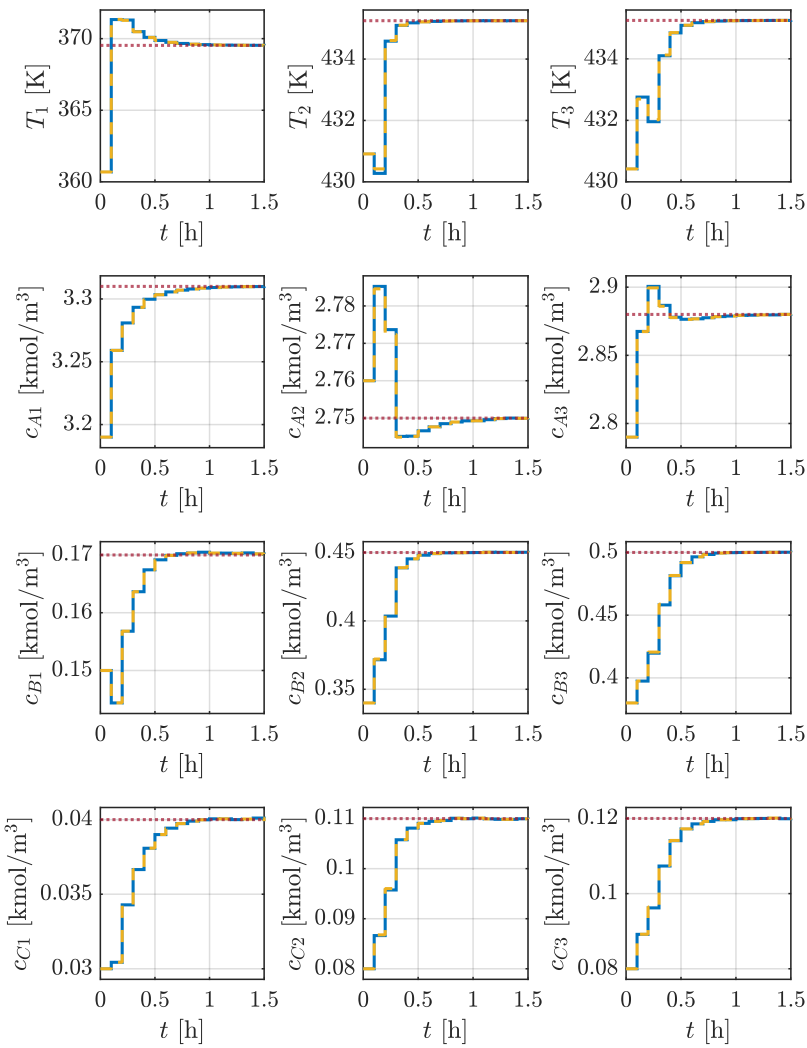


**Figure 5.4:** Closed-loop control trajectories of CVs for scaling factor $\rho = 0.5$: non-tunable tube MPC (solid blue), tunable tube MPC with relaxed constraints (dashed yellow), and steady-state values (dotted red).

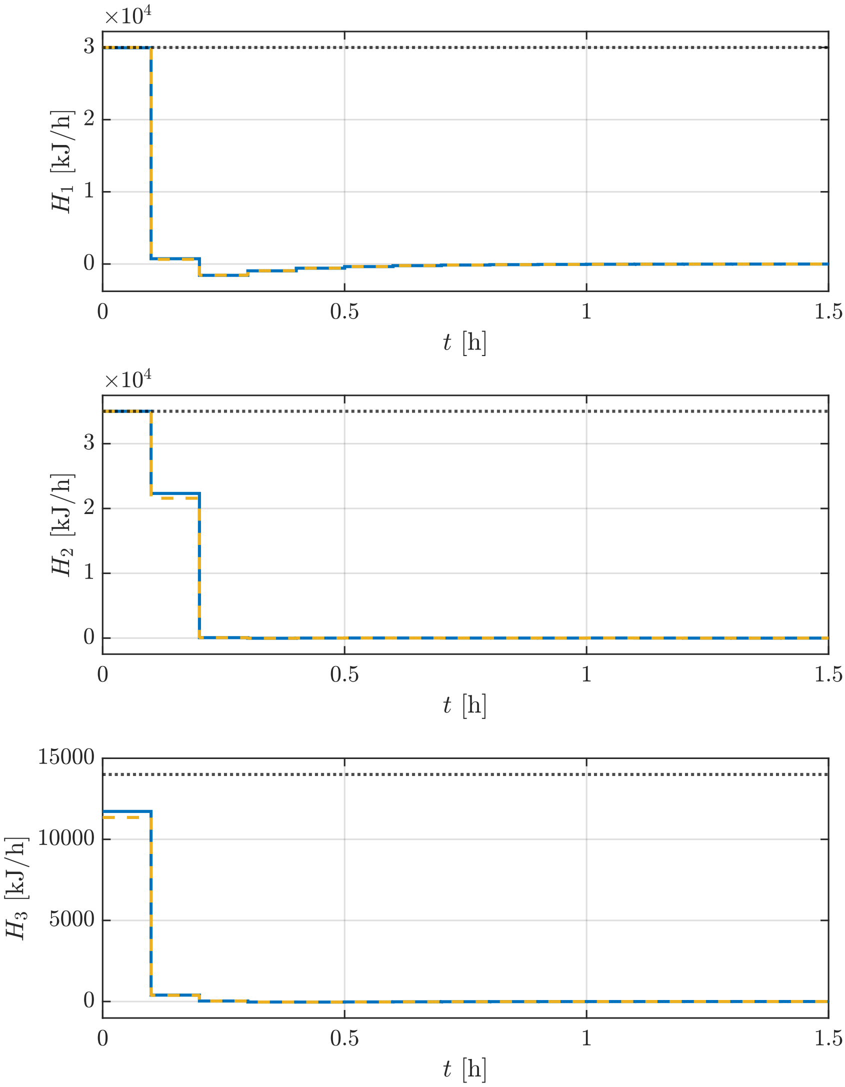


**Figure 5.5:** Closed-loop control trajectories of MVs for $\rho = 0.5$: non-tunable tube MPC (solid blue), tunable tube MPC with relaxed constraints (dashed yellow) and constraints on control inputs (dotted black).

**Table 5.2:** Performance analysis for the large-scale benchmark.

| Tuning | $N_{\mathrm{S}}^{\star}$ | $\alpha^{\star} \cdot 10^{-4}$ | $J^{\star} \cdot 10^{9}$ | $J_{\mathrm{rel}}^{\star} \cdot 10^{9}$ | $\hat{J}_{\mathrm{rel}} \cdot 10^{9}$ | $\Delta J[\%]$ |
|---|---|---|---|---|---|---|
| $\rho = 0$ | 13 | 24.4657 | 0.4762 | 0.4756 | 0.4756 | 0.1239 |
| $\rho = 0.25$ | 21 | 3.2873 | 7.4214 | 7.3506 | 7.3506 | 0.9536 |
| $\rho = 0.50$ | 23 | 1.9005 | 14.3635 | 14.1645 | 14.1645 | 1.3851 |
| $\rho = 0.75$ | 26 | 2.3704 | 21.3389 | 20.9725 | 20.9725 | 1.7170 |
| $\rho = 1$ | 29 | 2.1442 | 28.3491 | 27.7784 | 27.7784 | 2.0132 |

The numerical results of the closed-loop simulations are summarized in Table 5.2, where $J^{\star}$ denotes the closed-loop cost achieved by the non-tunable tube MPC optimization problem in (4.4) [56], $J_{\mathrm{rel}}^{\star}$ denotes the closed-loop cost obtained by the non-tunable tube MPC with relaxed constraints (5.1), and $\hat{J}_{\mathrm{rel}}$ denotes the closed-loop cost obtained by the tunable tube MPC optimization problem in (5.4) with relaxed constraints (5.1).

The fixed-parameter tunable design primarily trades optimality for computational simplicity. As reported in Table 5.2, the resulting performance loss $\Delta J$ remains below 2.01 % for all tuning setups, while completely eliminating the need for online recomputation of the tube parameters.

## 5.3 Discussion

This chapter has presented real-time tunable implicit tube MPC for constrained systems. The formulation allows the input-penalty matrix $\hat{R}$ to be adjusted through a scalar tuning parameter without repeating the complete tube MPC redesign. The controller preserves the robust stability and recursive feasibility properties of implicit tube MPC while making the closed-loop behavior adjustable after the offline design stage.

The main contribution is the use of appropriate fixed tube-design parameters $\hat{N}_{\mathrm{S}}$, $\hat{\alpha}$, and $\hat{f}$ over the admissible tuning range. This removes the need to recompute the tube-related quantities $N_{\mathrm{S}}^{\star}$, $\alpha^{\star}$, and $f^{\star}$ whenever the penalty factor is changed. The relaxed first-step constraints further simplify the real-time formulation by avoiding the direct inclusion of the tube cross-section in the initial state constraint, while preserving feasibility, constraint satisfaction, and closed-loop stability.

The reactor-separator benchmark, based on the results published in [52], indicates that the tunable controller gives closed-loop trajectories close to those of the non-tunable implicit tube MPC reference for the tested tuning values. Across the tested tuning values, the performance loss remained below $\approx 2\,\%$, while the repeated redesign of tube parameters was removed from the online tuning loop. The method is therefore aimed at operation in which the desired trade-off between fast response and conservative input use changes during runtime while robust constraint handling must be retained.

Chapter 6

# Conclusions

This thesis addresses the design of safe and tunable MPC for constrained systems affected by bounded disturbances, plant–model mismatch, online tuning requirements, and embedded implementation limits. Throughout the thesis, safety was understood in terms of constraint satisfaction, recursive feasibility, and robust closed-loop stability. Tunability was considered as the possibility of modifying closed-loop performance after the initial MPC controller construction, but without repeating the complete synthesis procedure. Three main groups of methods were discussed: set-based tube MPC, implicit tube MPC, and tunable implicit tube MPC.

A central part of the thesis focused on tube MPC. The set-based and elastic tube MPC formulations in Chapter 3 were implemented and validated on systems of different complexity. The rigid tube MPC experiment on the laboratory heat exchanger quantified how robust constraint margins affect the closed-loop response and hot-medium consumption. The results demonstrated that tracking performance, actuator use, and energy demand are closely coupled tuning decisions.

The elastic tube formulation was used in Chapter 3 to reduce the conservatism of a fixed tube cross-section by allowing the tube geometry to vary along the prediction horizon. This advantage was verified on the embedded heat-exchanger platform, where the designed MPC controller recovered from an actuation interruption without redesign or retuning.

Chapter 4 analyzed the scalability advantage of avoiding a set-based tube construction in implicit tube MPC. This was validated in the reactor-separator benchmark, where the implicit tube formulation was successfully implemented and validated, while the corresponding set-based tube design was not tractable due to the high dimensionality of the system. Experimental validation on the Versatile Simulator for Near-zero Emissions Agriculture (VESNA) smart greenhouse further confirmed that the designed tube MPC controller can handle various real-world challenges, including sensor noise, actuator limits, cloud communication, and coupled temperature–humidity dynamics. These results support the application of the designed implicit tube MPC formulations to complex systems.

The validation in Chapter 4 was also extended to cases with industrially oriented implementation and modeling requirements. In the HHIDiS case study, the offset-free implicit tube MPC formulation compensated for plant–model mismatch caused by changing fouling conditions. The selected implicit tube MPC tuning reduced the condenser-pressure tracking RMSE by approximately 35.4 % relative to the PID baseline in the considered control scenarios. In the reboiler-temperature tracking task, the conservative robust tuning eliminated overshoot for all considered fouling levels. These results demonstrated that robust controller tuning can be determined according to the operating priority: reducing settling time, smoothing control trajectories, increasing safety margins, or lowering heating-medium consumption. The same tuning approach also reduced the fuel cost and the associated $CO_2$ emissions, which confirms that the offset-free implicit tube MPC formulation can support both constraint-aware operation under fouling and more energy-conscious operation.

The software implementation presented in Chapters 3 and 4 is another relevant outcome of these robust MPC case studies. Rigid, elastic, and implicit tube MPC frameworks were integrated into the open-source MPT+ software toolbox, including controller construction, closed-loop simulation, visualization, and implementation. This reduces the manual work needed when moving from the theoretical tube MPC controller construction to a compact controller that can be evaluated in simulation or deployed experimentally. The MPT+ implementation therefore not only makes tube MPC design methods easier to use, but also provides a repeatable way to construct and analyze the controllers implemented in the simulation and experimental studies.

Chapter 5 presented a tunable implicit tube MPC formulation. The aim was to allow online adjustment of the penalty factors in the objective function without recomputing the tube-design parameters at every tuning instant. Fixed tube-design parameters were introduced to preserve recursive feasibility and robust stability over the admissible tuning interval. The relaxed first-step constraints were used to reduce the conservatism of the initial prediction step, extend the feasible set where possible, and improve the closed-loop cost without changing the constraints imposed on the remaining prediction steps. On the reactor-separator benchmark, the resulting performance loss remained negligible over the tested tuning range compared with the corresponding non-tunable implicit tube MPC designs, while repeated recomputation of $N_{\mathrm{S}}$, $\alpha$, and the constraint-tightening vector was avoided.

The results of this thesis demonstrate that robust and tunable MPC can be integrated into a compact design framework that preserves the relevant theoretical guarantees when the tuning mechanism is considered during tube MPC controller design. The resulting MPC controllers were evaluated not only in numerical simulations, but also through software implementation, laboratory experiments, and industrially motivated benchmarks. The tube-based methods provide the safety margins needed to handle disturbances and plant–model mismatch, while the tuning mechanisms modify performance within ranges for which the controller remains feasible, stable, and executable on the target platform.

## Main Contributions

The main contributions of this thesis include the development, implementation, and validation of safe and tunable MPC methods for embedded and implementation-oriented control problems. The specific contributions are summarized below, together with the corresponding publications in which the results were presented after peer review.

- **Safe tube MPC for uncertain systems: implementation, analysis, and validation.** The tube-based robust MPC strategies considered in Chapters 3–4 were systematically implemented, analyzed, and validated for constrained systems affected by bounded disturbances and plant–model mismatch. The validation covered the design and implementation of (i) rigid tube MPC on a laboratory heat exchanger, (ii) elastic tube MPC with embedded experimental validation, (iii) implicit tube MPC on a large-scale reactor-separator numerical benchmark and laboratory implementation on the smart greenhouse VESNA, and (iv) offset-free implicit tube MPC for the industrially oriented HHIDiS numerical case study. These results demonstrated that safe tube-based MPC can provide robust constraint satisfaction mechanisms in laboratory, embedded, large-scale, and industrially motivated settings. The corresponding results were published in:
  - **E. Pavlovičová** – J. Oravec – M. Trafczynski – M. Markowski – S. Alabrudzinski – P. Kisielewski – K. Urbaniec: Energy and Carbon Footprint Reduction for Hybrid Heat-Integrated Distillation Systems: Robust Model Predictive Control Approach. Energy, vol. 334, 2025.
    (WoS: D1/Q1, IF: 9.4, citations: 2)
  - J. Holaza – **E. Plšičík Pavlovičová** – S. Serhiienko – J. Oravec: End-to-End Elastic Tube MPC: Design, Analysis, and Embedded Implementation. In IFAC World Congress 2026, Busan, South Korea (**corresponding author**, accepted).
  - **E. Pavlovičová** – B. Daráš – P. Bakaráč – M. Fikar – J. Oravec: From Theory to Harvest: Robust MPC Supervising Smart Greenhouse System. In Proceedings of the 2025 25th International Conference on Process Control, IEEE, pp. 1–6, 2025 (**corresponding author**).
  - **E. Pavlovičová** – J. Holaza – L. Galčíková – J. Oravec: Introducing Implicit Tube Model Predictive Control to MPT+: Efficient Design for Large-Scale Systems. In American Control Conference 2025 (ACC25), Denver, Colorado, USA, pp. 33–38, 2025 (**corresponding author**).

   - J. Holaza – K. Kvasnicová – **E. Pavlovičová** – J. Oravec: Tube MPC Extension of MPT: Experimental Analysis. In Proceedings of the 2023 24th International Conference on Process Control, IEEE, Slovak University of Technology in Bratislava, Radlinského 9, 81237, Bratislava, Slovakia, pp. 120–125, 2023 (**presented by author, corresponding author**).

- **Real-time tunability of implicit tube MPC.** A novel tunable implicit tube MPC framework was developed to adjust closed-loop performance through penalty tuning without a complete redesign of the tube ingredients, see Chapter 5. The formulation uses fixed tube-design parameters to preserve recursive feasibility and robust stability guarantees over the admissible tuning range. Relaxed first-step constraints reduce the conservatism of the initial prediction step without changing the remaining tightened constraints. The reactor-separator benchmark confirmed that the tunable formulation avoids repeated tube-parameter redesign while maintaining closed-loop performance close to the corresponding conventional non-tunable implicit tube MPC designs. This contribution supports the goal of real-time tunability in implicit tube MPC and was recently published in:

   - **E. Plšičík Pavlovičová** – L. Galčíková – J. Holaza – J. Oravec: Real-Time Tunable Rigid Tube MPC Using Implicit Formulation. Journal of Process Control, vol. 163, article 103750, 2026.
     (**corresponding author**, WoS: Q2, IF: 3.9)

- **Open-source software-supported implementation of tube-based controllers.** Rigid, elastic, and implicit tube MPC methods were implemented in the MPT+ toolbox for MATLAB, providing controller design, closed-loop performance analysis, visualization, and implementation support. The implementation automates several geometric and optimization steps of the tube construction and makes the resulting MPC controllers available for analysis, comparison, and deployment. This contribution supports the goal of software-assisted tube-based controller design by translating the theoretical constructions into executable and reusable open-source controller-design tools.

  The MPT+ toolbox described in Chapters 3 and 4 of this thesis is freely available on GitHub:

   - `https://github.com/holaza/mptplus/wiki`

  The software-related peer-reviewed results were published in:

   - J. Holaza – **E. Plšičík Pavlovičová** – S. Serhiienko – J. Oravec: End-to-End Elastic Tube MPC: Design, Analysis, and Embedded Implementation. In IFAC World Congress 2026, Busan, South Korea (**corresponding author**, accepted).

– **E. Pavlovičová** – J. Holaza – L. Galčíková – J. Oravec: Introducing Implicit Tube Model Predictive Control to MPT+: Efficient Design for Large-Scale Systems. In American Control Conference 2025 (ACC25), Denver, Colorado, USA, pp. 33–38, 2025 (**corresponding author**).

– J. Holaza – K. Kvasnicová – **E. Pavlovičová** – J. Oravec: Tube MPC Extension of MPT: Experimental Analysis. In Proceedings of the 2023 24th International Conference on Process Control, IEEE, Slovak University of Technology in Bratislava, Radlinského 9, 81237, Bratislava, Slovakia, pp. 120–125, 2023 (**presented by author, corresponding author**).

APPENDIX A

# Resumé

Táto dizertačná práca sa zaoberá bezpečným a laditeľným prediktívnym riadením (angl. Model Predictive Control, MPC) ohraničených systémov, ktoré sú ovplyvnené neurčitosťami, nesúladom medzi predikčným modelom a reálnym riadeným procesom a implementačnými obmedzeniami. V priemyselných a laboratórnych aplikáciách regulátor často pracuje v blízkosti fyzikálnych, bezpečnostných alebo ekonomických limitov. Je nevyhnutné zohľadniť, že akčné členy majú obmedzený rozsah, stavové veličiny musia zostať v prípustnej oblasti a prevádzkové podmienky sa môžu meniť v čase. Prediktívne riadenie je vhodné na riešenie takýchto úloh, pretože umožňuje zahrnúť dynamiku systému, vstupné a stavové ohraničenia a požadované kritériá kvality riadenia priamo do optimalizačnej úlohy návrhu regulátora.

Schopnosť MPC pracovať s ohraničeniami je zároveň spojená s výpočtovou náročnosťou. Zložitosť optimalizačnej úlohy rastie s počtom stavov, vstupov, ohraničení a predikčných krokov. Tento problém je výrazný najmä pri robustných formuláciách, veľkorozmerných systémoch a implementácii na platformách s obmedzeným výpočtovým výkonom alebo pamäťou. Nominálne MPC dokáže reagovať na poruchy spätnou väzbou, ale to nezaručuje splnenie ohraničení pre všetky prípustné realizácie porúch. Robustné MPC preto rozširuje návrh a formuláciu regulátora tak, aby sa zachovala rekurzívna riešiteľnosť, robustná stabilita a splnenie ohraničení aj pri pôsobení ohraničených neurčitostí.

Ťažiskom tejto dizertačnej práce je MPC založené na tubách (angl. Tube MPC, TMPC). Základnou myšlienkou tejto triedy metód riadenia je predikovať nominálnu trajektóriu a zabezpečiť, aby skutočná trajektória systému zostala v jej okolí, teda v invariantnej množine označovanej ako tuba. Ohraničenia nominálneho systému sa následne sprísnia tak, aby pôvodné ohraničenia procesu boli dodržané pre všetky prípustné realizácie poruchy. Bezpečnosť je v rámci tejto dizertačnej práce chápaná ako splnenie ohraničení, a zabezpečenie rekurzívnej riešiteľnosti a robustnej stability uzavretého regulačného obvodu. Laditeľnosť znamená možnosť prispôsobiť správanie regulátora po jeho začiatočnej syntéze, teda počas riadenia v reálnom čase, bez potreby opakovať celý postup návrhu regulátora so zmenenými parametrami.

Prvá množina dosiahnutých výsledkov sa zameriava na implementáciu a validáciu robustného MPC založeného na tubách v rigidnej, elastickej a implicitnej formulácii. Rigidné MPC založené na tubách bolo navrhnuté a experimentálne overené na laboratórnom výmenníku tepla. Namerané výsledky kvantifikovali, ako sprísňovanie ohraničeniach a uvažovanie ohraničených porúch ovplyvňujú uzavretý regulačný obvod a spotrebu ohrevného média. Zároveň sa ukázalo, že maximálne pregulovanie, čas ustálenia, spotreba ohrevného média a energetická náročnosť riadenia predstavujú úzko previazané rozhodnutia pri ladení regulátora.

Elastická formulácia MPC založeného na tubách bola použitá na zníženie konzervatívnosti rigidného prierezu tuby. Na rozdiel od rigidnej tuby umožňuje, aby sa geometria tuby menila v každom kroku riadenia aj v rámci predikčného horizontu. Táto vlastnosť bola overená na vstavanej platforme výmenníka tepla. Navrhnutý regulátor dodržal ohraničenia akčných zásahov a po dočasnom výpadku akčného zásahu sa vrátil k riadeniu bez potreby nového návrhu alebo dodatočného ladenia. Namerané výsledky potvrdzujú, že flexibilnejšia reprezentácia tuby môže znížiť konzervatívnosť robustného riadenia a zároveň zachovať požadované bezpečnostné vlastnosti.

Ďalšia časť tejto práce analyzuje implicitné MPC založené na tubách ako škálovateľnú alternatívu ku klasickej konštrukcii založenej na množinových operáciách. Výpočet robustne invariantných množín, Pontryaginových rozdielov a terminálnych množín môže byť pri systémoch s väčším počtom stavov a ohraničení numericky náročné alebo neuskutočniteľné. Implicitná formulácia sa týmto náročným množinovým operáciám vyhýba tak, že tubu reprezentuje nepriamo pomocou pomocných premenných a ohraničení založených na podporných funkciách. Táto metóda riadenia bola validovaná na prípadovej štúdii systému reaktor–separátor, kde sa implicitná formulácia úspešne implementovala a analyzovala, zatiaľ čo zodpovedajúci rigidný MPC regulátor založený na tubách nebolo možné skonštruovať pre zložitosť riadeného systému.

Implicitné MPC založené na tubách bolo experimentálne overené aj na riadení inteligentného skleníka VESNA. Táto prípadová štúdia ukázala použiteľnosť navrhnutého regulátora pri reálnych implementačných vplyvoch, akými sú šum meraní, limitované akčné členy, sieťová komunikácia, poruchy z externého prostredia a previazaná dynamika riadených veličín. Úlohou navrhnutého regulátora bolo zabezpečiť sledovanie žiadanej hodnoty aj v prípade, keď zásah do jednej riadenej veličiny ovplyvňuje druhú riadenú veličinu. Táto vzájomná previazanosť riadených veličín neumožňuje efektívne využitie jednoduchších samostatných regulátorov, akým je napríklad PID regulátor.

Experimentálne výsledky podporujú výhody implementácie implicitného MPC založeného na tubách pre komplexnejšie systémy, pri ktorých je potrebné spojiť robustné ohraničenia s praktickou implementáciou.

Robustná implicitná formulácia bola rozšírená aj na úlohy s priemyselným aplikačným rámcom a na problémy riadenia spôsobené nesúladom predikčného modelu s riadeným procesom. V prípadovej štúdii hybridnej rektifikačnej kolóny s integrovaným ohrevom bolo použité implicitné MPC založené na tubách bez trvalej regulačnej odchýlky. Model bol rozšírený o poruchové stavy, aby regulátor dokázal kompenzovať zmenu vlastností zariadenia spôsobenú zanášaním teplovýmenných plôch. Pri sledovaní tlaku v kondenzátore navrhnuté robustné ladenie znížilo hodnotu RMSE približne o 35.4 % v porovnaní s referenčným PID regulátorom v uvažovaných riadiacich scenároch. Pri sledovaní teploty vo variči konzervatívne robustné ladenie navyše odstránilo preregulovanie pre všetky uvažované úrovne zanášania. Dosiahnuté výsledky ukázali, že robustné ladenie možno voliť podľa prevádzkovej priority, napríklad podľa požiadavky na kratší čas ustálenia, plynulejšie akčné zásahy alebo nižšiu spotrebu ohrevného média.

Súčasťou priemyselne orientovanej štúdie bola aj systémová analýza energetických a environmentálnych ukazovateľov. Použitie implicitného MPC založeného na tubách bez trvalej regulačnej odchýlky umožnilo znížiť náklady na spotrebu paliva a súvisiace emisie oxidu uhličitého. Tento výsledok práce potvrdzuje, že robustné prediktívne riadenie môže podporovať nielen bezpečnú prevádzku pri neurčitostiach a zanášaní, ale aj energeticky úspornejšie rozhodovanie. V kontexte procesného priemyslu je to dôležité, pretože kvalita regulácie, spotreba energie a dodržanie ohraničení sú navzájom úzko previazané.

Ďalším významným výstupom robustných prípadových štúdií je aj softvérová implementácia uvažovaných pokročilých metód riadenia. Rigidné, elastické a implicitné formulácie MPC založeného na tubách boli integrované do voľne prístupného softvérového nástroja MPT+. Implementácia pokrýva konštrukciu regulátora, simuláciu uzavretého regulačného obvodu, vizualizáciu a prípravu na praktické nasadenie na vnorených platformách. Tým sa znižuje množstvo manuálnej práce potrebnej pri prechode od teoretického návrhu k regulátoru, ktorý možno analyzovať v simulácii alebo overiť experimentálne. Softvérová podpora zároveň vytvára opakovateľný postup návrhu, porovnávania a implementácie MPC regulátorov založených na tubách.

Ďalšia skupina dosiahnutých výsledkov sa venuje laditeľnému implicitnému MPC založenému na tubách. Cieľom bolo umožniť v reálnom čase meniť váhové matice v účelovej funkcii bez potreby opakovane prepočítavať parametre návrhu tuby pri každej zmene ladenia. Zmena váhových matíc môže pri robustnom MPC ovplyvniť spätnoväzbové zosilnenie, sprísnené ohraničenia, terminálne podmienky aj samotnú tubu. Preto boli uvažované fixné parametre návrhu tuby, ktoré zachovávajú rekurzívnu riešiteľnosť a robustnú stabilitu pre celý prípustný interval ladenia.

V navrhnutej laditeľnej formulácii TMPC boli použité aj uvoľnené ohraničenia v prvom predikčnom kroku. Ich úlohou je znížiť konzervatívnosť začiatočného kroku, rozšíriť množinu prípustných počiatočných stavov vtedy, keď je to umožnené, ako aj zlepšiť hodnotu kritéria kvality bez zmeny sprísnených ohraničení pre ďalšie predikčné kroky. Na príklade riadenia systému reaktor–separátor zostala strata kvality riadenia v testovanom intervale ladenia zanedbateľná v porovnaní so zodpovedajúcimi neladiteľnými implicitnými MPC regulátormi založenými na tubách. Zároveň sa odstránila potreba opakovane prepočítavať pomocné parametre $N_\mathrm{S}$, $\alpha$ a vektor sprísnenia ohraničení. Navrhnutá formulácia tak umožňuje meniť správanie uzavretého regulačného obvodu v reálnom čase, pričom zachováva požadované teoretické garancie.

Hlavné prínosy dizertačnej práce možno zhrnúť do troch oblastí. Prvým prínosom je implementácia, analýza a validácia bezpečných robustných MPC stratégií založených na tubách pre systémy s ohraničenými poruchami a nesúladom medzi predikčným modelom a riadeným procesom. Validácia zahŕňala laboratórny výmenník tepla, vnorenú platformu, veľkorozmerný systém reaktor–separátor, inteligentný skleník VESNA a priemyselne motivovanú štúdiu hybridnej rektifikačnej kolóny. Druhým prínosom práce je formulácia laditeľného implicitného MPC založeného na tubách, ktorá umožňuje meniť penalizačné faktory v reálnom čase bez kompletného prepracovania návrhu tuby a bez straty rekurzívnej riešiteľnosti a robustnej stability v prípustnom rozsahu ladenia. Tretím prínosom je voľne dostupná softvérová implementácia týchto robustných prediktívnych regulátorov pre neurčité systémy v prostredí MPT+, ktorá podporuje návrh, ladenie, analýzu, simuláciu, vizualizáciu a prípravu experimentálnej implementácie. Prínosy tejto dizertačnej práce tak spoločne predstavujú komplexnú metodiku návrhu bezpečného a laditeľného prediktívne riadenie pre neurčité systémy, čím sa prepájajú teoretické garancie bezpečnosti s požiadavkami praktickej flexibility a implementovateľnosti.

Appendix B

# Author's Publications

The research activity of the author is represented by the following publications:

**Articles published in CC Journals:**

- **E. Plšičík Pavlovičová** – L. Galčíková – J. Holaza – J. Oravec: Real-Time Tunable Rigid Tube MPC Using Implicit Formulation. Journal of Process Control, vol. 163, article 103750, 2026 (**corresponding author**, WoS: Q2, IF: 3.9).
- **E. Pavlovičová** – J. Oravec – M. Trafczynski – M. Markowski – S. Alabrudzinski – P. Kisielewski – K. Urbaniec: Energy and Carbon Footprint Reduction for Hybrid Heat-Integrated Distillation Systems: Robust Model Predictive Control Approach. Energy, vol. 334, 2025 (WoS: D1/Q1, IF: 9.4, citations: 2).
- M. Markowski – M. Trafczynski – **E. Pavlovičová** – J. Oravec – S. Alabrudzinski – P. Kisielewski – K. Urbaniec – K. Elwertowski – D. Gostynski: Impact of Industrial Constraints on the Dynamic Performance of a PID-Controlled Hybrid Heat-Integrated Distillation System with a Plate Heat and Mass Exchanger. International Journal of Heat and Mass Transfer, vol. 252, 2025 (WoS: D1/Q1, IF: 5.8, citations: 2).
- M. Wadinger – R. Fáber – **E. Pavlovičová** – R. Paulen: Carbon neutral greenhouse: Economic model predictive control framework for education. European Journal of Control, vol. 83, pp. 101297, 2025 (WoS: Q2, IF: 2.5).

**Articles in Conference Proceedings:**

- J. Holaza – **E. Plšičík Pavlovičová** – S. Serhiienko – J. Oravec: End-to-End Elastic Tube MPC: Design, Analysis, and Embedded Implementation. In IFAC World Congress 2026 Busan, South Korea (**corresponding author**, accepted).

- P. Bakaráč – **E. Pavlovičová** – M. Klaučo – A. Oravec: Bayesian Optimization-Based Tunable Explicit MPC on a Pocket-Sized Embedded Platform. In IEEE 64th Conference on Decision and Control, IEEE, Rio de Janeiro, Brazil, pp. 4663–4670, 2025 (**presented by author, corresponding author**).
- **E. Pavlovičová** – B. Daráš – P. Bakaráč – M. Fikar – J. Oravec: From Theory to Harvest: Robust MPC Supervising Smart Greenhouse System. In Proceedings of the 2025 25th International Conference on Process Control, IEEE, pp. 80–85, 2025 (**corresponding author**).
- **E. Pavlovičová** – J. Holaza – L. Galčíková – J. Oravec: Introducing Implicit Tube Model Predictive Control to MPT+: Efficient Design for Large-Scale Systems. In American Control Conference 2025 (ACC25), Denver, Colorado, USA, pp. 33–38, 2025 (**corresponding author**).
- **E. Pavlovičová** – J. Vargan – P. Bakaráč – M. Fikar – J. Oravec: Offset-free MPC of Temperature in Smart Greenhouse VESNA. In Preprints of the 8th IFAC Conference on Nonlinear Model Predictive Control, IFAC, pp. 314–317, 2024 (**presented by author, corresponding author**).
- J. Oravec – P. Bakaráč – **E. Pavlovičová** – M. Fikar: Smart Eco Greenhouse VESNA. In IFAC World Congress 2023, Yokohama, Japan, pp. 10295–10300, 2023 (**presented by author**).
- R. Kohút – **E. Pavlovičová** – K. Fedorová – J. Oravec – M. Kvasnica: Real-Time Deep-Learning-Driven Parallel MPC. In 62nd IEEE Conference on Decision and Control, IEEE, Singapore, 2023.
- J. Holaza – K. Kvasnicová – **E. Pavlovičová** – J. Oravec: Tube MPC Extension of MPT: Experimental Analysis. In Proceedings of the 2023 24th International Conference on Process Control, IEEE, Slovak University of Technology in Bratislava, Radlinského 9, 81237, Bratislava, Slovakia, pp. 120–125, 2023 (**presented by author, corresponding author**).

Appendix C

# Curriculum Vitae


## Erika Plšičík Pavlovićová

| | |
|---|---|
| Email: | erika.pavlovicova@stuba.sk |
| Homepage: | https://www.uiam.sk/~pavlovicova |
| ORCID iD: | 0000-0003-4335-8347 |
| Web of Science: | GQQ-1878-2022 |
| Year of Birth: | 1998 |


## Education

- 2022 – present
  PhD-study: Faculty of Chemical and Food Technology, STU in Bratislava
  Study Program: Process Control
  - 2024 Dean's Award for activities for the benefit of the faculty
  - 2025 Dean's Award for activities for the benefit of the faculty
- 2020 – 2022
  Master's study: Faculty of Chemical and Food Technology, STU in Bratislava
  Study Program: Automation and Information Engineering in Chemistry and Food Industry
  - Graduated *Magna Cum Laude*
  - Award for outstanding master thesis by Humusoft
- 2017 – 2020
  Bachelor's study: Faculty of Chemical and Food Technology, STU in Bratislava
  Study Program: Chemistry, Medical Chemistry, and Chemical Materials
  - Graduated *Magna Cum Laude*

# International Visits and Study Stays

- 2026 – University of Pisa, Italy
  Supervised by Prof. Gabriele Pannocchia, 1 month

- 2025 – University of Pisa, Italy
  Supervised by Prof. Gabriele Pannocchia, 1 month

- 2023 – Shinshu University, Nagano, Japan
  Supervised by Prof. Yuichi Chida, 1 week

- 2023 – EECI International Graduate School on Control: Learning-based Predictive Control, Zurich, Switzerland
  Supervised by Prof. Melanie Zeilinger, 1 week

# Research Grants

The author of the thesis has been involved in several research projects focusing on robust and optimal control, scalable technologies, industrial monitoring, process automation, and energy-efficient operation.

## Internal STU Scheme

- 2026 – 2027 Optimal process control using computer vision
  Principal investigator

- 2025 – 2025 Distributed nonlinear model predictive control for sustainable control of chemical-technological plants
  Principal investigator

- 2024 – 2024 Carbon footprint reduction using optimization-based control methods
  Principal investigator

## European Projects

- 2022 – 2025 Fostering Opportunities Towards Slovak Excellence in Advanced Control for Smart Industries
  Investigator

### APVV Research Projects

- 2025 – 2028 Robust Optimal Control of Processes
  Investigator

### VEGA Research Projects

- 2026 – 2029 Balanced Optimal Control for Scalable Technologies
  Investigator
- 2025 – 2028 Safe and Reliable Industrial Monitoring, Optimization, and Control
  Investigator
- 2022 – 2025 Controller design methods for low-level carbon footprint process automation
  Investigator
- 2021 – 2024 Efficient control of industrial plants using data
  Investigator

## Teaching Activities

- Automatic Control Theory III (Master's study, laboratory exercises, 4 semesters)
- Fundamentals of MATLAB (Bachelor's study, laboratory exercises, 2 semesters)
- Laboratory Exercises of Process Control (Master study, laboratory exercises, 2 semesters)
- Robust Control (Master's study, seminars, 4 semesters)
- Semester Project I–III (Master's study, laboratory exercises, 6 semesters)
- Co-supervision of master theses:
  - 2023 – 2024 Richard Fodor: ALADIN-Based Distributed Model Predictive Control Design
    Award for outstanding master thesis by Humusoft
  - 2024 – 2025 Branislav Daráš: Robust Model Predictive Control Design for a Smart Greenhouse
    Award for outstanding master thesis by Humusoft
  - 2025 – 2026 Michal Hvolka: Advanced Controller Design and Implementation for Embedded Platforms

# Community Engagement

- 2022 – 2025
  International Student Scientific Conference, Vice-Chairperson of the Organizing Committee

- 2024 – present
  Academic Senate of the Faculty of Chemical and Food Technology, STU in Bratislava, student representative, Vice-Chairperson

# Bibliography

[1] A. Alessio and A. Bemporad. A survey on explicit model predictive control. In L. Magni, D. M. Raimondo, and F. Allgöwer, editors, *Nonlinear Model Predictive Control*, volume 384 of *Lecture Notes in Control and Information Sciences*, pages 345–369. Springer Berlin Heidelberg, 2009.

[2] L. Aolaritei, M. Fochesato, J. Lygeros, and F. Dörfler. Wasserstein tube MPC with exact uncertainty propagation, 2023.

[3] P. Bakaráč, E. Pavlovičová, M. Klaučo, and J. Oravec. Bayesian optimization-based tunable explicit MPC on a pocket-sized embedded platform. In *2025 IEEE 64th Conference on Decision and Control (CDC)*, pages 4663–4670, 2025.

[4] A. Bemporad, M. Morari, V. Dua, and E. N. Pistikopoulos. The explicit linear quadratic regulator for constrained systems. *Automatica*, 38:3–20, 2002.

[5] F. Borrelli, A. Bemporad, and M. Morari. *Predictive Control for Linear and Hybrid Systems*. Cambridge University Press, Cambridge, 2017.

[6] S. Chen, K. Saulnier, N. Atanasov, D. D. Lee, V. Kumar, G. J. Pappas, and M. Morari. Approximating explicit model predictive control using constrained neural networks. In *American Control Conference*, pages 1520–1527, 2018.

[7] L. Chisci, J. Rossiter, and G. Zappa. Systems with persistent disturbances: predictive control with restricted constraints. *Automatica*, 37(7):1019–1028, 2001.

[8] J. Coulson, J. Lygeros, and F. Dörfler. Distributionally robust chance constrained data-enabled predictive control. *IEEE Transactions on Automatic Control*, 67(7):3289–3304, 2022.

[9] S. Diaconescu, F. Stoican, B. D. Ciubotaru, and S. Olaru. Elastic tube model predictive control with scaled zonotopic sets. *IEEE Control Systems Letters*, 8:1343–1348, 2024.

[10] M. Farina and R. Scattolini. Tube-based robust sampled-data MPC for linear continuous-time systems. *Automatica*, 48(7):1473–1476, 2012.

[11] G. Frison, D. K. M. Kufoalor, L. Imsland, and J. B. Jørgensen. Efficient implementation of solvers for linear model predictive control on embedded devices. In *2014 IEEE Conference on Control Applications*, pages 1954–1959, 2014.

[12] T. Geyer, F. D. Torrisi, and M. Morari. Optimal complexity reduction of polyhedral piecewise affine systems. *Automatica*, 44(7):1728–1740, 2008.

[13] L. Grüne, F. Allgöwer, R. Findeisen, J. Fischer, D. Groß, U. D. Hanebeck, B. Kern, M. A. Müller, J. Pannek, M. Reble, O. Stursberg, P. Varutti, and K. Worthmann. Distributed and networked model predictive control. In J. Lunze, editor, *Control Theory of Digitally Networked Dynamic Systems*, pages 111–167. Springer US, 2014.

[14] M. Herceg, M. Kvasnica, C. N. Jones, and M. Morari. Multi-Parametric Toolbox 3.0. In *Proceedings of the European Control Conference*, pages 502–510, Zurich, Switzerland, 2013.

[15] R. Heydari and M. Farrokhi. Robust tube-based model predictive control of LPV systems subject to adjustable additive disturbance set. *Automatica*, 129:109672, 2021.

[16] J. Holaza, L. Galčíková, J. Oravec, and M. Kvasnica. A software package for MPC design and tuning: MPT+. In *62nd IEEE Conference on Decision and Control*, pages 5682–5689, Singapore, December 13–15 2023. IEEE.

[17] J. Holaza, K. Kvasnicová, E. Pavlovičová, and J. Oravec. Tube MPC extension of MPT: Experimental analysis. In *2023 24th International Conference on Process Control (PC)*, pages 120–125, 2023.

[18] J. Holaza, E. P. Pavlovičová, S. Serhiienko, and J. Oravec. End-to-end elastic tube MPC: Design, analysis, and embedded implementation. *IFAC-PapersOnLine*, 2026. 23rd IFAC World Congress, accepted.

[19] B. Houska, M. Müller, and M. Villanueva. Control lyapunov function design via configuration-constrained polyhedral computing. *Automatica*, 188:112896, 2026.

[20] B. Houska, M. A. Müller, and M. E. Villanueva. On stabilizing terminal costs and regions for configuration-constrained tube MPC. *IEEE Control Systems Letters*, 8:1961–1966, 2024.

[21] B. Houska, M. A. Müller, and M. E. Villanueva. Polyhedral control design: Theory and methods, 2024.

[22] D. Ingole. *Embedded Implementation of Explicit Model Predictive Control.* PhD thesis, Slovak University of Technology in Bratislava, November 2017.

[23] D. Kouzoupis, G. Frison, A. Zanelli, and M. Diehl. Recent advances in quadratic programming algorithms for nonlinear model predictive control. *Vietnam Journal of Mathematics*, 46:863–882, 2018.

[24] M. Kvasnica, P. Bakarac, and M. Klaučo. Complexity reduction in explicit MPC: A reachability approach. *Systems & Control Letters*, 124:19–26, 2019.

[25] M. Kvasnica and M. Fikar. Clipping-based complexity reduction in explicit MPC. *IEEE Transactions on Automatic Control*, 57(7):1878–1883, 2012.

[26] M. Kvasnica, J. Holaza, B. Takács, and D. Ingole. Design and verification of low-complexity explicit MPC controllers in MPT3. In *2015 European Control Conference*, pages 2595–2600, 2015.

[27] M. Kvasnica, J. Löfberg, and M. Fikar. Stabilizing polynomial approximation of explicit MPC. *Automatica*, 47(10):2292–2297, 2011.

[28] M. Kvasnica, I. Rauová, and M. Fikar. Simplification of explicit MPC feedback laws via separation functions. *IFAC Proceedings Volumes*, 44(1):5383–5388, 2011. 18th IFAC World Congress.

[29] W. Langson, I. Chryssochoos, S. Raković, and D. Mayne. Robust model predictive control using tubes. *Automatica*, 40(1):125–133, 2004.

[30] M. Ławrynczuk and P. Ocłon. Model predictive control and energy optimisation in residential building with electric underfloor heating system. *Energy*, 182:1028–1044, 2019.

[31] D. Limon, I. Alvarado, T. Alamo, and E. F. Camacho. Robust tube-based MPC for tracking of constrained linear systems with additive disturbances. *Journal of Process Control*, 20(3):248–260, 2010.

[32] J. Lofberg. YALMIP: A toolbox for modeling and optimization in MATLAB. In *Proceedings of the CACSD Conference*, Taipei, Taiwan, 2004.

[33] J. M. Maciejowski. *Predictive Control with Constraints.* Prentice Hall, London, 2000.

[34] M. Markowski, M. Trafczynski, E. Pavlovičová, J. Oravec, S. Alabrudziński, P. Kisielewski, K. Urbaniec, K. Elwertowski, and D. Gośtyński. Impact of industrial constraints on the dynamic performance of a PID-controlled hybrid heat-integrated distillation system with a plate heat and mass exchanger. *International Journal of Heat and Mass Transfer*, 252:127445, 2025.

[35] J. Mattingley and S. P. Boyd. CVXGEN: a code generator for embedded convex optimization. *Optimization and Engineering*, 13:1–27, 2012.

[36] D. Mayne and W. Langson. Robustifying model predictive control of constrained linear systems. *Electronics Letters*, 37:1422 – 1423, 12 2001.

[37] D. Mayne, S. Raković, R. Findeisen, and F. Allgöwer. Robust output feedback model predictive control of constrained linear systems. *Automatica*, 42(7):1217–1222, 2006.

[38] D. Mayne, M. Seron, and S. Raković. Robust model predictive control of constrained linear systems with bounded disturbances. *Automatica*, 41(2):219–224, 2005.

[39] D. Q. Mayne. Model predictive control: Recent developments and future promise. *Automatica*, 50(12):2967–2986, 2014.

[40] K. Meyer, T. Bisgaard, J. Huusom, and J. Abildskov. Supervisory model predictive control of the heat integrated distillation column. *IFAC-PapersOnLine*, 50(1):7375–7380, 2017.

[41] J. Oravec, P. Bakaráč, E. Pavlovičová, and M. Fikar. Smart eco greenhouse VESNA. *IFAC-PapersOnLine*, 56(2):9576–9581, 2023. 22nd IFAC World Congress.

[42] J. Oravec, M. Bakošová, M. Trafczynski, A. Vasičkaninová, A. Mészáros, and M. Markowski. Robust model predictive control and pid control of shell-and-tube heat exchangers. *Energy*, 159:1–10, 2018.

[43] J. Oravec and M. Klaučo. Real-time tunable approximated explicit MPC. *Automatica*, 142:110315, august 2022.

[44] G. Pannocchia. Robust model predictive control with guaranteed setpoint tracking. *Journal of Process Control*, 14(8):927–937, 2004.

[45] G. Pannocchia. Offset-free tracking MPC: A tutorial review and comparison of different formulations. In *2015 European Control Conference*, pages 527–532, Linz, Austria, 2015.

[46] G. Pannocchia, M. Gabiccini, and A. Artoni. Offset-free MPC explained: novelties, subtleties, and applications. *IFAC-PapersOnLine*, 48(23):342–351, 2015.

[47] G. Pannocchia and J. B. Rawlings. Disturbance models for offset-free model-predictive control. *AIChE Journal*, 49(2):426–437, 2003.

[48] E. Pavlovičová, B. Daráš, P. Bakaráč, M. Fikar, and J. Oravec. From theory to harvest: Robust MPC supervising smart greenhouse system. In *2025 25th International Conference on Process Control (PC)*, pages 1–6, 2025.

[49] E. Pavlovičová, J. Holaza, L. Galčíková, and J. Oravec. Introducing implicit tube model predictive control to MPT+: Efficient design for large-scale systems. In *2025 American Control Conference (ACC)*, pages 33–38, 2025.

[50] E. Pavlovičová, J. Oravec, M. Trafczynski, M. Markowski, S. Alabrudziński, P. Kisielewski, and K. Urbaniec. Energy and carbon footprint reduction for hybrid heat-integrated distillation systems: Robust model predictive control approach. *Energy*, 334:137587, 2025.

[51] E. Pavlovičová, J. Vargan, P. Bakaráč, M. Fikar, and J. Oravec. Offset-free MPC of temperature in smart greenhouse VESNA. In *8th IFAC Conference on Nonlinear Model Predictive Control (NMPC)*, Kyoto, Japan, 2024. Zenodo.

[52] E. Plšičík Pavlovičová, L. Galčíková, J. Holaza, and J. Oravec. Real-time tunable rigid tube MPC using implicit formulation. *Journal of Process Control*, 163:103750, 2026.

[53] S. J. Qin and T. A. Badgwell. A survey of industrial model predictive control technology. *Control Engineering Practice*, 11(7):733–764, 2003.

[54] S. Raković, E. Kerrigan, K. Kouramas, and D. Mayne. Invariant approximations of the minimal robust positively invariant set. *IEEE Transactions on Automatic Control*, 50(3):406–410, 2005.

[55] S. Raković and D. Mayne. A simple tube controller for efficient robust model predictive control of constrained linear discrete time systems subject to bounded disturbances. *IFAC Proceedings Volumes*, 38(1):241–246, 2005. 16th IFAC World Congress.

[56] S. V. Raković. The implicit rigid tube model predictive control. *Automatica*, 157:111234, 2023.

[57] S. V. Rakovic, B. Kouvaritakis, M. Cannon, C. Panos, and R. Findeisen. Fully parameterized tube MPC. In *Proceedings of the 18th IFAC World Congress*, 2011.

[58] S. V. Rakovic, B. Kouvaritakis, R. Findeisen, and M. Cannon. Homothetic tube model predictive control. *Automatica*, 48(8):1631–1638, 2012.

[59] S. V. Rakovic, W. S. Levine, and B. Acikmese. Elastic tube model predictive control. In *2016 American Control Conference*, pages 3594–3599, 2016.

[60] S. V. Raković and S. Zhang. Model predictive control with implicit terminal ingredients. *Automatica*, 151:110942, 2023.

[61] J. B. Rawlings, D. Q. Mayne, and M. Diehl. *Model Predictive Control: Theory, Computation, and Design.* Nob Hill Publishing, 2017.

[62] J. B. Rawlings, D. Q. Mayne, and M. M. Diehl. *Model Predictive Control: Theory, Computation, and Design.* Nob Hill Publishing, Santa Barbara, California, 2 edition, 2022.

[63] P. O. M. Scokaert and D. Q. Mayne. Min-max feedback model predictive control for constrained linear systems. *IEEE Transactions on Automatic Control*, 43(8):1136–1142, 1998.

[64] J. Sieber, A. Zanelli, A. P. Leeman, S. Bennani, and M. N. Zeilinger. Asynchronous computation of tube-based model predictive control, 2023.

[65] B. Stellato, G. Banjac, P. Goulart, A. Bemporad, and S. Boyd. OSQP: an operator splitting solver for quadratic programs. *Mathematical Programming Computation*, 12(4):637–672, 2020.

[66] P. Tatjewski. Disturbance modeling and state estimation for predictive control with different state-space process models. In *Proceedings of the 18th IFAC World Congress*, pages 5326–5331, Milano, Italy, 2011.

[67] Tubular Exchanger Manufacturers Association. *Standards of the Tubular Exchanger Manufacturers Association.* Tubular Exchanger Manufacturers Association, Tarrytown, NY, USA, 10th edition, 2019.

[68] B. P. G. Van Parys, D. Kuhn, P. J. Goulart, and M. Morari. Distributionally robust control of constrained stochastic systems. *IEEE Transactions on Automatic Control*, 61(2):430–442, 2016.

[69] M. Villanueva, M. Müller, and B. Houska. Configuration-constrained tube mpc. *Automatica*, 163:111543, 2024.

[70] K. Wang, Y. Jiang, J. Oravec, M. Villanueva, and B. Houska. Parallel explicit tube model predictive control. In *58th IEEE Conference on Decision and Control*, pages 7696–7701, Nice, France, December 11–13 2019.

[71] K. Wang, S. Zhang, S. Gros, and S. V. Raković. Tube MPC with time-varying cross-sections. *IEEE Transactions on Automatic Control*, 70(3):1851–1858, 2025.

[72] F. Wu, M. E. Villanueva, and B. Houska. Ambiguity tube MPC. *Automatica*, 146:110648, 2022.

[73] J. Xu. Lattice piecewise affine approximation of explicit linear model predictive control. In *60th IEEE Conference on Decision and Control*, pages 2545–2550, 2021.

[74] M. Zanon and S. Gros. On the similarity between two popular tube MPC formulations. In *2021 European Control Conference (ECC)*, pages 651–656, 2021.

[75] Z. Zhong, E. A. del Rio-Chanona, and P. Petsagkourakis. Tube-based distributionally robust model predictive control for nonlinear process systems via linearization. *Computers & Chemical Engineering*, 170:108112, 2023.